TUHH
POLYMER COMPOSITES

TUHH
Technische Universität Hamburg-Harburg

Failure mechanism under tensile loads in CFRP 0-90° cross-ply laminates containing voids.

FINAL DEGREE PROJECT

von

Carlos Lozano Pedrero

aus

Girona, Spanien

Matr. Nr.: 34278

26.04.2007

Betreuer:	Dipl.-Ing. Florian Gehrig
Erstprüfer:	Prof. Dr.-Ing. Karl Schulte
Zweitprüfer:	Dr. Josep Costa i Balanzat

DECLARATION

Hereby, I declare that I prepared this project by myself and without help of others. All used sources and tools were mentioned completely. Text, illustrations, pictures and drawings, which were taken word by word, have been marked in every individual case.

Hamburg (Germany), April 26th, 2007 ……..……

(Carlos Lozano Pedrero)

ACKNOWLEDGEMENTS

I would like to thank Prof. Dr.-Ing. Schulte for giving me the opportunity to do this Final Degree Project within the Department of Polymer Composites.
Many thanks to my supervisor Dipl.-Ing. Florian Gehrig for the idea of this project, his guidance and help in theoretical and practical support and for his patience.
Special thanks to Dipl.-Ing. Lars Böger for his help and hospitality. Many thanks to Dipl.-Ing. Leif Ole Meyer and Dipl.-Ing. Stephan Hinz for his support and trouble shooting. I would like to thank Dr. Ruby Dhamari for his important help with the FEM.
Furthermore, I am very grateful with Dr. Josep Costa i Balanzat for the valuable previous training and background formation received at his research group.

Special thanks to my parents for their unconditional support through all this years. Finally, thanks to everybody that contributed directly or indirectly in the culmination of my degree.

ABSTRACT

The failure mechanism of a voided CFRP 0-90° cross-ply laminate under tensile loads applied in one direction was studied in this Final Degree Project.

For this purpose, voided coupons were manufactured for being tested and a FEA was done. In both investigations, voids were placed in 90º and 0º direction, in order to understand the void location influence.

On the one hand, the behaviour of the voided laminates was investigated through a FEM in order to preview the stress distribution within the material.
On the other hand, voided specimens where manufactured by applying blowing agent in between the inner layers. These specimens were tested by a quasi-static step wise tensile test where data showing its real behaviour was collected. Specimens were X-rayed after each step of the test in order to investigate the failure mechanism of the composite.

Data from the test was studied so that relations such as strength of the laminates, crack density per stress, void length per first crack at the void and void area per first crack at the specimen could be characterized.

In conclusion, it was detected that big discrete void do not affect the location of final failure in cross-ply laminates. Furthermore, it was stated that transversal cracks for 90º appeared normally at the void section, but for 0º the first crack did not appear at the void. Transversal crack density developed earlier per 0º void lay-up than per 90º void lay-up. Finally, it was noted that strength decreases with parameters as void length and voided area although it was clear that other parameters may affect as well, because of the scatter.

Table of contents

1. INTRODUCTION

Fibre reinforced composite materials are widely used because of its superior properties. High stiffness, high strength, low density and adaptability to the intended function of the structure make these materials suitable for many engineering applications, from sports goods to aircraft structures.

Composites are complex materials exhibiting an anisotropic behaviour. This characteristic presents a positive characteristic when designing a certain component: there are multiple degrees of freedom in order to get an optimal configuration of the material.

But because of this characteristic it has been necessary to closely study its behaviour and properties by combining various disciplines within science and technology. Nowadays, composite materials are still under development although they have already reached a state of maturity.

Effective design parameters have been accumulated in composites, but its behaviour when there are anomalies is still being researched. A common problem when manufacturing composites is the formation of defects such as resin-rich regions, distorted fibres, foreign inclusions and voids. Most probably, voids are the greatest problem because they are difficult to avoid and are noticeable affecting the mechanical properties.

Much research has been done in order to study the mechanical behaviour of composites with porosity, like for example, its interlaminar fracture toughness, its interlaminar shear strength, its bending strength or its transverse and longitudinal tensile strength. However, there is no general agreement in which is the failure mechanism occurring in these materials when tensile loads are applied in a laminate containing voids. This is mainly because most of the research done relates the void volume fraction with these material properties. Therefore, the scope of this project was to study the failure mechanism in a CFRP 0-90º cross-ply laminate when it contains discrete voids.

2. THEORY

2.1 CFRP

"A structural composite is a material system consisting of two or more phases on a macroscopic scale, whose mechanical performance and properties are designed to be superior to those of the constituent materials acting independently. "[1]

These phases that complement each other are usually clearly differentiable. One of them, called reinforcement, is the responsible of the stiffness and strength of the resultant, and the other component, called matrix, is the weaker and responsible of the ductile properties.
In terms of morphology, normally, the fibres are discontinuous at least in one direction whereas the matrix is continuous in all direction and surrounds the fibres. A resultant region is defined because of this combination. It is called interfacial region and is where the interface between the two phases is. Both components can be seen in *figure 2.1*

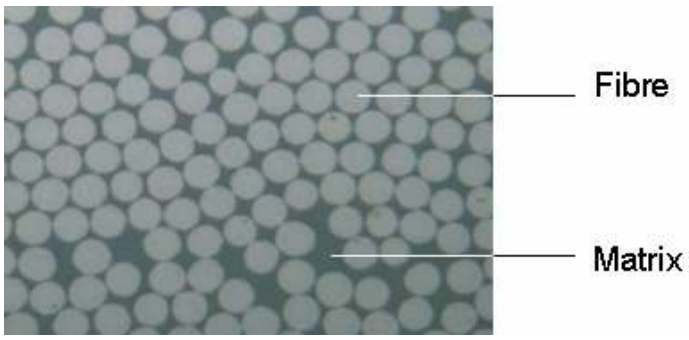

Fig. 2.1. Matrix and fibres [2]

As stated in the definition, the aim for combining this system is to achieve a new material which presents new and/or superior properties than each of the components.

Moreover, polymers, metals and ceramics can usually act as matrix or fibre in the common system.

The influence of these properties depends in the manufacturing process but mainly on how the reinforcement is related within the matrix.

Therefore, factors such as the reinforcement size, its dispersion, its orientation and its geometry become crucial when defining the final material properties.

Reinforcements can be configured as particles dispersed in the matrix or fibres that can be either continuous or discontinuous. [1] [3] [4]

As this Final Degree Project is based on carbon fibre reinforced plastics with continuous fibre, from now on a focus in this configuration and these materials is done.

In contrast to short fibre composites, continuous fibre composites produce a significant improvement in strength.

Furthermore, by combining fibres and resin (matrix) a composite material is created with a strength and stiffness close to that of the fibres and with chemical resistance and ability to absorb energy during deformation of the resin. *Fig.2.2*

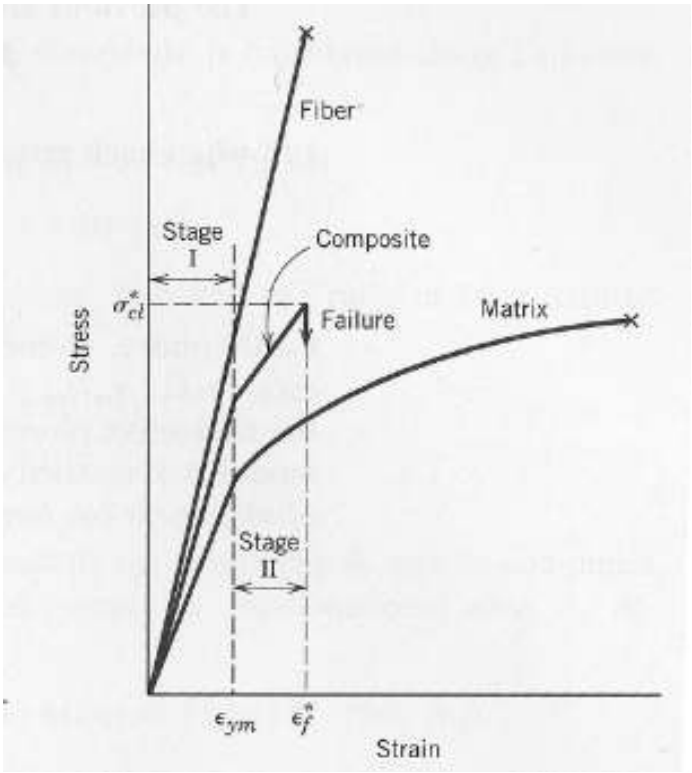

Figure 2.2. Stress-strain behaviour for composite material and its components. [4]

Nowadays, the use of fibre reinforced composites turned to be the most issued to fulfil required technological requests.

Mainly, these materials present an optimal behaviour when high strength, high stiffness and low density are required. Composites present these properties together due to its high specific strength and high specific stiffness. Comparing its behaviour with metals, composites present better properties as stated in the example in *Table 2.1*.

	High strength Al-Zn-Mg alloy	**Carbon Fibre-epoxy resin unidirectional laminae, parallel to fibres**
Density (Mg m-3)	2,80	1,62
Young's modulus (GN m-2)	72	220
Tensile strength (MN m-2)	503	1400
Elongation to fracture (%)	11	0,80
Coefficient of thermal expansion (10-6ºC-1)	24	-0,20
Specific Young's modulus (GN m-2)	25,70	135
Specific tensile strength (MN m-2)	280	865
Heat resistance (ºC)	350	260

Table 2.1. Comparison between properties of an alloy and a composite.

2.1.1 Matrix

Polymeric are the most commonly used matrices. Within this type, there are two kinds of resins: thermoplastics and thermosets.

Thermoplastics change from the crystalline phase to an amorphous viscous liquid when heating.

In contrast, thermosets, more used in industry, remain as brittle rigid solids when cured and do not soften when heating.

Focusing in thermosets, they can be classified in three main groups: epoxies, polyimide and polyester. [1]

The resin acts as a fibre union element, binding them together and protecting them against mechanical abrasion or chemical environments, although the main task is to help distributing the applied load in the fibres.

Normally, within the composite, the matrix is responsible for isolating, chemical behaviour and coefficient of expansion. [4]

2.1.2 Fibres

The fibres are responsible for the composites stiffness and strength.
A wide range of fibres can be found as reinforcement for composites, as the use of one or another fibre affects the properties in the final product, main characteristics per each kind of fibre are shown in *Table 2.2*

Fiber	Advantages	Disadvantages
Glass	High strength Low cost	Low stiffness Short fatigue life High temperature sensitivity
Aramid (Kevlar)	High tensile strength Low density	Low compressive strength High moisture absorption
Boron	High stiffness High compressive strength	High cost
Carbon	High strength High stiffness	Moderately high cost
Graphite	very high stiffness	Low strength High cost
Ceramic	High stiffness High use temperature	Low strength High cost

Table 2.2. Types of reinforcing fibres and their main advantages and disadvantages. [1]

The content of fibres has a strong influence in the composite properties. For example, a high content of fibres increases the strength and the elastic modulus.

2.1.3 Elastic properties

First of all a distinction has to be done between longitudinal and transverse direction. As indicated in Figure 2.3 where the applied load is in longitudinal direction.

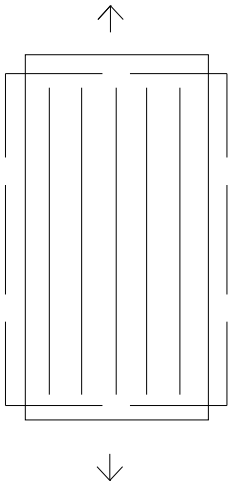

Fig. 2.3 Deformed and undeformed orthotropic laminate under longitudinal load

As a main property composite materials present anisotropy. Because of the orientation of the fibres the mechanical response of the system varies depending on several factors such as the direction in which the stress or load is applied and the direction in which the properties are measured.

Assuming the anisotropy characteristic, a more detailed specification is used for the unidirectional laminates: orthotropy.
Orthotropic materials present principal axis aligned with the longitudinal reinforcement and its transverse directions. Because of being orthotropic, a material does not present shear strains if it is subjected to a loading aligned parallel to any of the principal axis, *Figure 2.3*.

A basic explanation on the material response under loading in the longitudinal direction is required.
Talking in terms of elastic micromechanical behaviour a further supposition is made: the interface between fibres and matrix is excellent. In consequence, an isostrain situation is achieved so that matrix and fibre strains are equal. [4]
On the one hand, in the longitudinal direction, the elastic behaviour is defined as follows:

$$\varepsilon_c = \varepsilon_1 = \varepsilon_f = \varepsilon_m \tag{2.1}$$

Where, ε_c is the elongation of the composite

ε_1 is the elongation due to tensile stress in 1 direction

ε_f is the elongation of the fibre

ε_m is the elongation of the matrix

$$F_c = F_1 = F_f + F_m \tag{2.2}$$

$$\sigma_c = \sigma_1 = \sigma_f \frac{A_f}{A_c} + \sigma_m \frac{A_m}{A_c} = \sigma_f V_f + \sigma_m V_m \tag{2.3}$$

$$E_1 = E_f V_f + E_m V_m \tag{2.4}$$

In this same situation, the longitudinal strength is defined by the following equations.

$$F_c = F_1 = F_f + F_m \tag{2.5}$$

$$\sigma_{1u} = \sigma_{fu} V_f + \sigma_m^* V_m \tag{2.6}$$

Where, σ_m^* is the stress in the matrix at fibre failure

σ_{1u} is the ultimate longitudinal tensile strength of the composite

It is assumed that the strength of the fibres is greater as that of the matrix as they bear the major part of the applied load.

On the other hand, the behaviour of the transverse direction when longitudinal loads are applied can be approached by the following equations:
In this case the load is conducted equally to the matrix and the fibres.

$$F_2 = F_f = F_m \tag{2.7}$$

Considering an isostress strain:

$$E_2 = \frac{E_f E_m}{E_f V_m + \varepsilon_m V_f} \tag{2.8}$$

As a simplification, it can be assumed that the strength of the transversal direction is dominated by the matrix strength.

$$\sigma_{2u} = \sigma_m^* \tag{2.9}$$

Although it has to be commented that it has been proved that in praxis the strength is higher than the matrix strength [5]

When a deeper study is required, taking into account anisotropy and high loads, matricial mathematics are needed and computational analysis by finite elements.

2.2 Classical laminate theory (CLT).

As seen before, lamina present good properties for being a structural component, but they are rarely used alone but rather as a part of a laminate. A laminate is made up of two or more unidirectional lamina or plies that are stacked together at various orientations.
Composite laminates are identified by its stacking sequence (lay up) orientation of the different ply. Concerning this Project, a cross ply symmetric laminate could be designated as $[0,90]_{s,}$ where s stands for symmetry to its middle layers.

In order to characterize the elastic macromechanical properties of a laminate, the properties of each lamina have to be considered in classical lamination theory.

Before, an assumption has to be noted when bonding lamina. The bond between layers is supposed to be infinitely strong so that displacement is constant in two bonded lamina. However, in reality because of small off-axis alignment or fibres or stress, severe shear stresses may affect the composite in the boundary region.
This stresses can induce delamination between layers affecting the composite properties.

Always, the stress strain behaviour can be described by the stiffness relation matrix, which characterises the material properties

$$\begin{bmatrix} \sigma_1 \\ \sigma_2 \\ \sigma_3 \\ \tau_{23} \\ \tau_{31} \\ \tau_{12} \end{bmatrix} = \begin{bmatrix} A_{11} & A_{12} & A_{13} & B_{14} & B_{15} & B_{16} \\ A_{12} & A_{22} & A_{23} & B_{24} & B_{25} & B_{26} \\ A_{13} & A_{23} & A_{33} & B_{34} & B_{35} & B_{36} \\ B_{14} & B_{24} & B_{34} & D_{44} & D_{45} & D_{46} \\ B_{15} & B_{25} & B_{35} & D_{45} & D_{55} & D_{56} \\ B_{16} & B_{26} & B_{36} & D_{46} & D_{56} & D_{66} \end{bmatrix} \begin{bmatrix} \varepsilon_1 \\ \varepsilon_1 \\ \varepsilon_1 \\ \gamma_{23} \\ \gamma_{31} \\ \gamma_{12} \end{bmatrix} \tag{2.10}$$

This expression can be formulated by defining strain as a function of stress, known as the compliance matrix, which obviously is the inverse matrix of the stiffness matrix. [6]

In the case of orthotropic lamina, the stress in 3-direction is neglected because it is assumed that it is very thin. By this assumption, the following relations are defined:

$$\sigma_1 = \sigma \tag{2.11}$$

$$\sigma_2 = \sigma_3 = \tau_{23} = \tau_{31} = \tau_{12} = 0 \tag{2.12}$$

Where,

σ is the tensile stress applied at the lamina in 1-direction

Thus, the plane stress equations are expressed as follows. [6]

$$\begin{bmatrix} \sigma_1 \\ \sigma_2 \\ \tau_{12} \end{bmatrix} = \begin{bmatrix} A_{11} & A_{21} & 0 \\ A_{12} & A_{22} & 0 \\ 0 & 0 & A_{66} \end{bmatrix} \begin{bmatrix} \varepsilon_1 \\ \varepsilon_2 \\ \gamma_{12} \end{bmatrix} \tag{2.13}$$

Where,

$$A_{11} = \frac{E_1}{1-\upsilon_{12}\nu_{21}}; A_{22} = \frac{E_2}{1-\upsilon_{12}\nu_{21}};$$

$$A_{12} = \frac{\nu_{12}E_2}{1-\upsilon_{12}\nu_{21}} = \frac{\nu_{21}E_1}{1-\upsilon_{12}\nu_{21}}; A_{66} = \frac{1}{2}(A_{11} - A_{12}) = G_{12}$$

2.3 Edge weakness

Before having a closer look on the failures modes and appraisal should be done in a particular weak region of the specimens: the free edge surface.
In the edge free region appear types of damage such as interlaminar delamination and transverse cracks in the 90º plies.

Furthermore, because of the production process, the edges of the specimen could result damaged.
Polishing the edges of the specimen is important because it has been proved, in the study made by Clements and Lee, that this action increases the strength of the specimens in a 15% to 25% factor. [7]

Damaged edges produce two effects that contribute to create a week region in the free edge surface.

- Damaged fibres get scratches and cavities in the surface that induce early crack initiation in this region.
- There will be a higher local stress in the cut fibres when the decrease in its cross section area is greater than the decrease in the bonding matrix area.

  This will occur when more than half of the fibre cross section area has been removed. In this condition, the load applied to these fibres will induce higher stresses in these damaged fibres rather than in undamaged ones. Once one of these damaged fibres fails, the adjacent fibre will get a stress increase as result which may produce cracks

2.4 Failure mechanism

A laminate, formed by stacking several bonded laminae, responds under a certain load depending on the properties of each individual laminae and the interaction with each other.

It must be noted before having a closer introduction in laminates failure mechanism that strength is no longer a fixed parameter for composites. Thus, a laminate may continue to support an increasing load although it can have happened that one of the laminae did fail. Therefore, the final application of the material is normally the parameter that fixes the strength of a composite laminate.

Failure in composite laminates under load appears as a result of the sum of several different failure modes, such as matrix longitudinal cracks, matrix transversal cracks, interfacial debonding, delamination and fibre breaks. *Figure 2.4.*

All this failure modes are going to be deeply explained later. Some parameters such as temperature, lay up or interface between fibres and matrix have to be considered because they may affect the final failure as well.

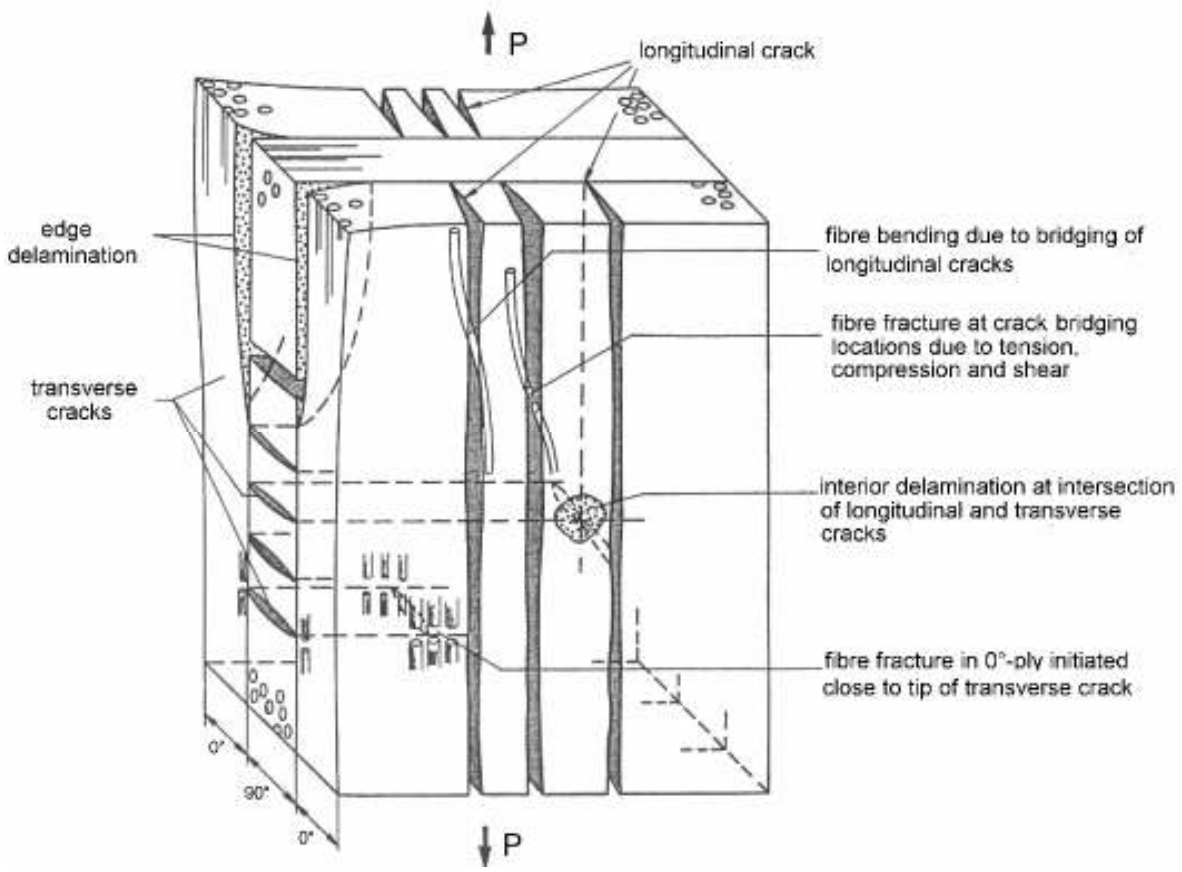

Fig.2.4. Overview of the damage mechanisms possibly occurring in a cross-ply laminate. [6]

The failure of an individual lamina does not imply total failure of the laminate, but it starts the progressive failure of the laminate [1]. When a lamina fails, the stresses are redistributed so that the rest of the laminas receive the stress that was sustaining the one that failed.
The bonding between laminas becomes then crucial when reassigning the stress after the failure of a lamina in a laminate.

Consequently, it is difficult to predict precisely the final failure of a composite because of so many failure modes involved that are degrading the material properties.

From now on, due to the scope of this Project, a focus in damage development under static loading is done regarding cross-ply laminates. Concerning this kind of laminates, it has to be noted that failure modes in quasi-static test appear later than in fatigue. Transverse cracks start appearing earlier while longitudinal cracks and fibre fracture appear close to the ultimate strain. Delamination is encountered rarely in quasi-static test.

2.4.1 Transverse cracks

The transverse tensile strength of a lamina is determined by factors such as properties of the matrix (mainly), interface bond strength and presence and distribution of voids.

This is in general the first failure occurring in laminates with cross-ply lay up. The cracks start to grow in the matrix located at the free edge region and keep on growing to the inner centre until they meet forming a large transverse crack through the thickness of the ply. Transverse cracks appear in the 90º plies, usually, after a strain of 0.3% has been applied. *Fig. 2.5*

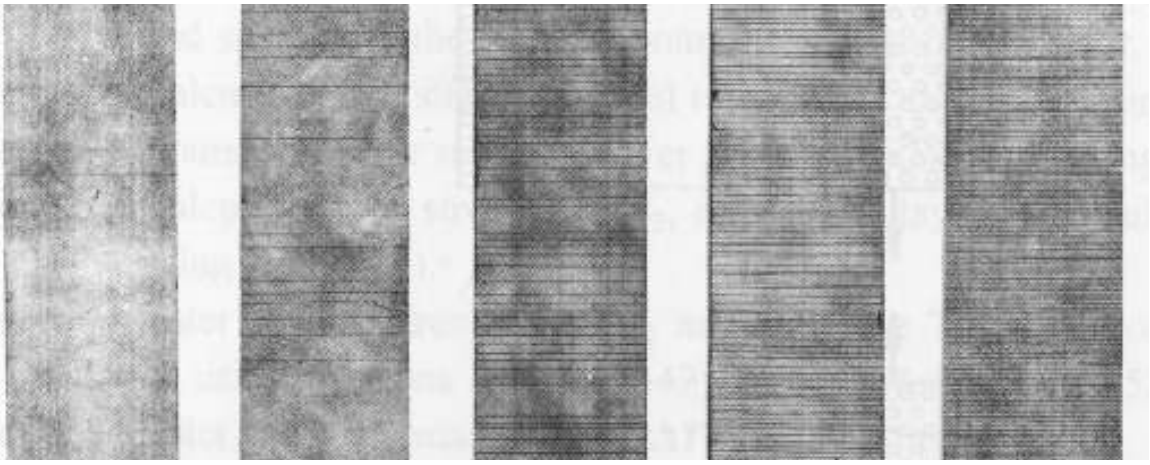

Fig. 2.5. Radiographies from a $[0,90_2]_s$ cross-ply laminate under tensile stress at 221, 276, 414, 517 and 662 MPa respectively [1].

This kind of defect is influenced by the matrix ductility and the bonding characteristics between fibres and matrix.

When a crack through the matrix reaches a fibre, the stress σ_1 (in fibre direction) tends to cause fibre fracture, while σ_2 (crack growing direction) leads to tensile separation at the interface (consequent crack propagation through the matrix) as shown in *Fig. 2.6.*
As damage grows, the stiffness of the damaged ply is reducing and therefore the stiffness of the entire composite.

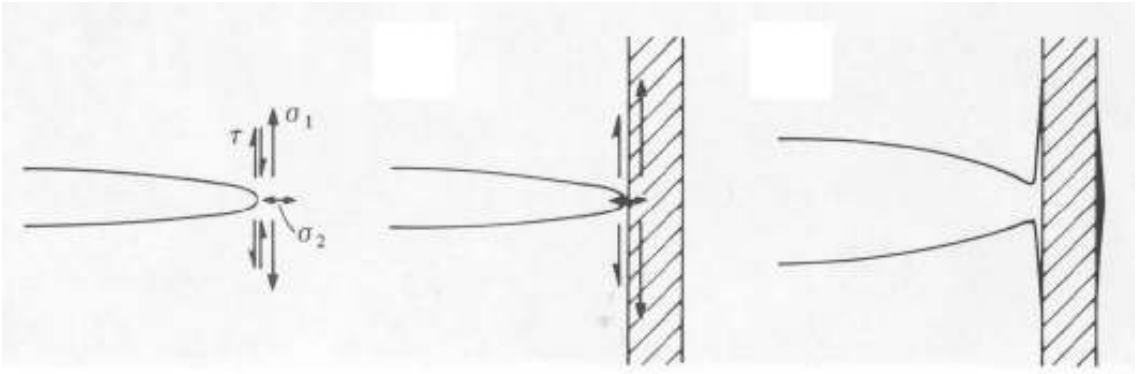

Fig. 2.6. Damage evolution when a matrix crack meets a fibre [3]

After the first crack, the following cracks appear, so that the specimen is being divided in equal parts by the cracks. This fact is produced because the redistribution of load places the next critical point in the middle of the two halves of the specimen. *Figure 2.7.*

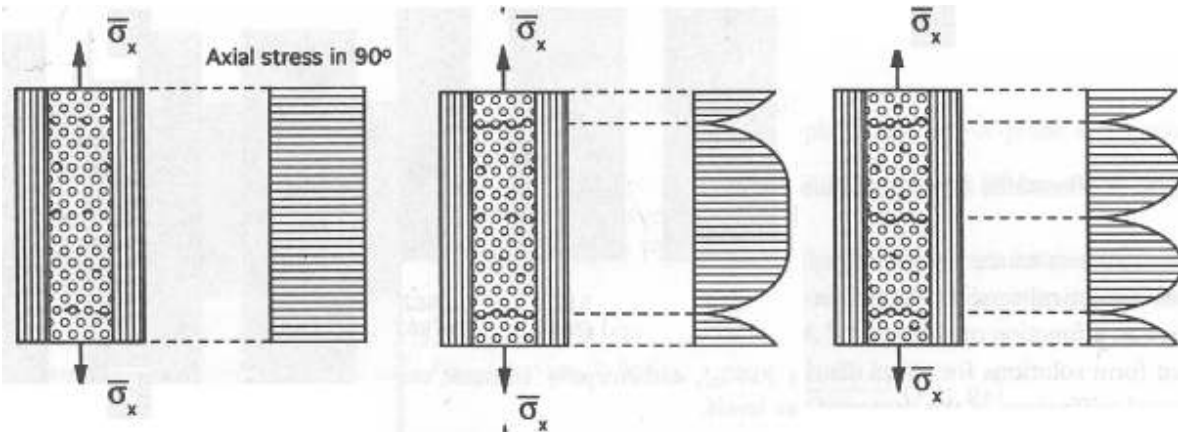

Fig.2.7. Progressive failure and stress distributions in transverse ply of cross ply laminate under uniaxial tension. [1]

While increasing the load, the crack density increases too until it reaches a certain value. This saturation point is a characteristic of each laminate and depends on the constituents and on the stacking sequence. [8] The reason why this saturation point is reached is because after a lot transversal cracks have occurred; the stress redistribution does not present a tensile strength value anymore. [1]

2.4.2 Longitudinal cracks

Longitudinal cracks appear in the matrix following the axial direction where the load is being applied. It was noted in laboratory that this kind of crack appears short before final failure when being tested.

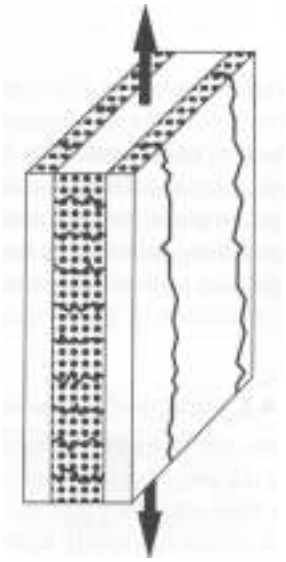

Fig. 2.8. Longitudinal crack (vertical) for a cross-ply laminate

Longitudinal cracks are produced due to the mismatch of the poisons ratio between the different orientated plies. Under stress, 0º plies tend to contract in its transversal length while the 90º plies tend to hinder.

When a transversal crack appears, some of the energy liberated is trespassed to the neighbouring 0º layers, increasing the stress in these layers. *Fig. 2.9*. The sum of these facts produces the longitudinal cracks. *Fig. 2.8*

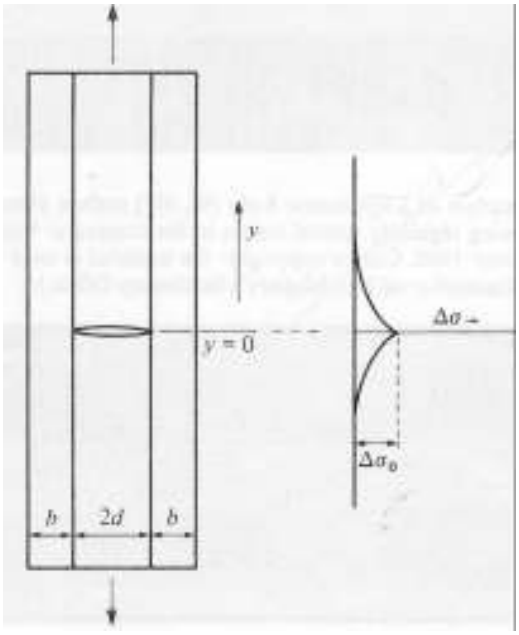

Fig. 2.9. Transverse crack in a cross-ply laminate illustrating additional stress on longitudinal layers. [3]

The intersection between transverse and longitudinal cracks is likely to develop local delamination.

2.4.3 Delamination: Edge effect

It is a fact that a laminate with different orientation plies under a certain load gets interlaminar shearing stresses because of the mutual restrain against Poisson's deformations between plies.
Two kinds of stresses can induce delamination, also known as interlaminar separation.

- Normal tensile interlaminar stress, which tends to separate two bonded laminas.
- Shear interlaminar stress, which tends to slide one lamina over the other.

Interlaminar stresses can be mainly controlled by selecting an accurate stacking sequence of laminas. For example, it can happen that a tensile interlaminar normal stress is transformed into a compressive stress by rearranging the layer sequence. *Figure 2.10* [1].

Focusing in cross-ply laminates, under stress applied the different component layers (0º and 90º) undergoes a different transverse deformation because of the different Poisson's ratios.

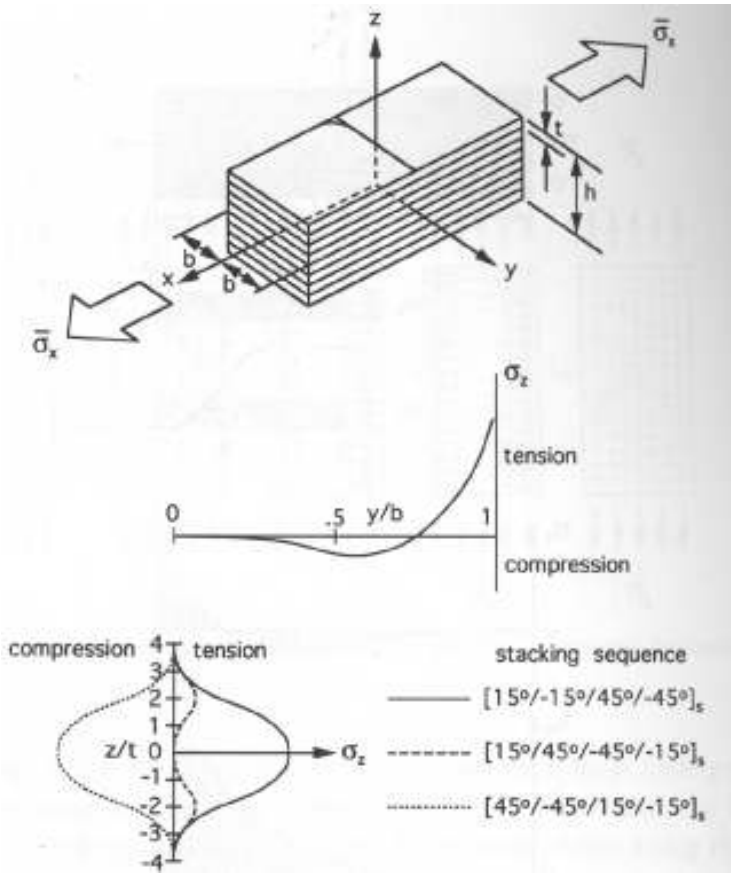

Figure 2.10. Stacking sequence effect on interlaminar stresses. [1]

As plies are bonded together the transversal strain has to be equal for all of them. As a result, the stress distribution stated in *Fig.2.11* appears in the interlaminar region.

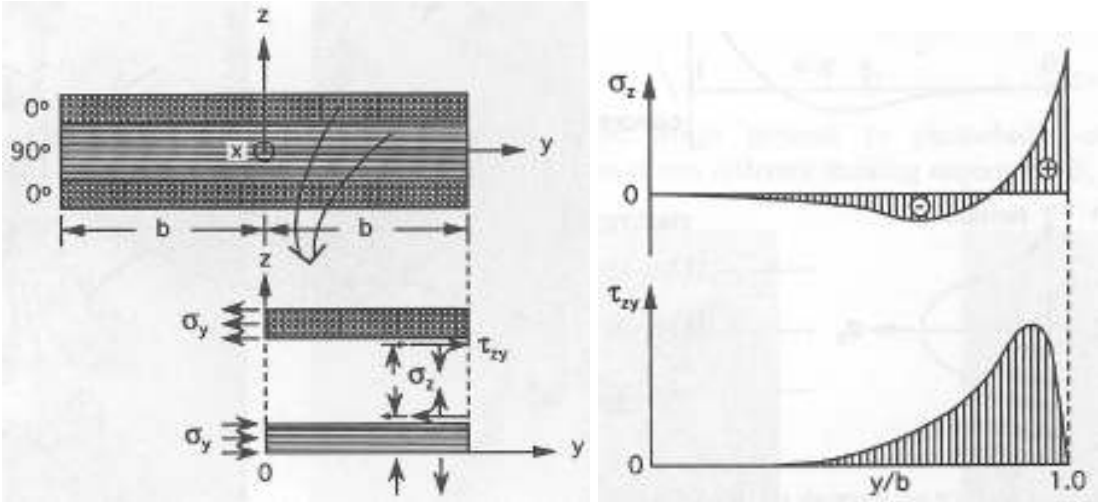

Fig. 2.11. Distribution of interlaminar normal stress σ_z and interlaminar shear stress τ_{zy} in [0/90]s [1]

In order to exactly characterise and analyze the interlaminar stresses in a composite, complex numerical mathematical methods are required.

2.4.4 Fibre failure

This failure mode is normally related to the composite laminate final failure.
In a cross-ply laminate, failure of 0º fibres can be determined at those locations, where internal transverse cracks reach 0º plies.
Another cause of failure can be because of defects in the fibre structure. Flaws in fibres are assumed to be randomly distributed. Because of this, as the load increases, the fibres tend to break at the weakest point. [3]
When a fibre breaks it immediately transfers the load as an increase to the neighbouring region.

In case of having a broken fibre three different processes can occur in the composite. *Figure 2.12*

a. The crack propagates into the adjacent matrix as a brittle crack.
b. The matrix around the crack yields
c. The interface fails in shear provoking that the fibre shrinks back

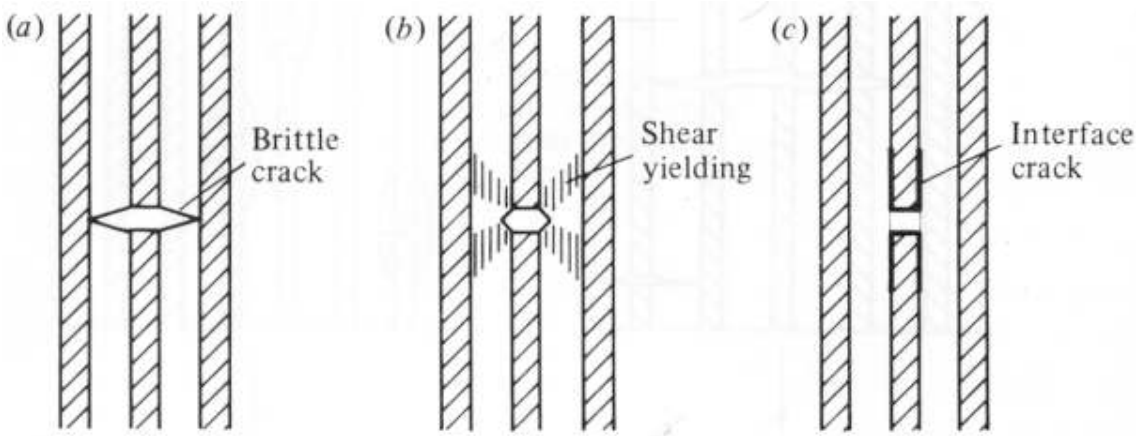

Figure 2.12. Failure processes when having a broken fibre a) brittle crack of the matrix b) shear yielding of the matrix c) interface failure [3]

If the assumption of having the fibres strongly bonded to a brittle matrix is possible, it can be considered that the fracture is immediately propagating through the section.

In any case, the failure of several fibres may produce fatal effect to the failure of the composite. [3] [6]

2.5 Voids

It is a fact that the presence of small defects, for example voids, resin rich areas or inclusions, in CFRP affects negatively the mechanical properties and structural integrity of the material. Within these defects, voids are a quite common type of defect in CFRP. [9]
The manufacturing process implies always a certain amount of voids in the material. Although the void volume fraction can be reduced by controlling the cure cycle pressure [10], an increase in cost is noted so that a commitment between product performance and cost is achieved.

For studying the properties prediction of models, normally, has been considered the void volume fraction underestimating the void structure. It has been noted that knowing the microstructure of the defect, as well as the volume fraction is important when analyzing the defects effects. For example, different material systems and/or processes types, such as RTM or autoclave, produce voids of different shape, size, and at different location.

As the specimens for the experimental part of this Project were manufactured by autoclave process, a closer look in the kind of voids that this process induces is done.
In autoclave process, there is a first void nucleation phase where micro spherical voids are formed. Afterwards, the pressure and vacuum applied during the cycle, induces the voids to more easily diffuse into nearby existing air voids, rather than nucleate forming a new void. [11]

It has been proved; that for a certain temperature, a void cannot grow by diffusion if the inner pressure is greater than the saturated vapour pressure. [9] While curing in the autoclave, the equilibrium of the void is ruled by the following equation:

$$P_{void} - P_{re\sin} = \frac{\gamma_{LV}}{m_{LV}} \tag{2.14}$$

Where,

P_{void} is the pressure inside the void

$P_{re\sin}$ is the pressure inside the resin

$\frac{\gamma_{LV}}{m_{LV}}$ is the surface tension

This fact produces a morphology of the voids which tends to be elongated with an elliptical shape along the fibre direction an elliptical shape in the cross section as well. These ellipses have their short axis in the laminate thickness direction. *Fig 2.13* [12]

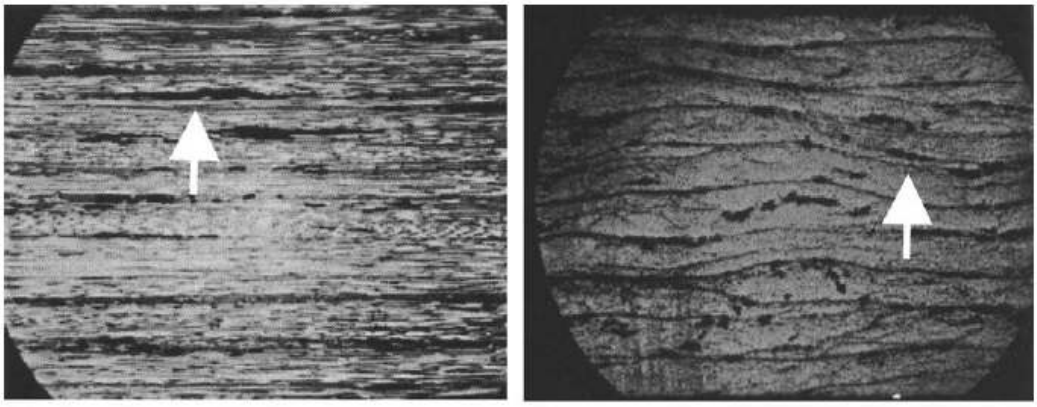

a b

Fig. 2.13. Voids in unidirectional composite laminates [11]. Arrow in each section points to a typical void. a) Section parallel to the fibre direction b) section perpendicular to the fibre direction

2.5.1 Types

If considering the void microstructure, types of voids can be classified in two main categories. [13]

- Voids located along individual fibres.
- Voids in the lamina bonding region

Usually, geometry tends to be spherical or ellipsoidal. If the content of voids is lower than 1.5% in volume fraction, voids present an spherical shape with diameters between 5 and 20μm, also called porosities, otherwise for a higher void contents, they tend to present a cylindrical or ellipsoidal shape, always parallel to fibres on the long axis, with lengths greater than for the previous case. In this case they are not anymore considered as porosity rather than a discrete void defect, large enough to be of structural significance. *Figure 2.14* [14]

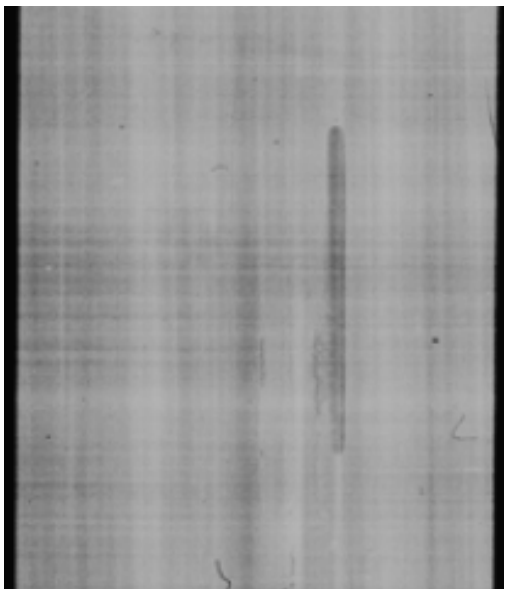

Figure 2.14: Elliptical kind of void in laminates.

2.5.2 Causes

Voids tend to be formed mainly because of three causes: [13]

- Gross defects due to errors in manufacturing
- Entrapment of air in between fibres due to incomplete wetting out during the impregnation of the fibre with the resin. This effect is more likely to happen in systems where the fibres are closely located and the resin has a high viscosity.
- Volatiles arising from the resin during the curing cycle. These volatiles may appear as a result from chemical reaction, residual solvents or low molecular weight components of the resin at curing temperature.

Thus, the parameters that influence void creation, despising voids due to manufacturing errors, are resin type, volatile components, viscosity of the resin, and the cure cycle (defined by pressure, temperature and time).

A focus in the causes of voids in the curing autoclave process used in this Project is done. During the process at the autoclave, voids are mainly formed because of the evaporation of volatiles or water trapped inside the prepreg during curing or because of trapped air during lay-up at the ply interfaces. As stated in some articles, major part of the voids is situated between the plies. [15]

2.5.3 Void influence on mechanical properties

The influence of voids in the mechanical properties of CFRP has become more important as the use of composites has grown too. It has been proved, as stated later, that the effect of voids, even in small amounts, influences negatively the mechanical properties of a composite.

When being formed, voids push aside surrounding fibres and resin as they expand. All fibres remain in the composite and are still continuous, only more packed together around the void. In essence, only the resin is replaced by voids. Therefore, the laminate retains almost all of its stiffness in the fiber direction. [10].

It has to be noted that for an elliptical void, the stress is not any longer distributed uniformly along the section, rather than distributed as seen in *Figure 2.15*.

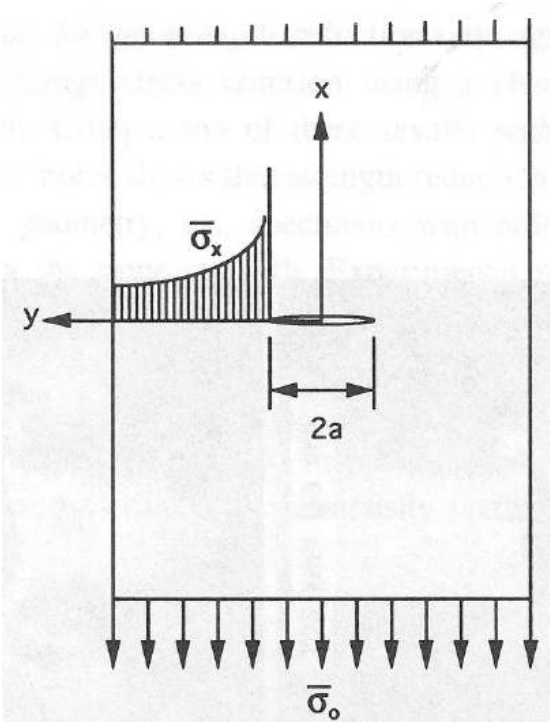

Figure 2.15.. Composite laminate with transverse void under uniaxial tensile loading. [1]

Thus, near the crack tip a high stress concentration is created.

It has been proved by numerous experiments that there is a decrease in properties such as transverse strength and flexural modulus, longitudinal strength and flexural modulus, interlaminar shear strength, compressive strength and modulus and fatigue resistance due to the presence of voids. Alternatively, there are some properties that increase due to the existence of voids, as impact strength and water absorption. [13]

It has been proved that regardless of fibre or resin type the interlaminar shear strength (ILSS) of a composite decreases by about 7% for each 1% voids up to a total void content of about 4%. [13]

The decrease in other properties has been determined too for the first one percent of voids. This decrease is as high as 30% for flexural strength, 9% for torsional shear and 3% for tensile properties. [16]. Furthermore, the correlation relation between void content and its absorption coefficient with mechanical properties such as interlaminar shear strength, tensile strength and flexure strength has been studied through experimental test that showed good correlation. [9]

2.6 FEA

2.6.1 History

It was in 1943 when Finite Element Analysis (FEA) was first developed by R. Courant, who analyzed some vibration systems by the use of the Ritz method, using the calculus of variation to compute the eigenvectors and eigenvalues of a Hamiltonian system. [17]
It wasn't till 1960 when FEA was first termed because of the paper published by M. J. Turner, R. W. Clough, H. C. Martin, and L. J. Topp dealing with "stiffness and deflection of complex structures".
The method became widely used in aerospace industry during the 60s.
In the 70's, FEA expanded to other technology fields where the inversion, in powerful but expensive computers, to run it was possible. Therefore it became common in industries such as nuclear, military, automotive and aeronautics.
As the micro-computers became popular and affordable in the 80's, the method became widely used for engineers in almost every field.

2.6.2 Definition

FEA is a numerical technique by which the solution of a set of differential equations is performed.

Finite element methods are predominantly used to perform analysis of structural, thermal, and fluid flow situations. They are used mainly when hand calculations cannot provide accurate results. This is often the case when the geometry or process in question is very complex. By using FEM (Finite Element Method) many complicated engineering phenomena can be accurately approximated by the use of its governing equations and its boundary conditions.

Fig.2.16. Fem approximation to engineering phenomena

In order to solve the equation system, the applied forces [F] and the stiffness of the material [K] are introduced by the user as parameters. The FEM solves the equation so that the displacements [u] are determined after the analysis. *Fig. 2.16.*

This solution is reached with FEA by using a complex system of points called nodes which make a grid called mesh. This mesh is programmed to contain the material and structural properties which define how the structure will react to certain loading conditions. Nodes are assigned at a certain density throughout the material depending on the anticipated stress levels of a particular area. Regions which will receive large amounts of stress usually have a higher node density than those which experience little or no stress. Points of interest may consist of: fracture point of previously tested material, corners, complex detail, and high stress areas. The mesh acts like a spider web relating all adjacent nodes. This web of vectors is what carries the material properties to the object,

creating many elements (portions of the problem domain, surrounded by nodes).

2.6.3 FEA procedure

Normally, three steps are followed in order to do an analysis in any computer-aided engineering task as stated in *Fig. 2.17*
These steps that were followed as well during the performance of the FEA of this Project are pre-processing, processing and Post-processing of results.

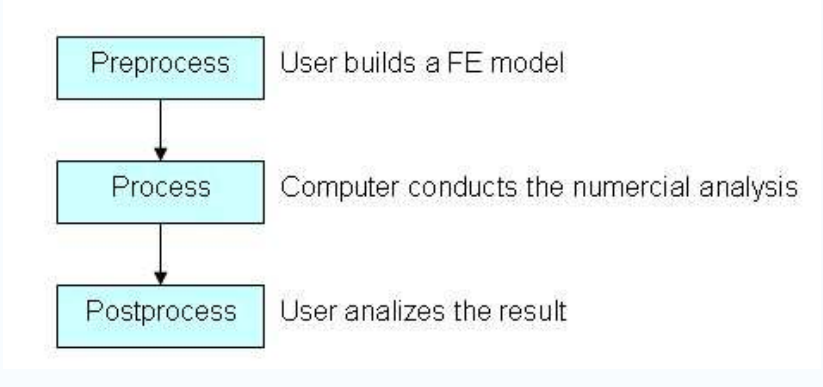

Fig. 2.17. FEA steps

First, pre-processing is required when making a FEA, so that a finite element model of the structure to be analysed is constructed. This can be in either 1D, 2D or 3D form, modelled by lines, shapes or surfaces representation respectively. The primary objective of the model is to realistically simulate the real model.
Once the finite element geometric model has been created, a meshing procedure is used to define and divide the model into a certain number of finite elements. In general a finite element model is defined by a mesh network, which is made up of the geometric arrangement of elements and nodes. Elements are bounded by sets of nodes, and define localised mass and stiffness properties of the model.

Then, the processing step is run in order to solve by the FEM the equation system defined in the previous step. [18]

Finally, in the post-process, the obtained results are studied using a visualisation tool within FEA environment to view and to fully identify the implications of the analysis. Numerical and Graphical tools allow the precise location of data such as stresses and deflections to be identified.

3. EXPERIMENTAL

3.1 Finite Element model

A FE analysis was made in order to investigate and predict the behaviour of a certain CFRP 0-90º cross-ply laminate containing a significant void under the effect of tensile load.
A macroscopic model was produced to predict the failure mechanism and the possible location of the initial failure, in order to get a deeper view in the material behaviour.
Furthermore, two different models where created varying in the orientations of the void within the laminate, one along 0º direction and the other along 90º direction.

3.2 Geometry (plate, void)

Due to symmetrical conditions applied, only an eighth of the geometry had to be modelled. *Fig. 3.1.*
The specimen was simulated by a representative volume cell defined by a rectangular section of 79.5 per 12.7m, being these measures the total ones, although only half of it hat to be represented because of symmetry.

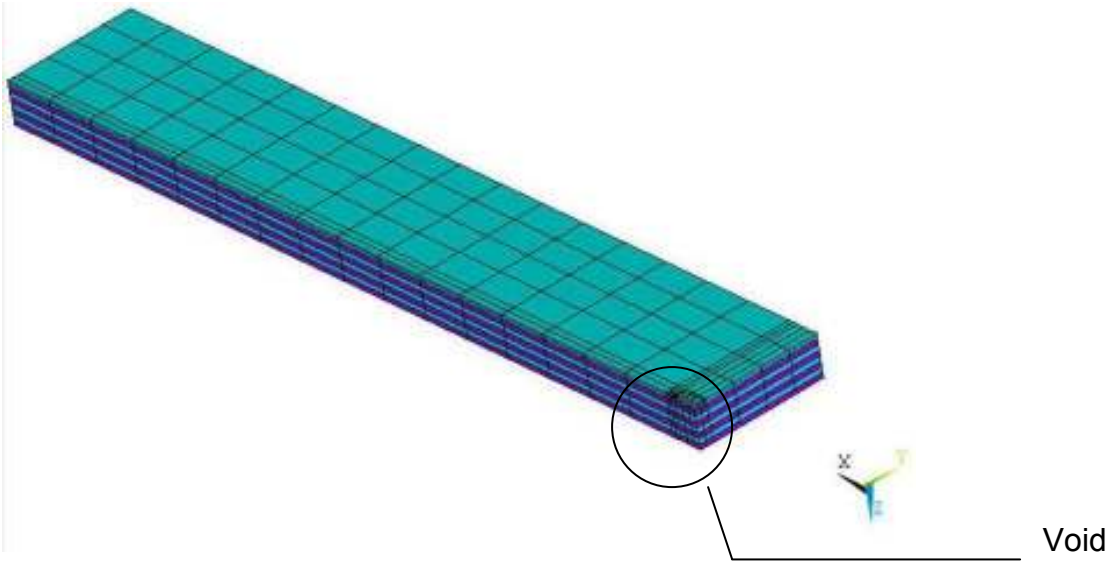

Fig. 3.1. FEA specimen simulation

The measures that define the complete specimen can be obtained by extrapolating this model to the complete eight layered model.

Length (x) = 79.5 mm
Width (y) = 12.7 mm
Thickness (z) = 0.250*8 mm
Ply thickness = 0.250

This measures where chosen in order to refer to the tests specimens, although the goal of the FE analysis was to determinate its qualitative behaviour rather than to obtain an accurate quantitative response.

The void was applied in the middle of the geometry *Fig.3.1*. In both possible orientation cases, the void was defined by two ellipses (longitudinal section and cross-section Fig. 3.2. in order to get a more accurate geometry to the voids formed during autoclave process [11], as stated in the theoretical part of this Project. *Fig. 2.14*

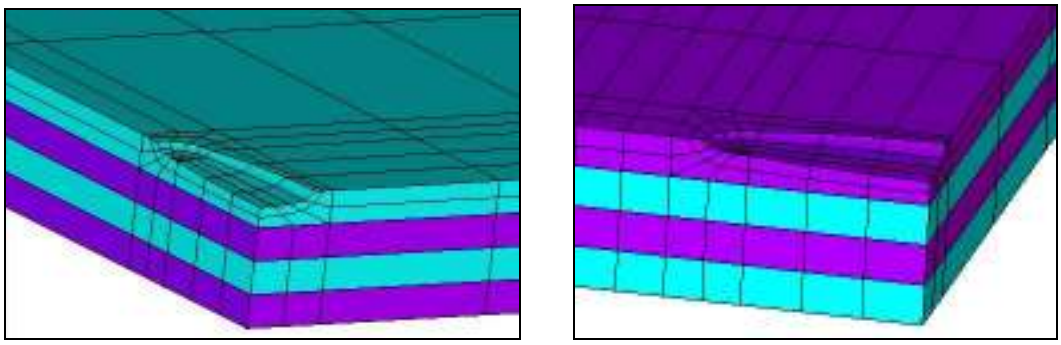

Fig. 3.2 Void detail in 0º and 90º respectively

In both void cases, the long axial direction of the longitudinal section was aligned with the fibre direction of the surrounding composite material.
Void measures were chosen in order to represent a big critical defect:

Length (x) = 3.0 mm
Width (y) = 1.0 mm
Height (z) = 0.2 mm

A two-phase approach was made embedding voids in a homogenized composite material because voids and fibres present different shapes and geometric scales and because modelling fibres as an inclusion phase required micromechanics models, which might bring in unnecessary error. Although it is not the case, a more accurated model could have been created by applying a third phase of resin rich area at the ends of the void.

The cross ply lay up had a total of 8 layers, each one of them with a thickness of 0,250mm.
The lay up was designed in two different formats so that the analysis could be made for two different void alignments within the composite.
In order to interpret the figures it must be noted that 90º layers are represented in purple colour, while 0º layers are those represented in green colour.
In both void orientation models, border assumptions were established in order to create a symmetric laminate.

On the one hand, $[90,0]_{2,\ S}$ lay up was modelled in order to locate the void oriented along the 0º in the inner layers. *Fig 3.3*

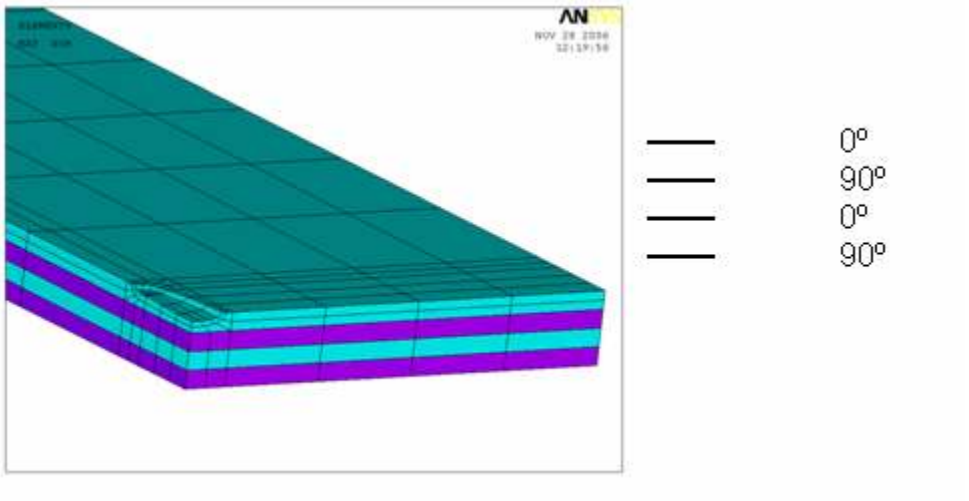

Fig.3.3. Model $[90,0]_{2,\ S}$ for 0º void.

On the other hand, $[0,90]_{2,\ S}$ lay up was modelled so that the void could be oriented along the 90º layers located in the middle of the specimen. *Fig. 3.4*.

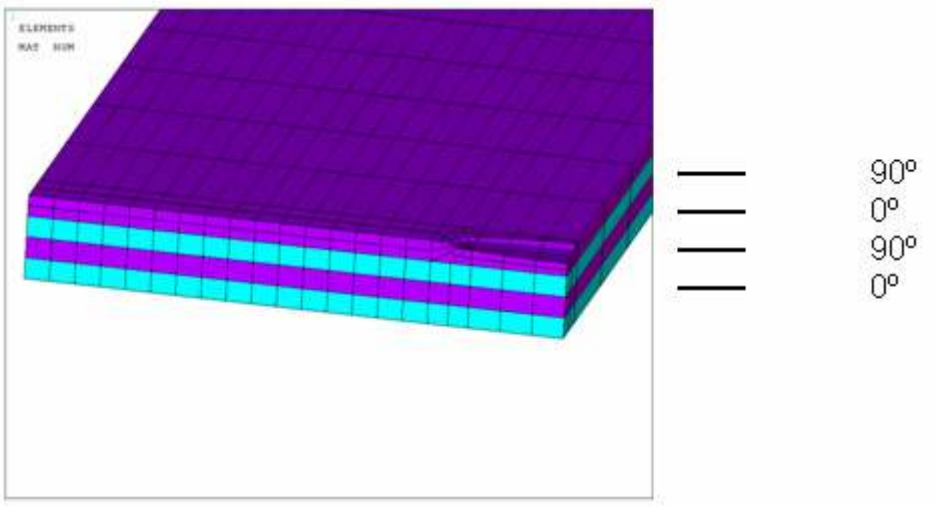

Fig.3.4 Model $[0,90]_{2,\ S}$ for 90º void.

3.3 Material Properties

Because of the orthotropic nature of the model, nine material constants where defined in order to describe the stiffness tensor of the specimen. The homogenized composite material properties where defined for both possible layer orientation as stated in *Table 3.1*

	0° Direction	90° direction
E_1	172000	8500
E_2	8500	172000
E_3	8500	8500
ν_{12}	0,25	0,0128
ν_{23}	0,0128	0,2525
ν_{13}	0,4	0,4
G_{12}	3500	3500
G_{23}	3000	3000
G_{13}	3000	3000

Table 3.1. Defined material properties for FE Analysis. [19], [20]

Where E in MPa refers to the elastic modulus in each axis, ν refers to the Poisson's ratio per each axial plane and G in MPa refers to the shear modulus per each axial plane as well.

These values were used based on datasheet for Matrix 977-2 and Fibre IMS Toho Tenax.

Although the decay of Poisson's ratio due to the effect of voids has been investigated [16] it was not contemplated for this study.

3.4 Element type

The element used was SOLID 95, already defined in *Ansys*, which is a 3D, 20-node structural solid. Fig. 3.5. This element was chosen because an accurate mesh around the void and its surroundings was needed. Its tolerance to irregular shapes without as much loss of accuracy as well as its well suitness to model curved boundaries, were the main reasons that justified its election. [21]

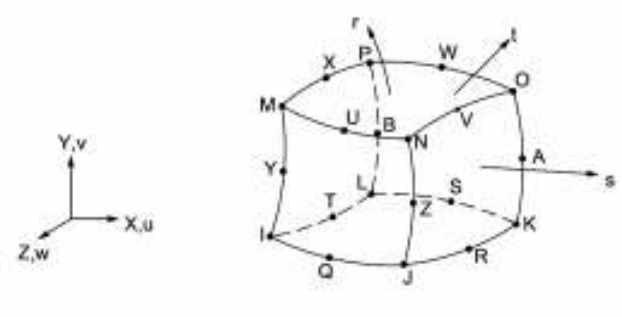

Fig. 3.5. Used element type Solid 95 [21]

3.5 Meshing

A total of 1174 elements were used in the modelling. The mesh was carefully refined around the void zone in order to get there an accurate appraisal from the response of the material and in order to have a smooth adaptation to the curved shape. *Fig 3.2.*

For the whole model, the mesh was defined and applied as shown in *Figure. 3.6*

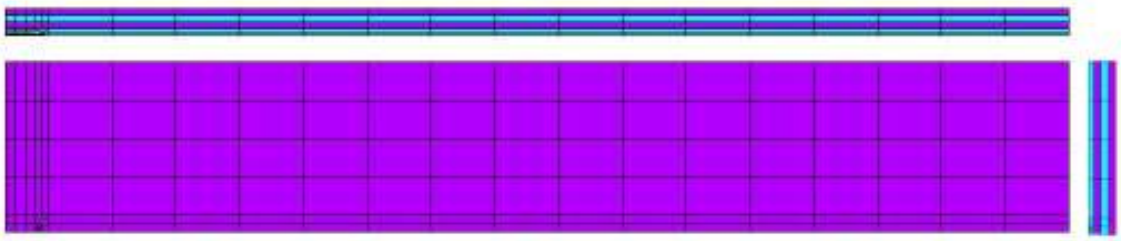

Fig. 3.6. Top, front and side view of the specimen

3.6 Loading and Boundary Conditions

First of all, an explanation in model geometry has to be done so that all the mentioned load or boundary conditions can be precisely identified by the reader. *Fig. 3.7*

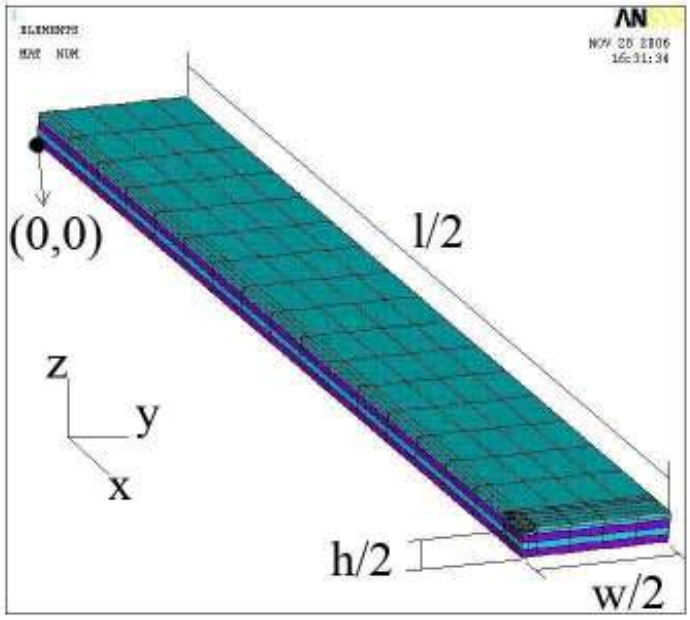

Fig. 3.7. Specimen measurements

The axial load was modelled by applying a constant displacement on the boundary surface along x direction defined per:

$$u(0, y, z) = -ctt \tag{3.1}$$

In this case a strain of 1% was applied instead of a force in order to avoid undesired deformations.

This strain is equivalent to an applied force that can be related by the following equations.

$$E = \frac{\sigma}{\varepsilon}\ ;\ \sigma = \frac{F}{A} \tag{3.2}$$

As it is a symmetric laminate:

$$E = \frac{E_{0^\circ} + E_{90^\circ}}{2} \tag{3.3}$$

Finally an expression of the applied force depending on the area of the specimen is obtained.

$$F = (\frac{E_{0^\circ} + E_{90^\circ}}{2})\varepsilon A \tag{3.4}$$

3.7 Boundary Conditions

Because of the geometric symmetry, displacements in the model will be also symmetric with respect to the symmetry planes x=l/2, y=0 and z=0.
Due to this fact, on the symmetry planes the displacements were defined as zero by applying the boundary conditions to both kinds of void models as defined next.

$$u(\frac{l}{2}, y, z) = 0 \tag{3.5}$$

$$v(x,0,z) = 0 \tag{3.6}$$

$$w(x, y,0) = 0 \tag{3.7}$$

The applied boundary conditions are graphically presented in the following figure. *Fig. 3.8.*

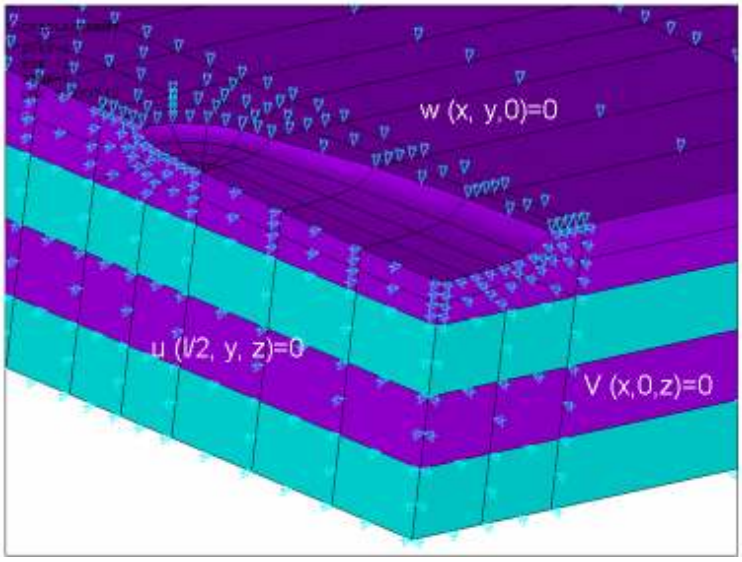

Fig. 3.8. Boundary conditions

3.8 Coupon Testing

3.8.1 Specimen description

The test coupons were designed mainly according to the pattern defined in ASTM D 3039 with the following measures: 250 mm. long and about 2.5 mm thick.
However, a width of 15mm was chosen as done in the study performed by M.C. Lafarie-Frenot & Hénaff-Gardin, were they studied the formation and growth of 90º ply fatigue cracks in carbon/epoxy laminates. [8]

Furthermore, glass/epoxy end tabs, 50mm long, were used for gripping in the tensile machine. They were placed in the machine by the use of two grips that applied sufficient lateral pressure to prevent slippage between the grip face and the coupon.

Coupons were labelled so that they were easy to distinct from each other and traceable back to the raw material.
The nomenclature used was as follows in *Fig. 3.9*.

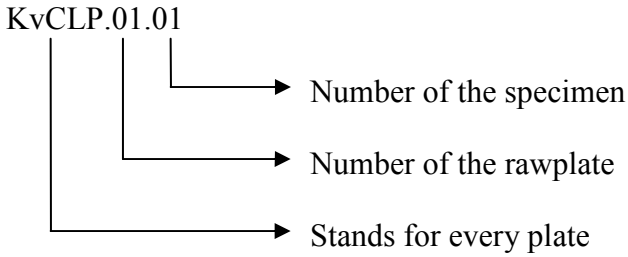

In order to identify the kind of void that had been produced in every specimen, the following nomenclature was chosen:

- Vv: Void aligned within the specimen in the 0º direction
- Hv: Void aligned within the specimen in the 90º direction

Fig. 3.9. Picture of a 0º voided specimen where the nomenclature is noted

3.9 Specimen preparation

3.9.1 Material

The specimens were made of prepreg, composite industry's term for continuous fibre reinforcement pre-impregnated with a polymer fibre sheet. The polymer can be partially cured.
This prepreg was constituted by *IMS 5131* (Intermediate Modulus) fibres, comercialized by *Toho Tenax* and a *977-2* matrix, supplied by *Cycom*.

Tenax IMS carbon fibres are tailored to suit applications where strength and stiffness are a priority, fulfilling high mechanical requirements. This fibre presents a high strength and a high modulus, as well as low density, low creep rate and low fatigue.
Some characteristic values were obtained from the product data sheet and are listed in the *Table 3.2. [20]*

	Tenax IMS 5131
Number of filaments	12000
Filament diameter (µm)	5
Density (g/cm3)	1,8
Tensile strength (Mpa)	5600
Tensile modulus (Gpa)	290
Elongation at Break (%)	1,9

Table 3.2- Material data of the fibre [20]

Moreover, Cycom 977-2 is a 177 ºC curing epoxy resin specially designed for autoclave or press molding.
Its characteristic values were obtained too from the product data sheet [18] and listed in the following *Table 3.3.*

	Cycom 977-2
Density (g/cm3)	1,31
Tensile strength (Mpa)	81,4
Tensile modulus (Gpa)	3,52
Flexural Strenght (Mpa)	197
Flexural Modulus (Gpa)	3,45

Table 3.3. Material data of the Matrix [19]

3.9.2 Prepreg Lay-up

The specimens were obtained from laminates manufactured by use of the Prepreg moulding technique.
In this art of manufacturing, fibres are pre-impregnated by the material manufacturer, under heat and pressure or with solvent, with a pre-catalysed resin. This resin is near-solid at ambient temperatures, and so the pre-impregnated materials (prepregs) have a light sticky feel. The prepregs were laid up by hand, vacuum bagged and then heated under a certain pressure in an autoclave.

Four composite laminates were manufactured each of them formed by ten bonded individual laminas (or plies). These laminas were all obtained from the same unidirectional carbon fibre roll detailed previously.
The plies were cut in an area of 300*300mm (they were already 250µm thick), so that the resultant laminates measured 300*300*2,5mm.

Two different stacking sequences were manufactured in order to adjust the orientation of the inner plies to the desired orientation of the applied voids.

In both cases the resultant laminate was created with a cross ply stacking sequence.

Detailed view on stacking sequence for composite laminate containing voids oriented in the 0° direction. *Fig. 3.10.a*

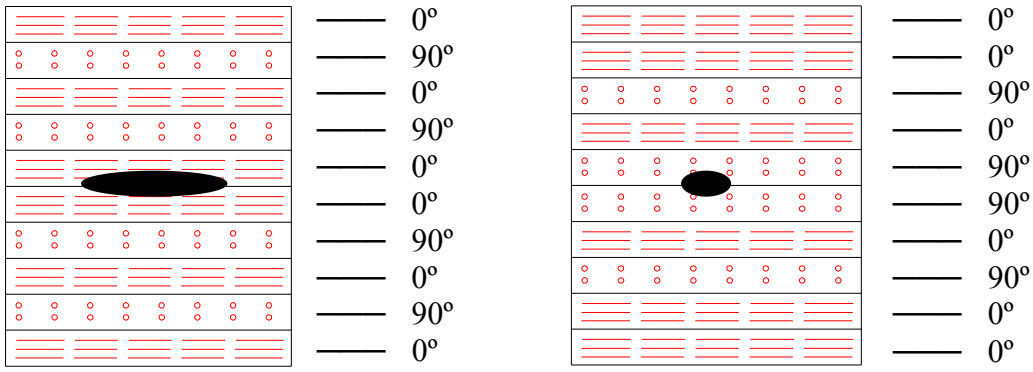

a) *b)*

Fig. 3.10. a) Lay up for voids in 0º, b) Lay up for voids in 90º

On the other hand, detailed view on stacking sequence for composite laminate containing voids oriented in the 90° direction. *Fig. 3.10.b.*

Composite prepreg used *977-2-35 24k IMS 268 presented a 65% in content of fibres.* It's tensile strength was ranged between 2400 and 3100 MPa, and it's tensile modulus between 155 and 185 GPa. [22]

Improper fibre alignment could be critical, so that it affects the composite properties and therefore induce an increase in the variation of the results.

To avoid this effect, a cutting pattern was always used as shown in *Figure 3.11*.

Fig. 3.11. Cutting pattern and roller used for proper stacking

During lay-up, in order to achieve a proper consolidation of the layers and to remove non-desired voids, every layer was rolled while applying pressure with the roller showed in *Figure 3.11.*

Moreover, always after bonding 5 layers the resultant part was vacuum bagged as an extra measure to avoid non-desired voids while bonding the layers, as shown in *Figure 3.12.*

Fig. 3.12. Vacuum bagging for the degassing of laminated plies.

Next, two packs of 5 layers were vacuum bagged together, with a separation foil in between that contained some metal cylindered wires with a length of 5mm.
The separation foil helped not to bond the two layered plates together and the small metal cylinders in between were used to induce some cavities where the blow agent would be applied afterwards.
The metal cylinders (especially in horizontal voids) where carefully placed in order not to induce a void linear propagation along the plate as the aim of the manufacture was to obtain discrete voids in each specimen. The cavities were produced as shown in *Figure 3.13.*

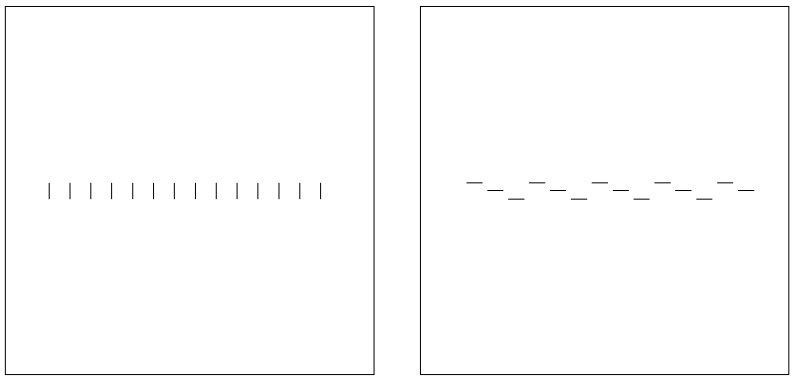

Fig. 3.13. Vertical and horizontal void location in plates.

Once the cavities where formed the blow agent was carefully applied with a powder doser so that the amount of blow agent was constant in each specimen. Despite this careful homogenization of the dose it resulted difficult to obtain constant measures in the voids.
Radiographies of the voids within the laminates are presented in *Annex 1*

The blow agent used was sodium bicarbonate, a crystalline solid which looks as fine powder. Fig. 3.14.

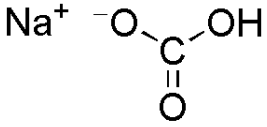

Fig. 3.14 $NaHCO_3$ structure

This agent reacts because of the heat added during the curing cycle in autoclave as shown in the following equation.

$$2NaHCO3 \rightarrow Na_2CO_3 + H2O + CO2 \qquad (3.8)$$

Finally the parts were bonded and vacuum bagged with the blow agent inside obtaining the final plate that would be cured in the next step.

3.9.3 Curing

In order to completely solidify the composite plate, a curing process was designed so that the epoxy (thermosetting material) was transformed from liquid to solid, obtaining in this procedure its final characteristics

This curing process was done in a laboratory autoclave of *Scholz Maschinenbau*, which consists of a large pressure vessel equipped with a temperature and pressure control system. *Fig. 3.15*

Fig. 3.15 Pressure vessel of the autoclave

The purpose of applying heat was to induce the formation of gel, a three-dimensional molecular network, by a chemical reaction that would get solidified

afterwards. This chemical reaction is highly exothermic. On the other side, pressure helped to consolidate the plies and squeeze out the excess of resin while this is liquid. [23]

The curing cycle is shown in *Figure 3.16*

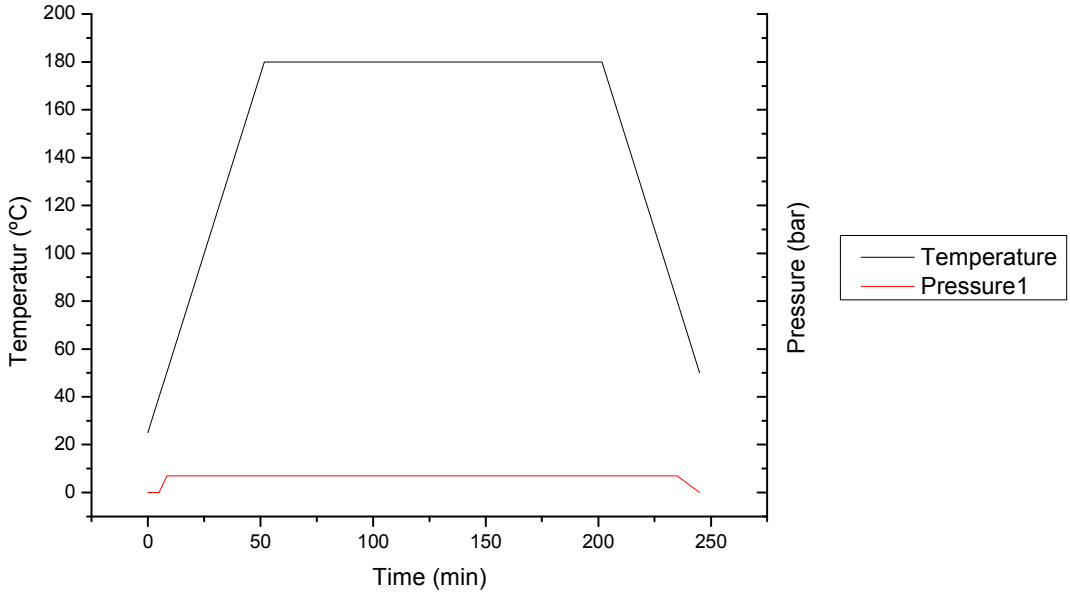

Figure 3.16. Cycle behaviour in autoclave

In order to cure the prepregs inside the autoclave a special certain vacuum bag lay up sequence was build as showed in *Figure 3.17*. The whole package was built on an aluminium plate doted with vacuum connections. Before starting the manufacture of the package, the plate had to be carefully cleaned with acetone, so that no rests of previous uses could affect the smoothness of the resultant plate. First of all, a sheet of release film was stacked on the aluminium plate so that the rest of the lay up was easily removable after the curing process.

Then, the prepreg stack was covered by two Teflon sheets, paying special attention that no wrinkles or raised regions remained because these sheets give to the carbon fibre plate its final required surface finish.

Next, a strip of adhesive cork was placed along the edge of the panel. By this action, a protection was applied around the laminate in order to fix its displacement on the aluminium plate and to minimize the resin flow through the edges of the laminate.

All around this cork, a metal grid strip was placed paying special attention in the fact that it had to lay on the vacuum connections. The purpose of this metal grid was to distribute the vacuum equally over the aluminium plate

After this, the bagging adhesive was applied at the borders of the aluminium plate making sure that it encircled all the previously mentioned components.

One more release ply was laid over all the previous components except from the bagging adhesive.

Finally, the vacumm bagging film was applied over the entire plate and sealed over the bagging adhesive.

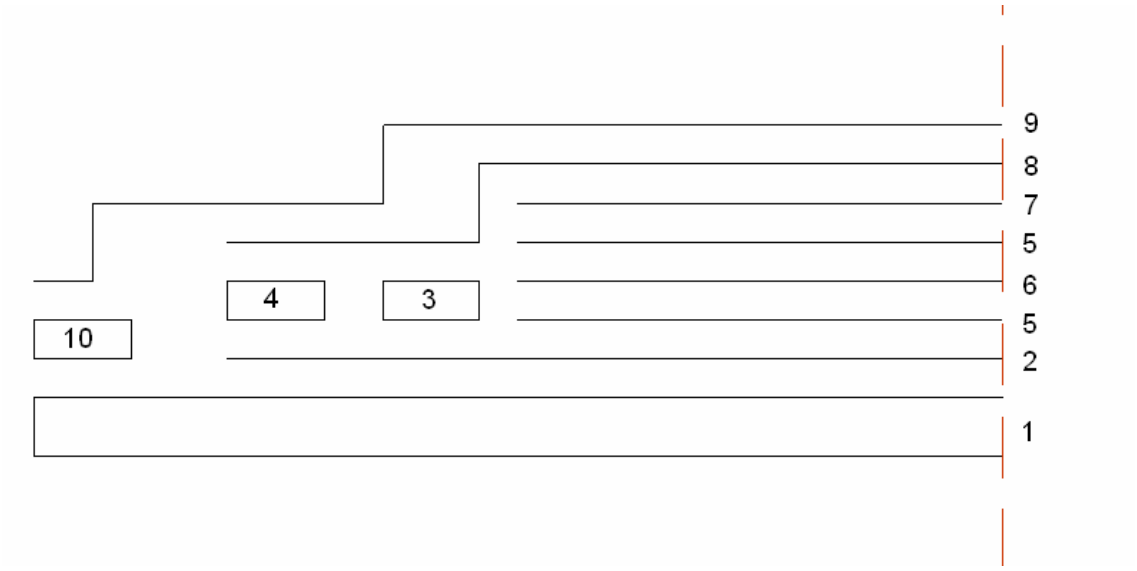

Figure 3.17. Vacuum bag lay up sequence

Where,

1. Aluminium plate
2. Release foil
3. Cork
4. Aluminium grid
5. Teflon sheet
6. Carbon fibre plate
7. Pressure aluminium plate
8. Release Ply
9. Vacumm bag
10. Adhesive

This vacuum bag lay up was applied on an aluminium plate that would be placed in the bed detailed in *Figure 3.18*, specially adapted to cure three vacuum bags at once inside the autoclave.

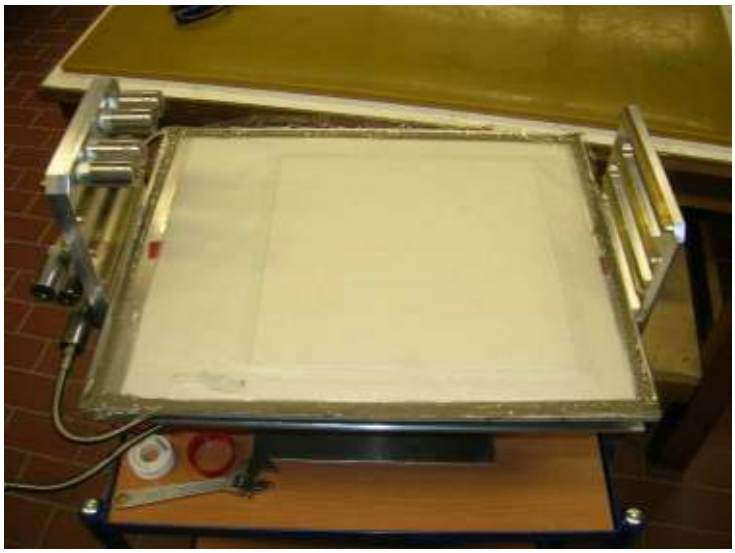

Fig. 3.18. Detail of vacuum bag placed in autoclave bed

As a preventive measure, before running the autoclave process, a vacuum test was performed in order to probe that it contained no leads.

3.9.4 Tabs

Tabs are not always required in tests; it is a fact that they are firmly recommended while testing strongly unidirectional dominated laminates. [24]
Therefore, they where used in order to assure that acceptable failure modes occur with reasonable frequency in the specimens.
The main purpose in the selection of using tabs was to assure a successful introduction of load into the specimen and to prevent a premature failure due to significant discontinuity.
The material used was glass fibre-reinforced with a lay up of ±45°. These were applied at 45° to the loading direction to provide a soft interface.
The tabs were applied in the specimens as shown in the *Figure 3.19*

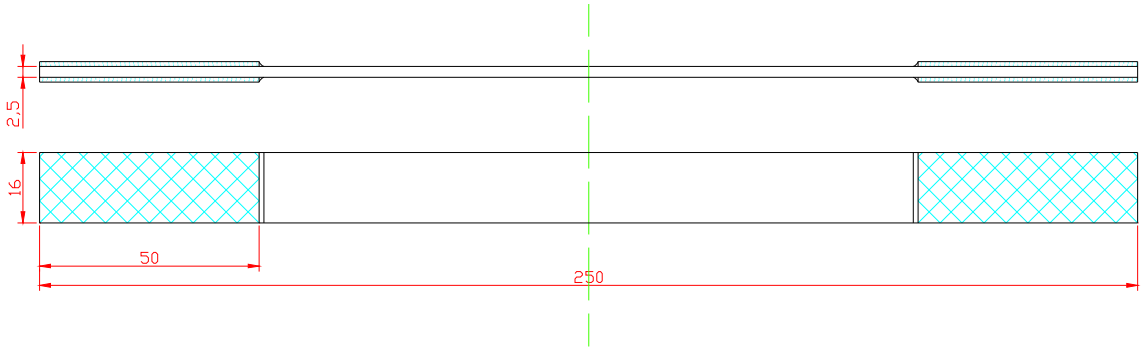

Fig. 3.19. Detailed tabs with fibre orientation

A high-elongation adhesive system *UHU plus endfest 300* was used when bonding tabs to the material under test. This adhesive is a solvent-free two component adhesive on an epoxy resin base. A particularly high bonding strength of 2000 N/cm2 was obtained by hardening in an oven at 70° during 45 minutes as indicated by the adhesive producer.

A uniform bond line of minimum thickness was desired in order to reduce undesirable stresses in the assembly.

3.9.5 Cutting, grinding and measuring

In order to get the final specimens, composites plates were cut to the measures detailed in *Figure 3.20*.The specimens were cut with a *Mutronic Diadisc 4500* industrial saw machine equipped with a diamond tooling blade.

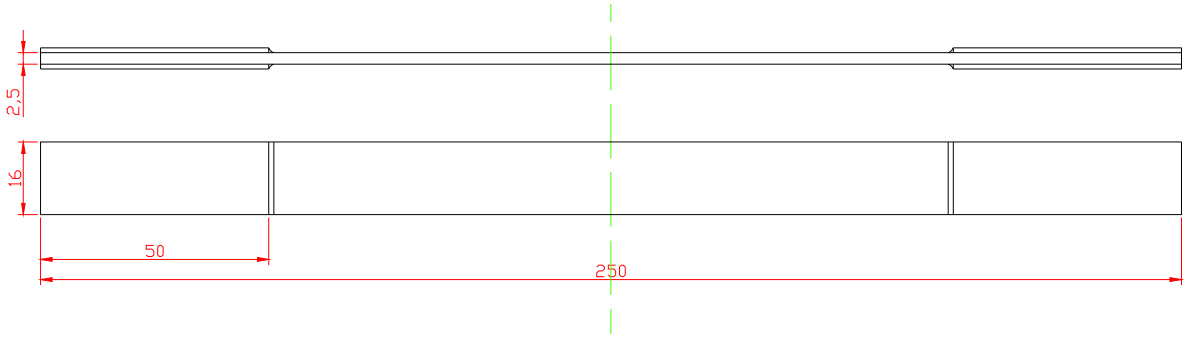

Fig. 3.20. Specimen geometry of coupons used in quasi tension test of cross ply laminates.

As edges flat and parallel were hardly desired, all the specimens were grinded afterwards. Thus, final dimensions were obtained by 320 and 800 water-lubricated grinding paper. Polishing the edges of the specimen is important because it has been proven, in the study made by Clements and Lee [25], that this action increases the strength of the specimens by a factor 15% to 25%.

Before testing all specimens were measured in thickness with a micrometer and in width with a cantilever. As a reference, final dimensions obtained after this procedure are detailed in *Annex 2*

3.10 Tensile test

In order to characterize the material response, several tensile tests were made in the *Miele Zwick 1474* machine, so that data on the material behaviour could be obtained.

Before running the test, the specimens were mounted in the grips of the testing machine taking special care to place them so that the longitudinal axis of the specimen was coincident to the direction of the load applied by the grips. It is proved that poor system alignment can cause premature failure of the specimen because of inducing undesired bending. The grips were fixed strongly enough to assure that no slippage between grips and tabs was possible.

First of all, non-voided specimens were tensile tested so that a reference was obtained for further tests with voided specimens. This test was done by applying quasi-static a load while measuring the strain of the specimen with a strain indicating device mounted at the machine. Further material responses were automatically recorded by test machine software, such as, ultimate tensile strain and tensile modulus of elasticity.

The stress-strain behaviour was monitored and recorded during the test, as well as the ultimate strength of the material, determined from the maximum load carried before failure.

3.10.1 Step wise tensile test

For the voided specimens, a stepwise test method was required in order to be able to study the damage propagation after each step.

The same procedure as for the reference test was followed, although the test was stopped at each load step in order to examine by X-Ray the inner defects of the specimen.

For each load step, the test was stopped as well, short before reaching the desired load in order to apply the penetrant as specified before in this section.

An example of the step wise tensile test followed for a certain specimen is shown in *Figure 3.21.*

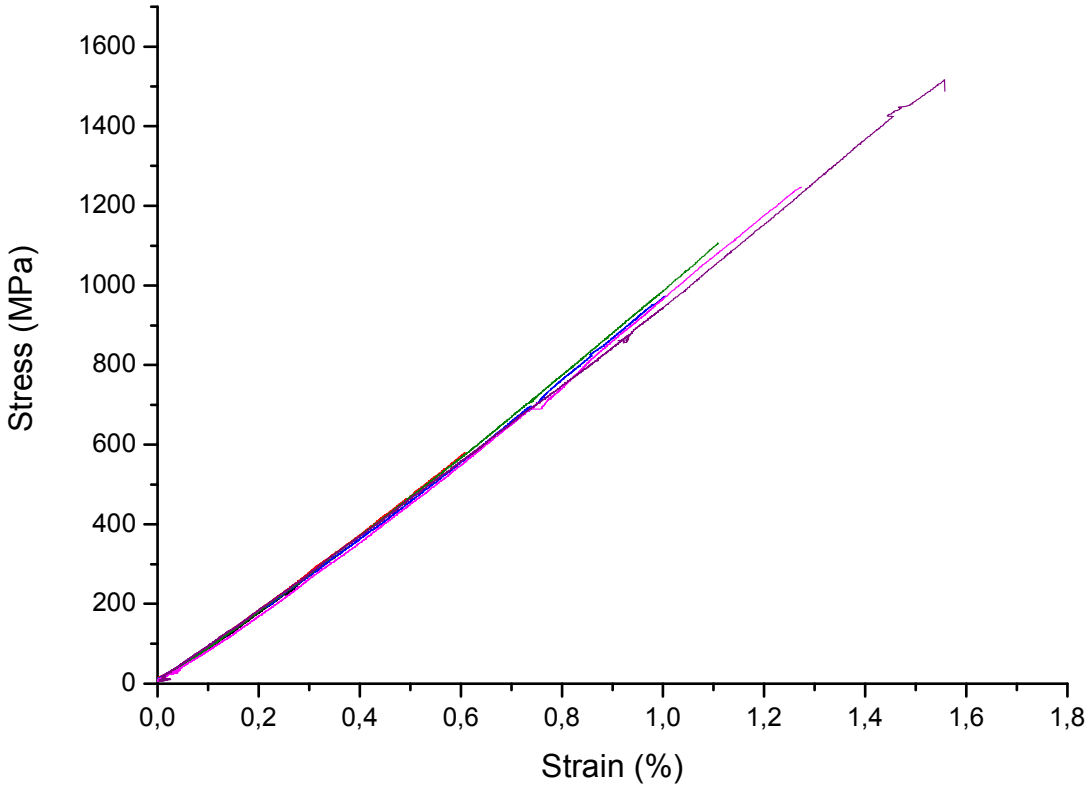

Figure *3.21. Step wise tensile test for a [0,90,0,90,0]$_2$ carbon fibre specimen*

3.11 Detection of damage in composite materials

When using composite materials, many different material properties have to be examined because of their heterogeneous behaviour.
In order to complement the general material properties, detailed information on the microscopic level is sometimes desired.

Non-destructive testing (NDT) techniques are used so that an inner characterization of the composite becomes possible.
Although visual inspection of the specimen is the simplest NDT, further techniques are required in order to detect and examine defects such as, matrix cracks, fibre breakage, debonding and delaminations.

Most NDT of composites are conducted by use of X-radiography or ultrasonic C-scan.
Ultrasonic C-scan is a valuable technique when the goal of the measure is to determine the void content (porosity) of a certain composite [25]. But due to the nature of voids induced in the specimens (discrete long voids) the use of X-radiography was needed for this work.
Nevertheless, as stated by Prakash, phenomena such as fibre debonding and interlaminar debonding are generally hard to detect with this technique. [27]

3.11.1 Radiography

The specimens where X-rayed in a *Hewlett Packard Cabinet X-Ray system Taxitron Series* after each load step in order to study the damage induced and its development.

First of all, it has to be noted that composite materials components present low density (low atomic number) and very small defects.

This two facts cause that the energy of the radiation used during the X-ray process has to be reduced in order to get an appropriate contrast.
Hence, a compromise had to be done concerning the test voltage and the exposure time. [28]
This compromise was achieved by referring to the following *Figure 3.22*.

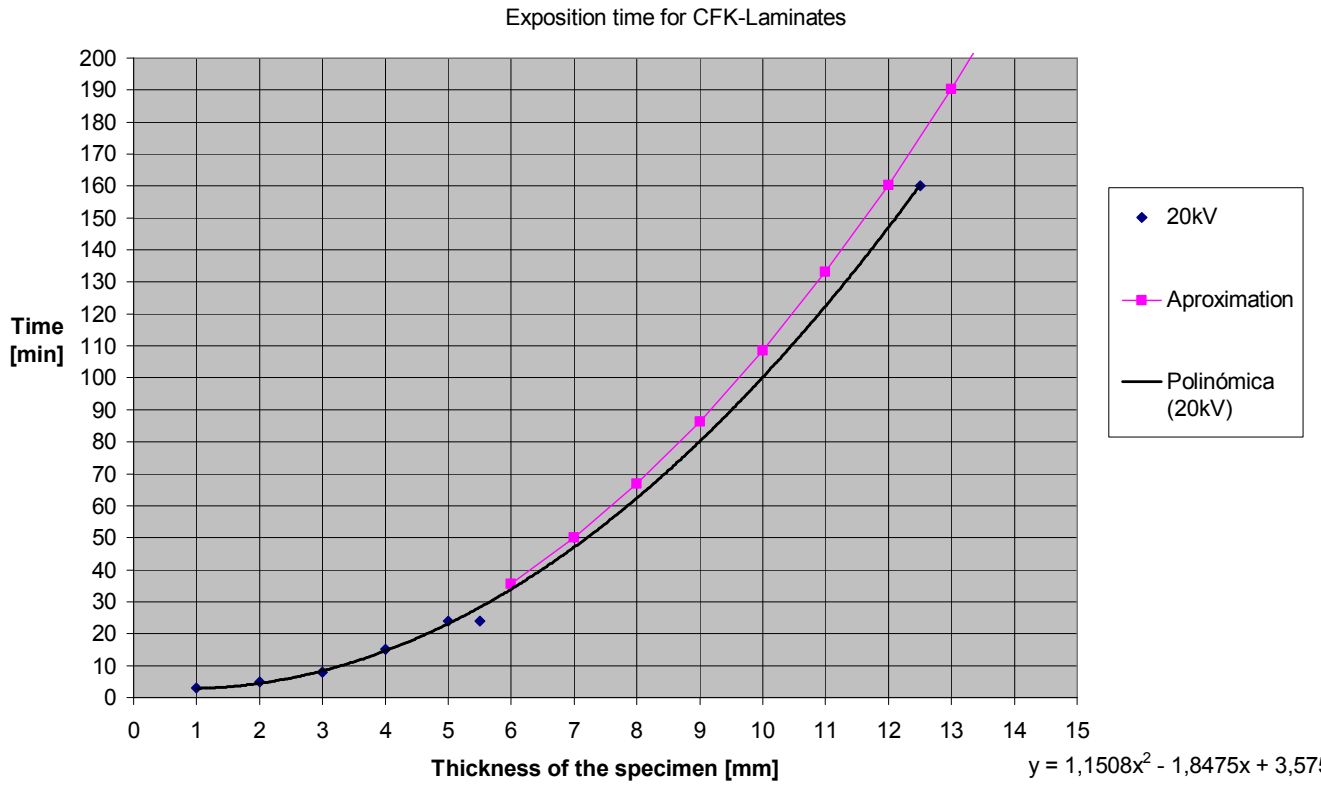

Figure 3.22. Exposure time for CFK-Laminate depending on its thickness.

The applied voltage of 20kN was chosen in order to receive long wavelength of the X-rays. [29]
As the average width of the specimens was of 2.5mm, an exposure time of 6 minutes was set.

3.11.2 Developing

The film used for these radiographies was X-Ray Film: *Structurix D2 FW*
All films obtained from the X-Ray method were manually developed.

This process began by sinking the film in a developing liquid while shaking it regularly, then the film was introduced in a recipient with fixing liquid for another five minutes. Finally, after rinsing out the fixing liquid with flowing water for a minute the film was dried in an oven for ten minutes.

3.11.3 The penetrant

Large cracks and material properties can easily be observed by the use of low-voltage X-ray, but if small matrix cracks should be detected too, then the use of an X-Ray opaque penetrant becomes compulsory.

Following some authors recommendation [6][29], Zinc Iodide penetrant, doted with high opacity, was prepared and used. This solution consists of:

- 60g of Zinc iodide
- 10ml of H_2O
- 10ml of isopropyl alcohol
- 10ml of “Agfa Agepon” or “Kodak photo-Flo 200”

The main advantage of using this penetrant is that it is not toxic in contrast with the other possible options.
Nevertheless, this penetrant presents the inconvenient that cannot be removed from the specimen once applied. This could induce additional damage during the following tests of a same specimen in the step wise test.

3.11.4 The penetration method

Specimens can be penetrated mainly by two different methods:

- Submersion penetration
- Edge penetration

Due to the relatively large size of the specimens the selected method was edge penetration.

During the test, the raising tension was maintained at a certain value (normally 30KN) in order to apply the penetrant with a pipette. *Fig.3.23.*

The reason for pre-tensing the specimen before applying the penetrant was to facilitate the introduction of the liquid through the already created cracks.

Fig.3.23.Edge penetration method

The surfaces of the specimens had to be carefully cleaned after each load step was done so that the X-ray image obtained was not distorted.

3.11.5 Image analyze

In order to obtain and analyze the result, all radiographies were digitalized by scanning and, afterwards, classified by specimen and applied load. *Annex 3*

After scanning it was necessary to use the image processing software *Image J* so that the radiographies could precisely be analyzed. [30] [31] *Fig.3.24.*

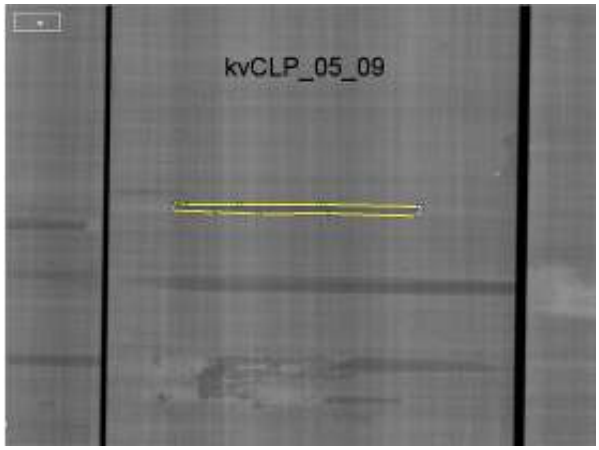

Fig.3.24 Example of void area calculation with Image J

By using this software each void area and length were calculated.
These measures were obtained by referring the area selected to the width of each specimen, used as a reference.

With this data, further graphics, shown in the results section of this project, were created.
When studying the crack growth behaviour, a distinction had to be done in the behaviour of two different zones within the 0º voided specimens as can be seen in *Figure 3.25.*

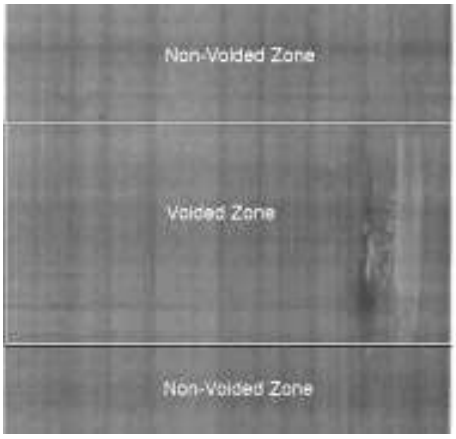

Figure 3.25. Definition of non-voided zone and voided zone in 0º voided specimens.

4. RESULTS

Obtained results are presented for both studies carried out during the work done for this project: FEA and experimental results.
The behaviour of the material under stress is characterised in this chapter. In both cases a distinction is done between voids located along the 0º direction and the 90º direction in cross-ply laminates

4.1 FEA results

As stated before, the results of the FEA were obtained with the visualization module. In order to study the response of the model, different properties were captured from obtained results.
For both typologies of voided plates designed properties such as applied deformation, stress distribution along the X, Y and Z axis and Von Misses stress distribution in XY, YZ and XZ were noted.

4.1.1 Results obtained for 0º void model

First of all, the results for the model where the void was applied along the 0º direction are presented.

As mentioned in the experimental part, a strain of 1% was applied in X direction obtaining the resultant strain distribution showed in *Figure 4.1*

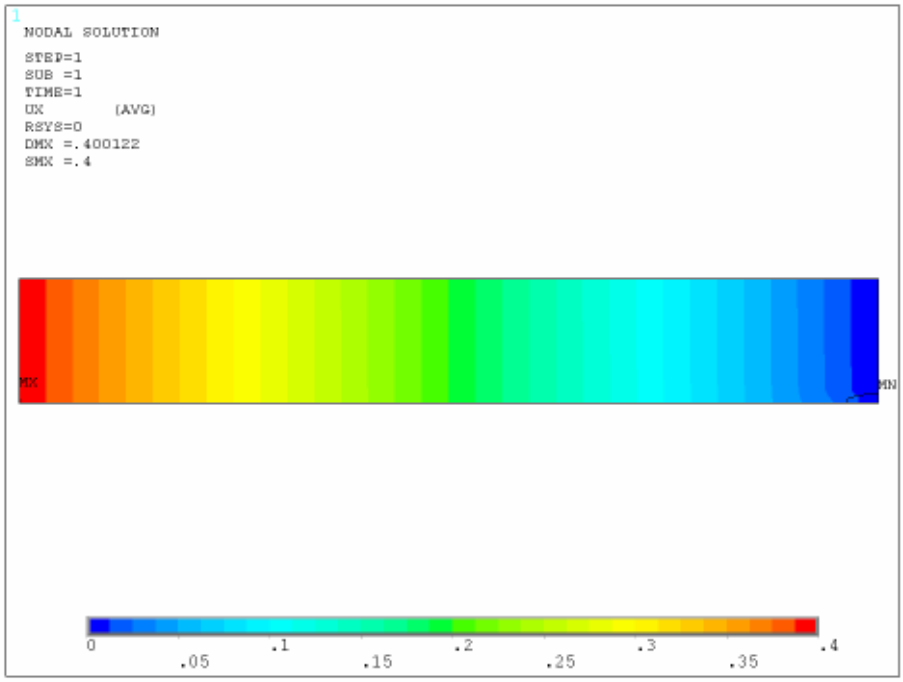

Fig. 4.1 Displacement range in 0º voided specimens with a strain of 1%

The stress distributions were studied for axis defined as follows:

X – parallel to the 0º fibre direction and to the major length of the void.
Y – parallel to the 90º fibre direction and perpendicular to the major length of the void.
Z – along the thickness direction

Stress distributions in these directions are presented in *Figures 4.2, 4.3 and 4.4.*

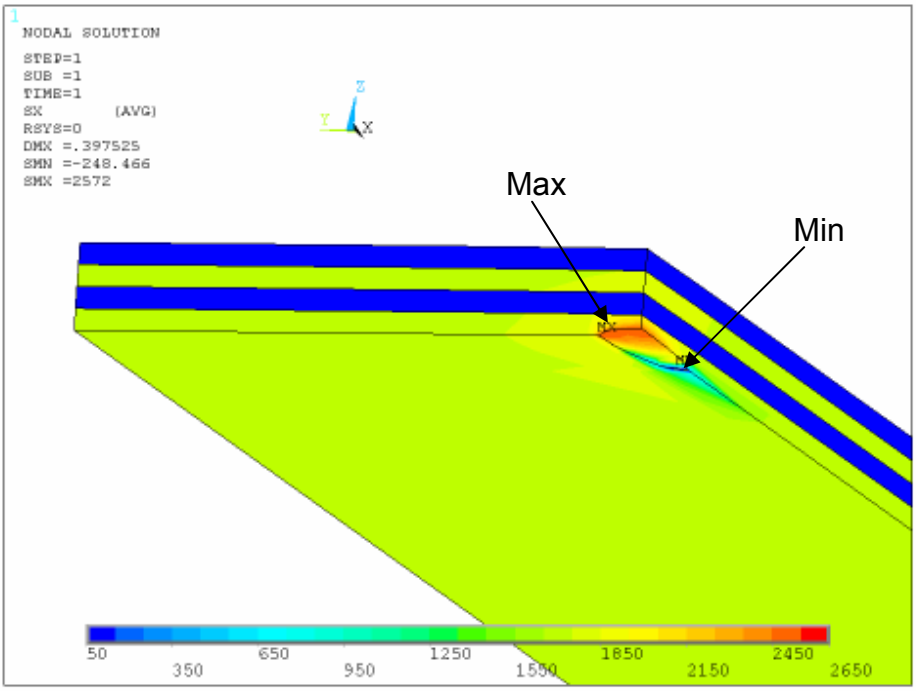

Fig. 4.2 Stress distribution in X direction for the 0º voided model

In figure 4.2 stress in X-direction is shown. Peak stresses can be recognized at the red zone pointed as Max. The stress there (2450) is about double than in the rest of the layer (1250).

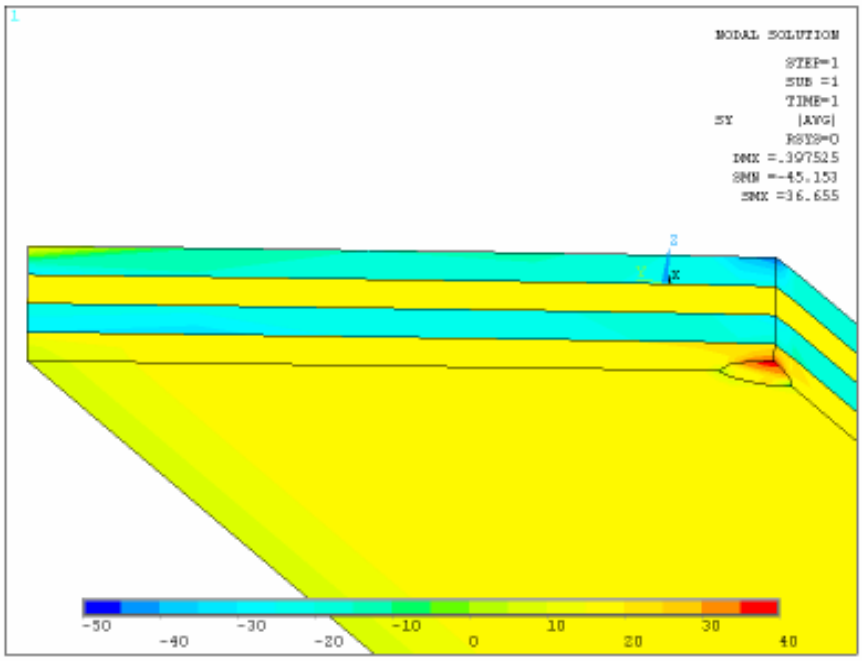

a)

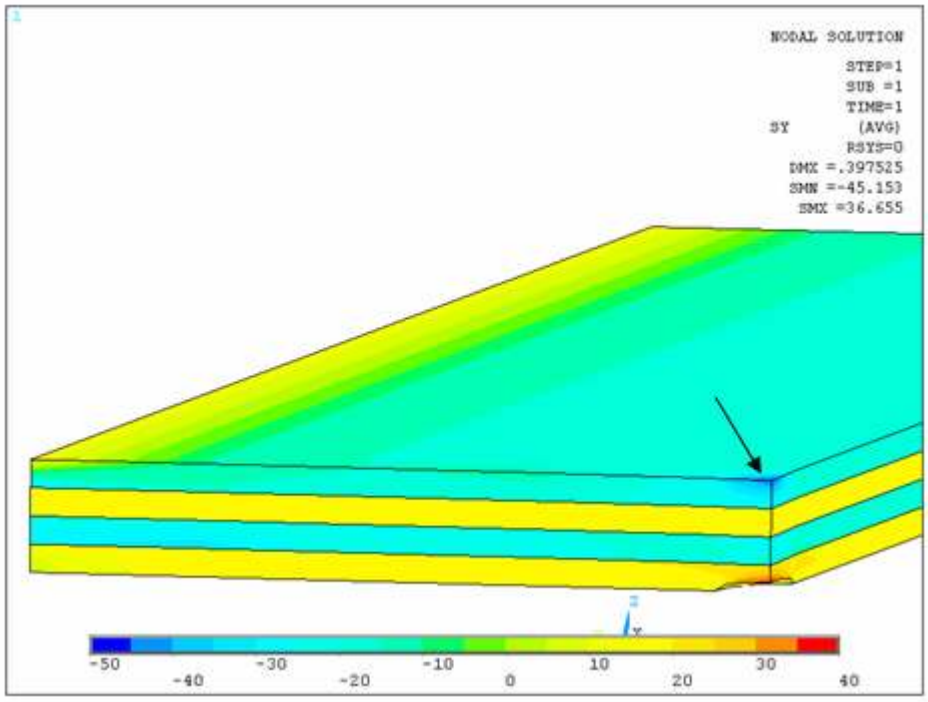

b)

Fig. 4.3b Stress distribution in Y direction for the 0º void model

Figure 4.3 shows lower stresses in 90º direction than in 0º direction. A peak stress point (-45MPa) can be located in *Figure 4.3b* in the middle of the outer 90º layer.

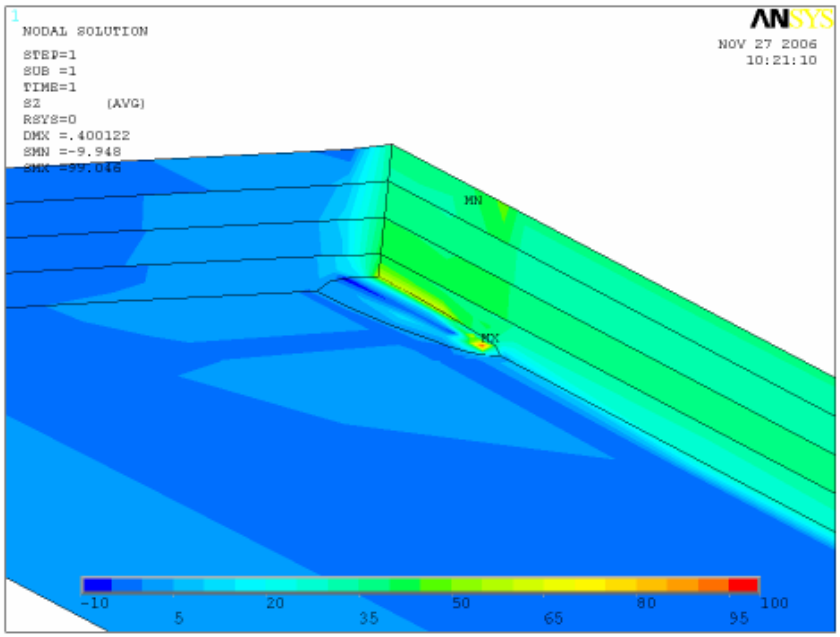

Fig. 4.4 Stress distribution in Z direction for the 0º voided model

Von Misses distribution can be seen in the following *Figures 4.5, 4.6, 4.7 and 4.8.*

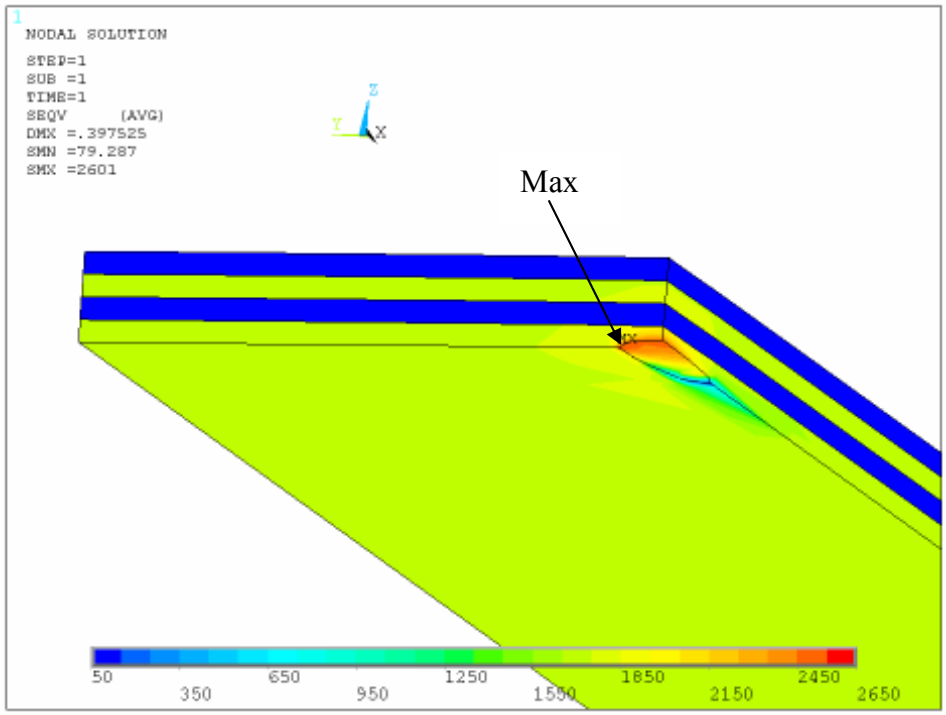

Fig. 4.5 Von Misses distribution for the 0° voided model.

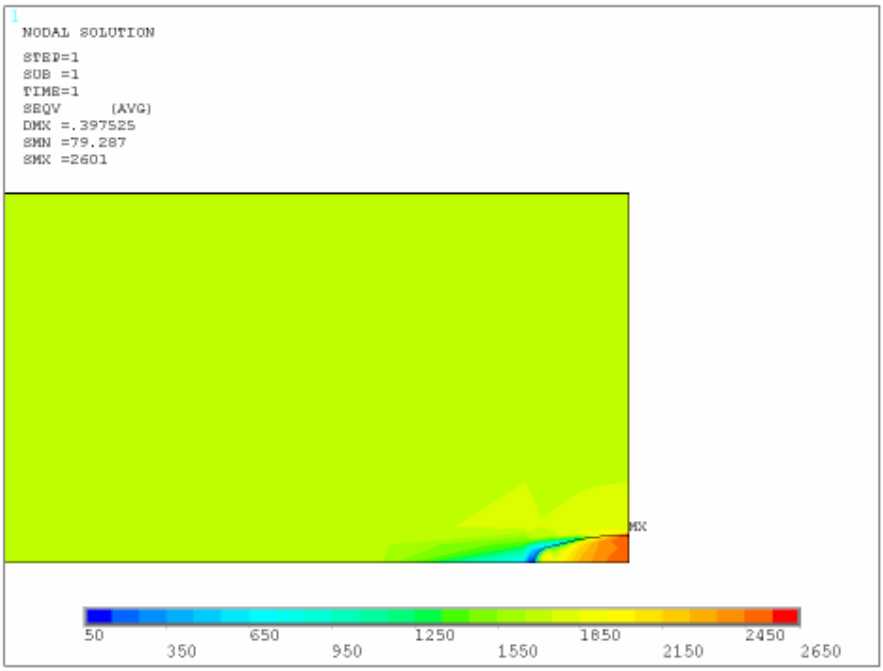

Fig. 4.6 Von Misses distribution in XY plane for the 0° voided model

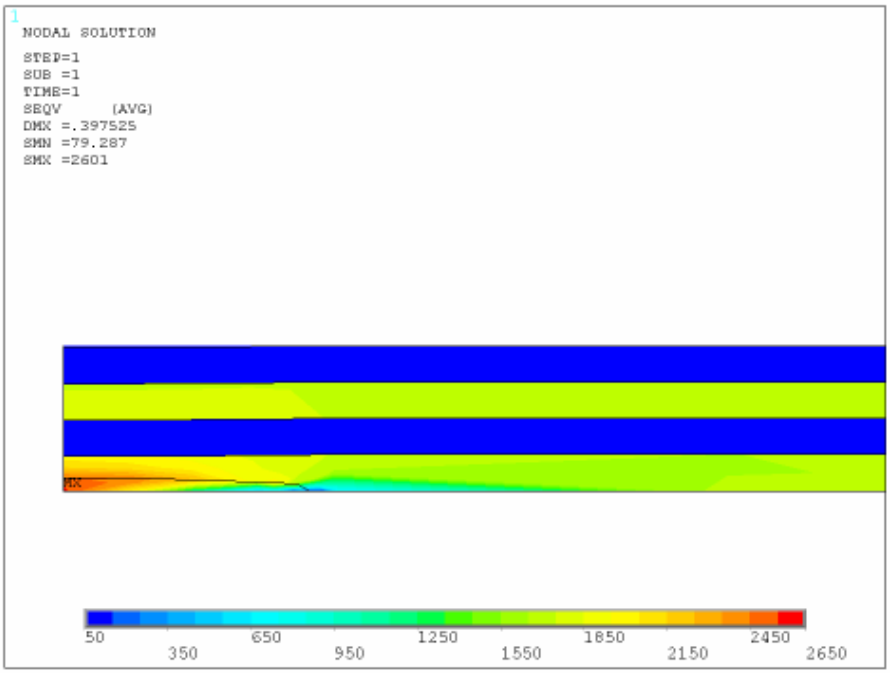

Fig. 4.7 Von Misses distribution in XZ plane for the 0° voided model

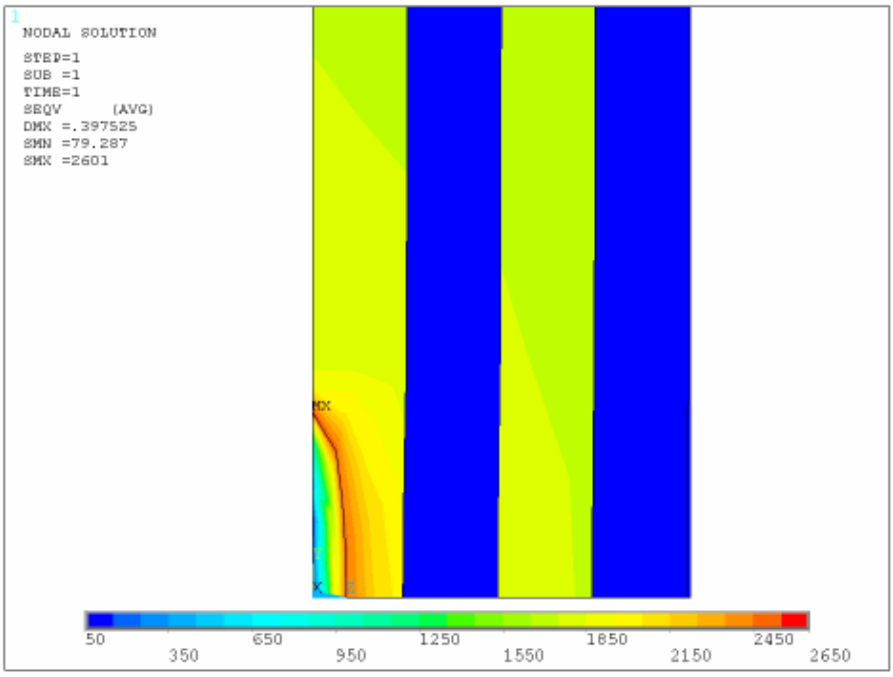

Fig. 4.8Von Misses distribution inYZ for the 0° voided model

As a result from analysing Von Misses figures, it is observed that, definitely, a stress peak is located at the void surface. Actually, it is located in the middle plane of the specimen.
It has to be taken into consideration that this model does not contemplate punctual defects or irregularities in the specimen, which resulted more influent for failure during the experimental part.

4.1.2 Results obtained for 90º void model

The obtained results for the model with the void applied in 90º direction (transversal) are now presented.

As done for the previous model, a displacement of 1% in the 0º direction was applied so that it produced the following strain distribution in X direction. *Figure 4.9*

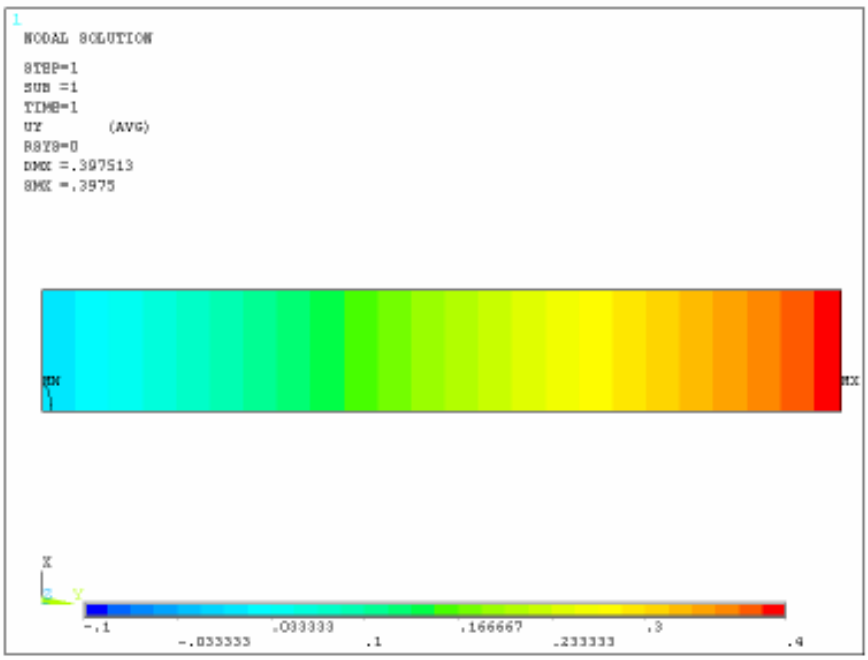

Fig. 4.9 Displacement range in 90º voided specimens with a strain of 1%

As previously done for the 0º voided model, stress distributions were studied for axis defined as follows:

X –parallel to the 0º fibre direction and to void major length.
Y – parallel to the 90º fibre direction and perpendicular to void major length
Z – along the thickness direction

Stress distributions in these directions are presented in *figures 4.10, 4.11 and 4.12*

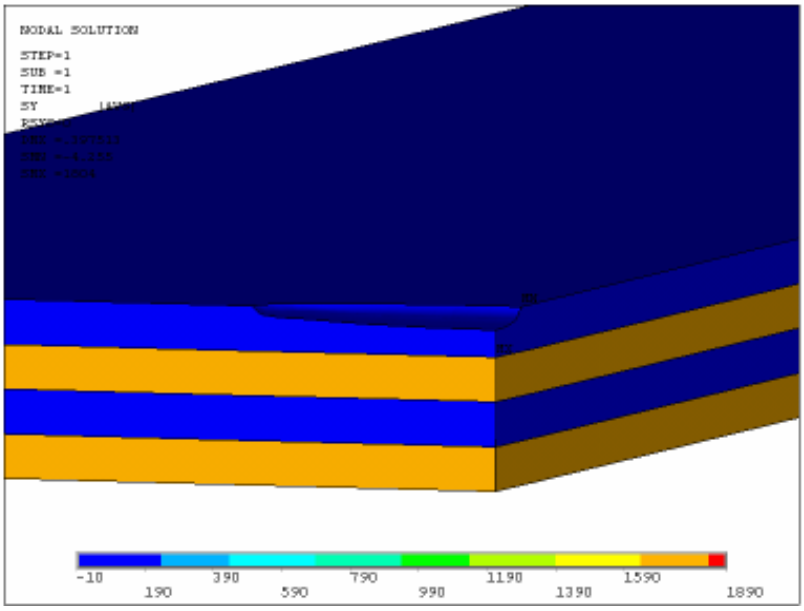

Fig. 4.10 Stress distribution in X direction for the 90º void model

In contrast to the 0º void, the void is located in a 90º layer due to the fact that voids have their long axis along the fibre direction. There is no x-stress peak point. The resultant stress is 1804MPa uniformly distributed along the 0º layers. The 90º layers present a compression in their principal direction due to the Poisson's ratio of the material.

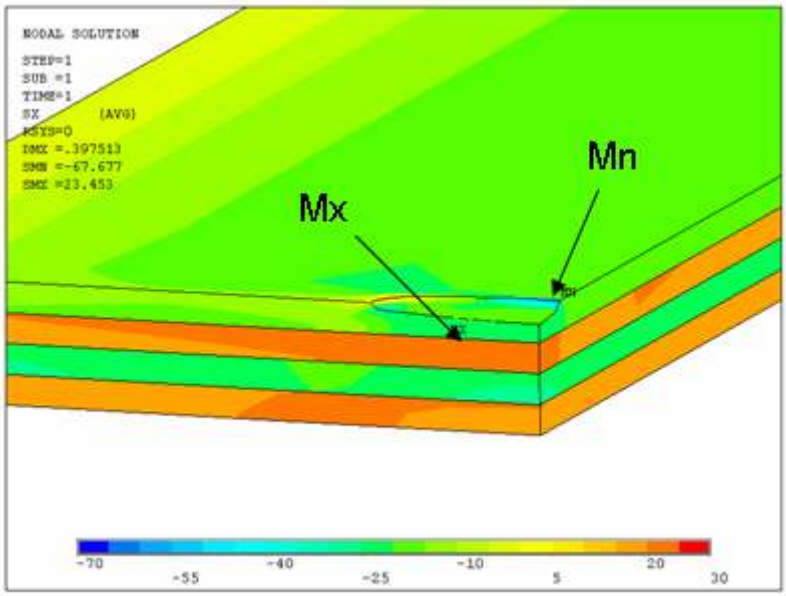

a)

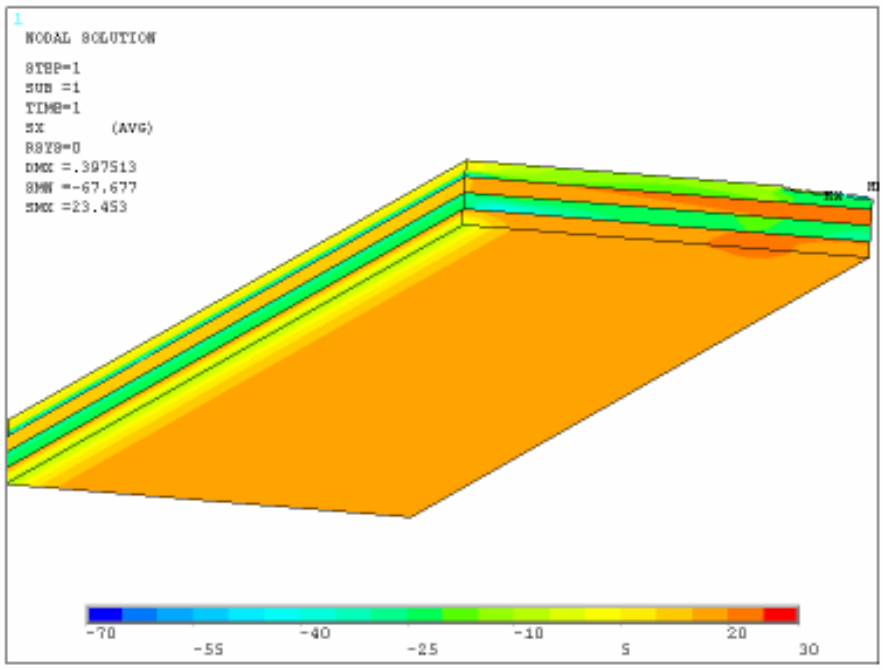

b)

Fig. 4.11 Stress distribution in Y direction for the 90º voided model

In *figure 4.11*, lower stresses appear in the 90º direction when comparing to those obtained in the longitudinal direction. Nevertheless, they are higher than those obtained when the void was located along the 0º direction.

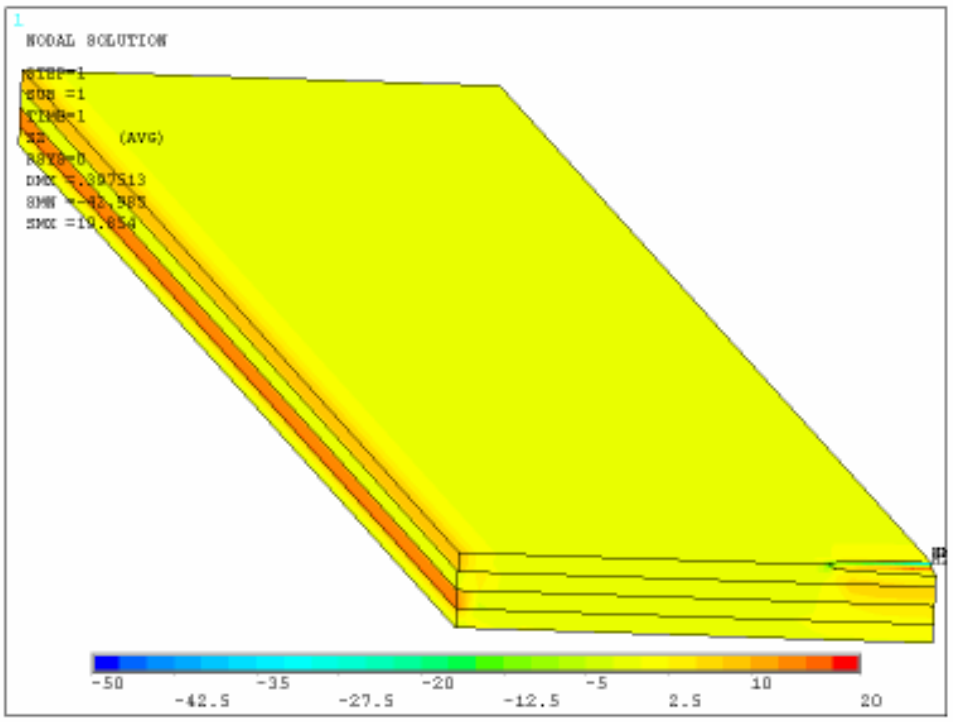

a)

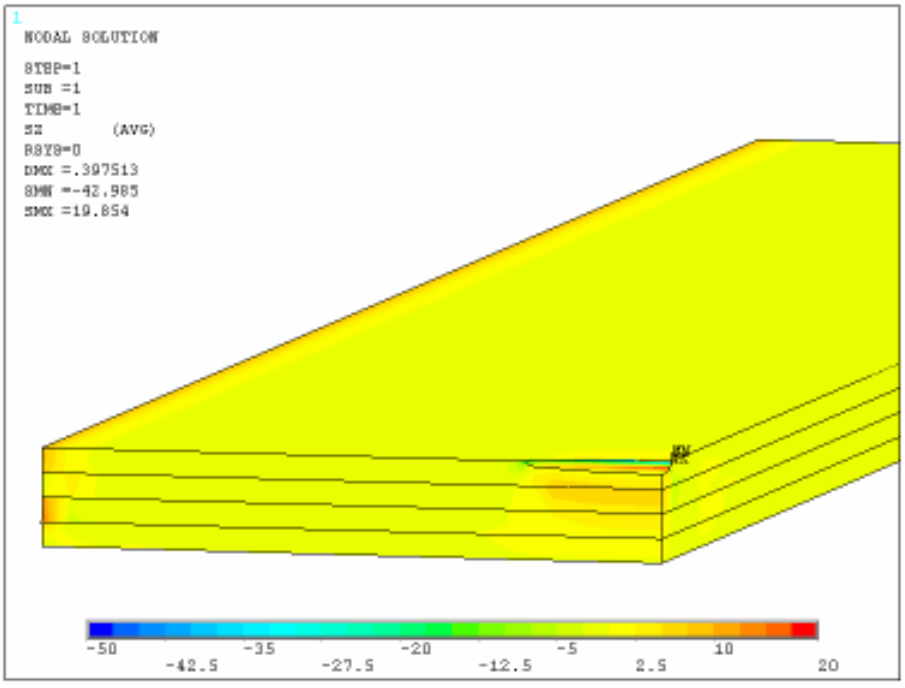

b)

Fig. 4.12 Stress distribution in Z direction for the 90º voided model

In *Fig. 4.12*, as a result from the Z stress distribution, it is noted that a compression zone appears along the long axis of the void region and some small stresses appear near the free edge region.

Von Misses distribution is represented in *Figures 4.13, 4.14, 4.15 and 4.16*

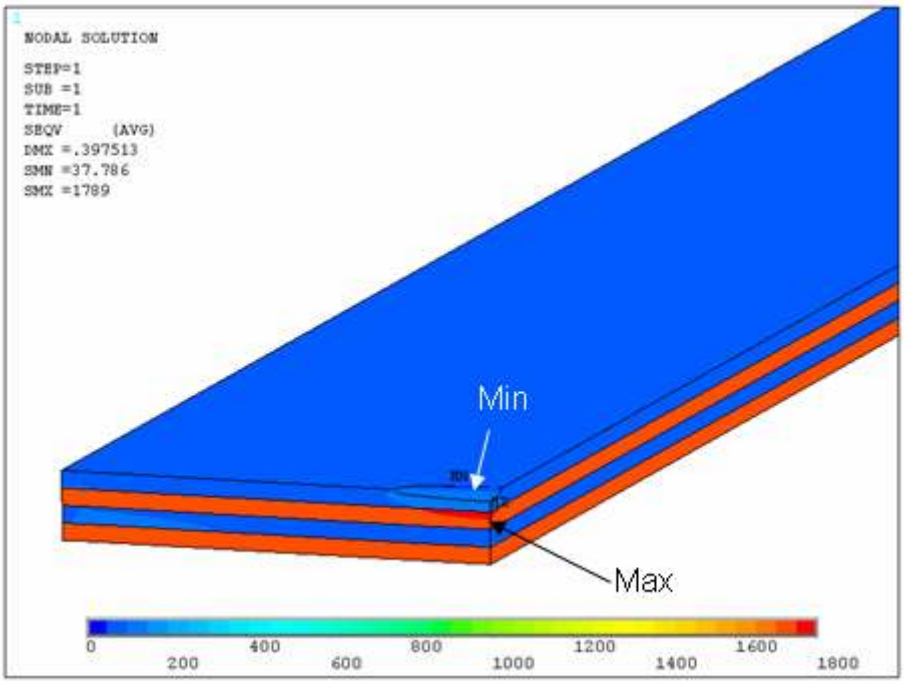

Fig. 4.13 Von Misses distribution for the 90º voided model

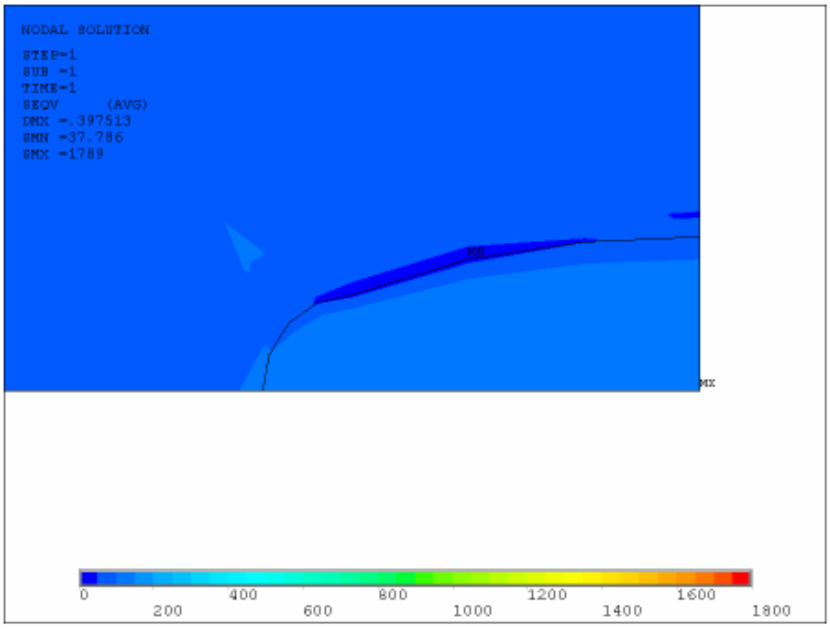

Fig. 4.14 Von Misses distribution in XY plane for the 90º voided model

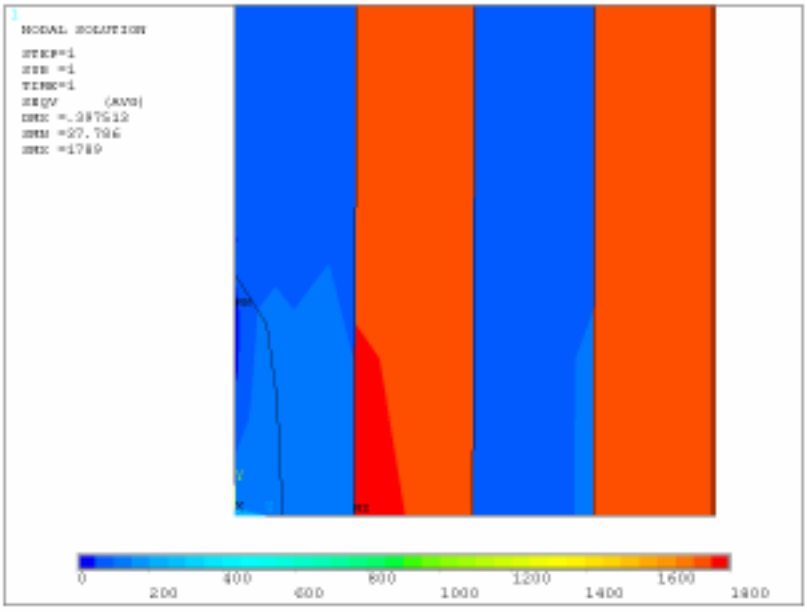

Fig. 4.15 Von Misses distribution in XZ plane for the 90º voided model

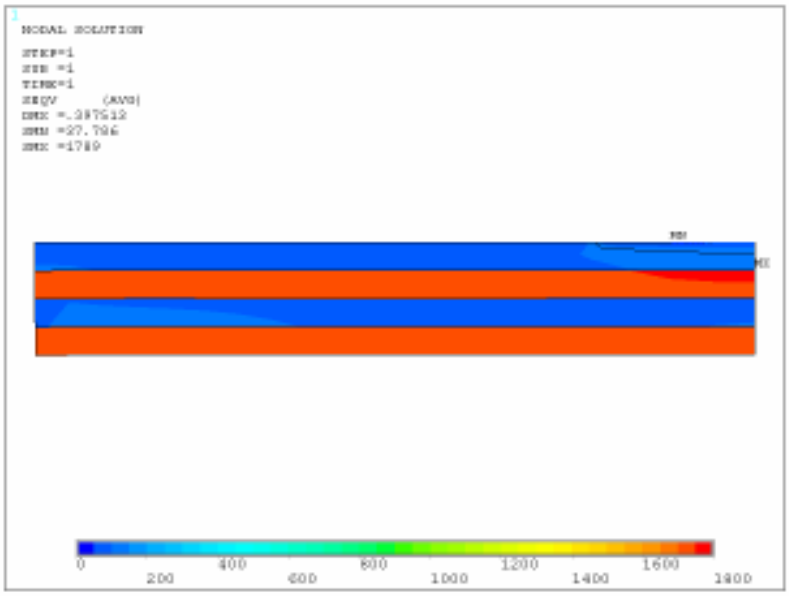

Fig. 4.16 Von Misses distribution inYZ for the 90º voided model

From this figures it can be extract that the stress applied is mainly sustained by the 0º layers, although there is some influence from the void that can be noticed.

For example, in the 90º layer where the void is applied, the void singularity produces a relaxation that provokes an irregular stress distribution around the void. As a consequence, the 0º layer placed next to the voided 90º layer

receives an extra stress at the vicinity of the void. This stress is the highest stress in the specimen (1789 MPa).

4.2 Coupon testing results

4.2.1 Reference characterization

Before testing the voided coupons, six tests until fracture were made with non-voided specimens in order to characterise its reference behaviour.
Respectively six non-voided and voided specimens were tested too until fracture occurred so that its strength and strain could be compared to the non-voided specimens

Results obtained from these tensile tests are presented in *Figure. 4.17*

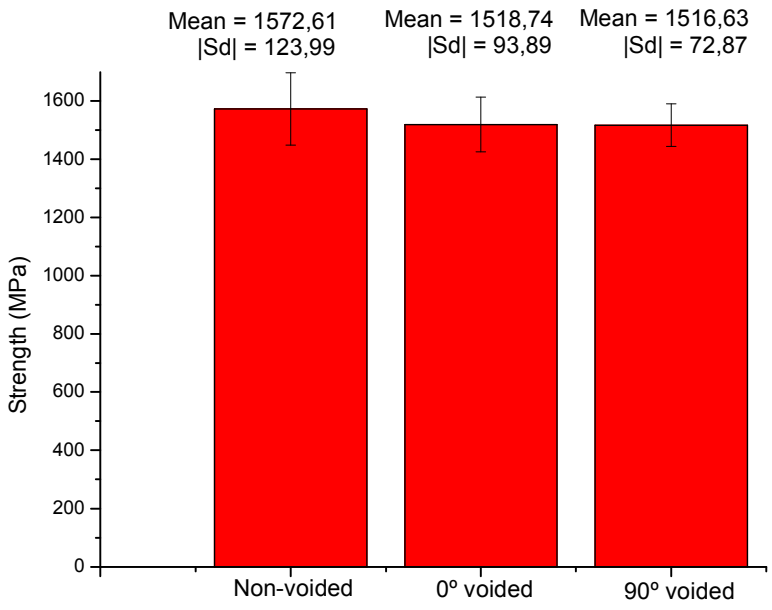

a)

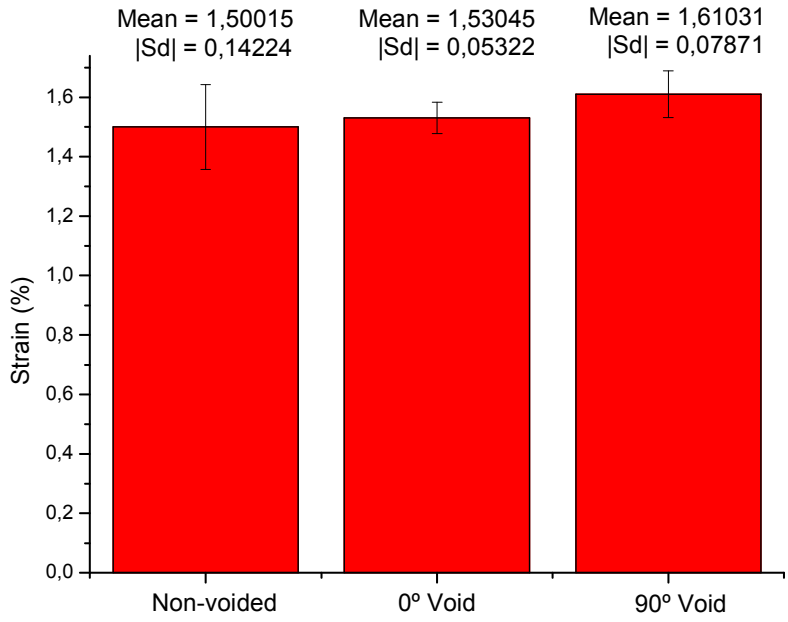

b)

Figure. 4.17. Reference behaviour for the non-voided, 0º void and 90º void specimens on unidirectional tensile test. a) Ultimate strength b) Ultimate strain.

4.2.2 Experimental observation

Major part of the voids obtained presented an elliptical shape as shown in *Fig. 4.18*

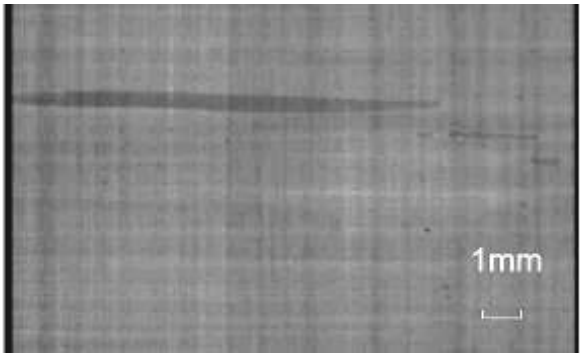

a)

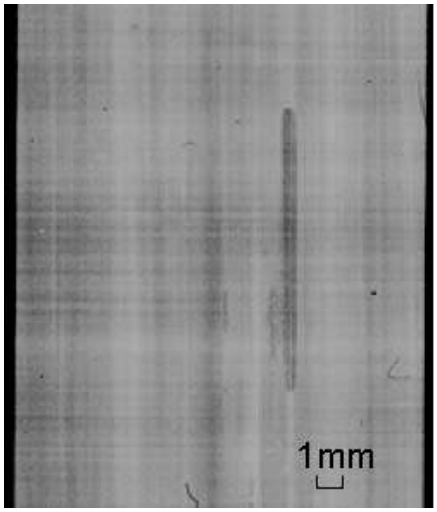

b)

Figure 4.18. X-Radiography with elliptical shape of void in laminates. a) 90º void. b) 0º void.

In addition, different failure modes were observed in the X-Ray pictures taken at the different load steps during the step wise tensile test.

Independently from the void alignment the cracks always start from the edge because of the weakness at the edge due to the manufacturing process as shown in *Figure 4.19* where cracks appear from the specimen edges clearly seen by the dark small areas.

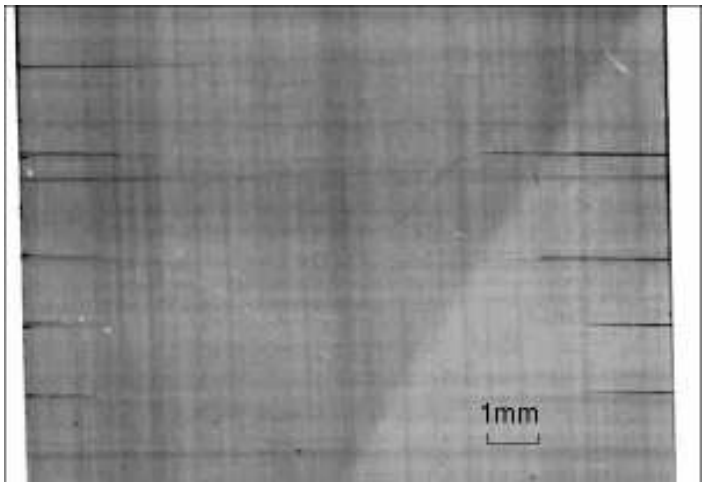

Fig. 4.19. Initiating edge cracks due to edge surface weakness at 30% of the ultimate strength.

These cracks develop as the load in the specimen grows until they meet or overlap another crack at the middle of the coupon. This provokes transversal cracks that start to appear at earliest 30% of the ultimate strength and continued forming until they reach the saturation. *Figure 4.20*

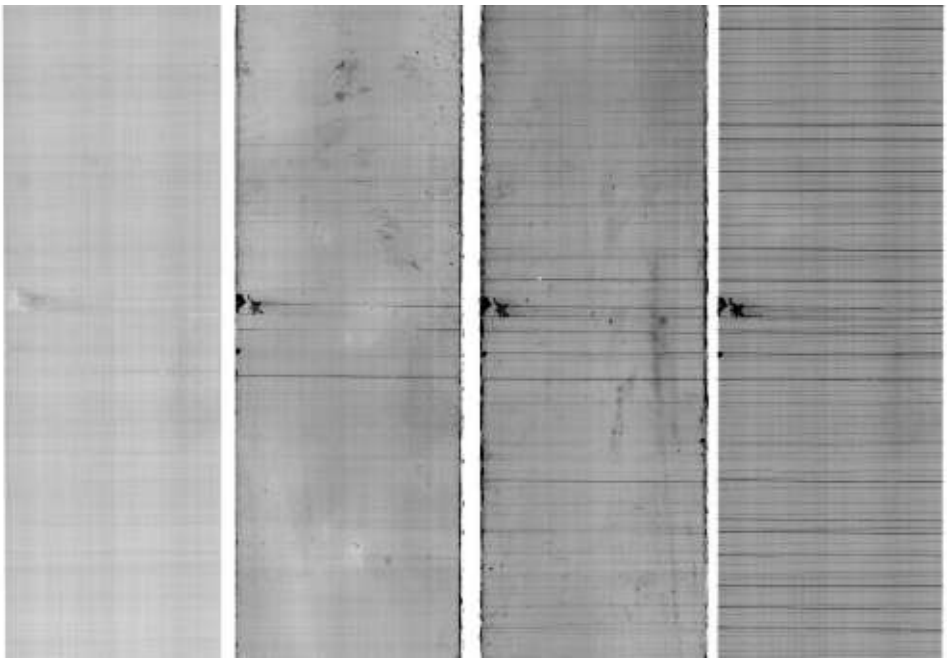

Fig. 4.20. Transverse cracking evolution for cross-ply laminate [0,90,0,90,0] at 0MPa, 67%, 82% and 93% of the ultimate strength respectively.

Short before final failure, longitudinal cracks appear. Because of this late appearing they were rarely detected. *Figure 4.21*

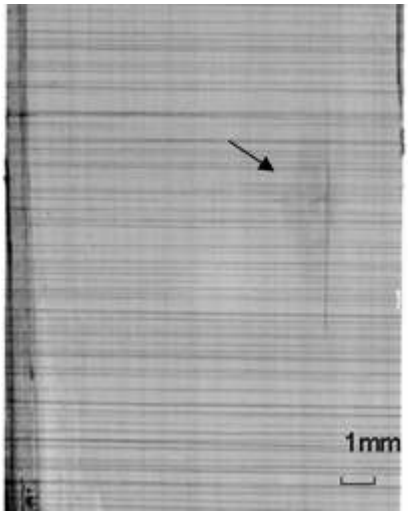

Fig. 4.21 Longitudinal crack (vertical) for a cross-ply laminate at 95% of the ultimate strength

Finally, fibre failure occurred. Although it could not be detected by X-Ray, some specimens did present a typical fibre failure. *Figure 4.22*

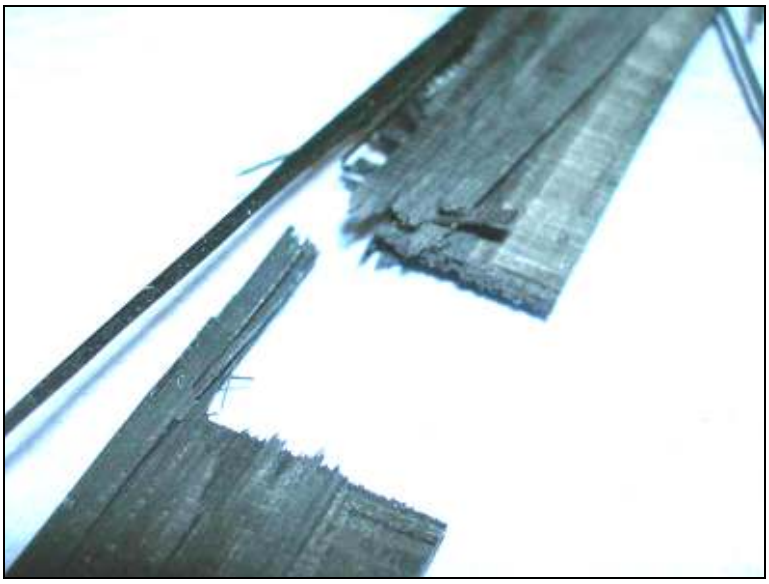

Fig. 4.22. Failure of a $[0,90,0,90,0]_s$ laminate

In this picture, the only one that failed at a 0º void, it can be seen how some fibres did break because of the void (in the left part of the specimen) and when the stress was too high to be sustained by the remaining fibres, the specimen presented a brittle straight fracture.

As expected and noted in the theory part of this project, no edge or interior delamination could be detected.

4.2.3 Results obtained from the tensile test for specimens with voids oriented in 0º direction

A total of 14 CFRP specimens were tested in order to characterize its behaviour and to study the influence of void orientation in the failure process.

All data that characterizes the specimens is presented in *Annex 2*

It has to be noted that specimens with 0º voids, present double adjacent layers oriented in 0º because of their particular lay up. This fact produced that the thicknesses (Z direction) of the 90º cracks, which appear first in tensile test, were smaller than those in specimens with voids oriented in the 90º direction. Because of this reason, it resulted more difficult to visualize the crack growth from the X-ray pictures.

In order to characterize the number of voids obtained per each specimen in the longitudinal direction, the following diagram is presented *in Figure 4.23.*

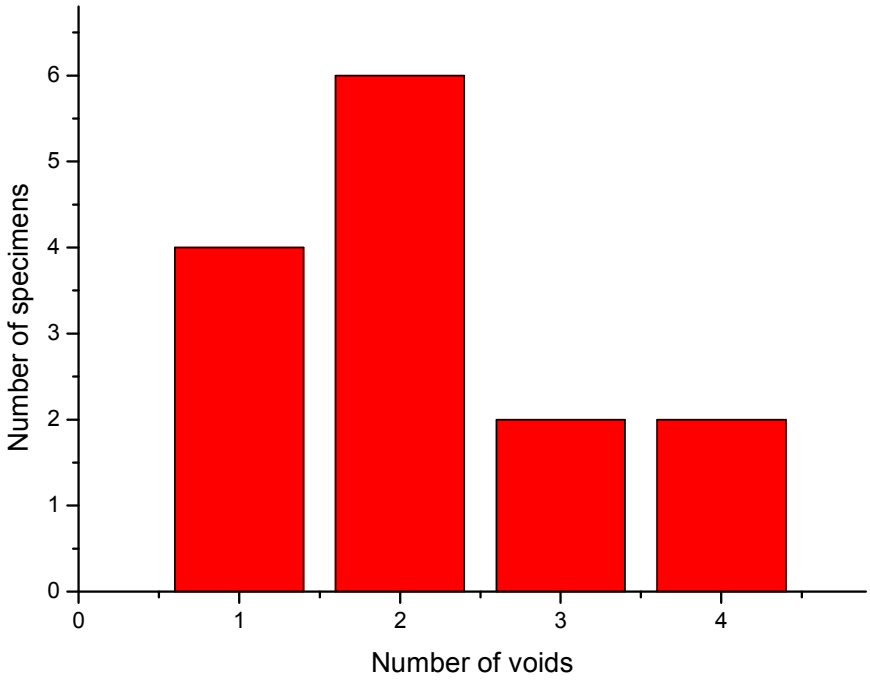

Figure 4.23. Number of voids per number of 0º voided specimens manufactured

Concerning 0º voided specimens, most of them had two voids applied. These voids present an averaged void length in 0º direction of 7,34mm as presented in *Figure 4.24*

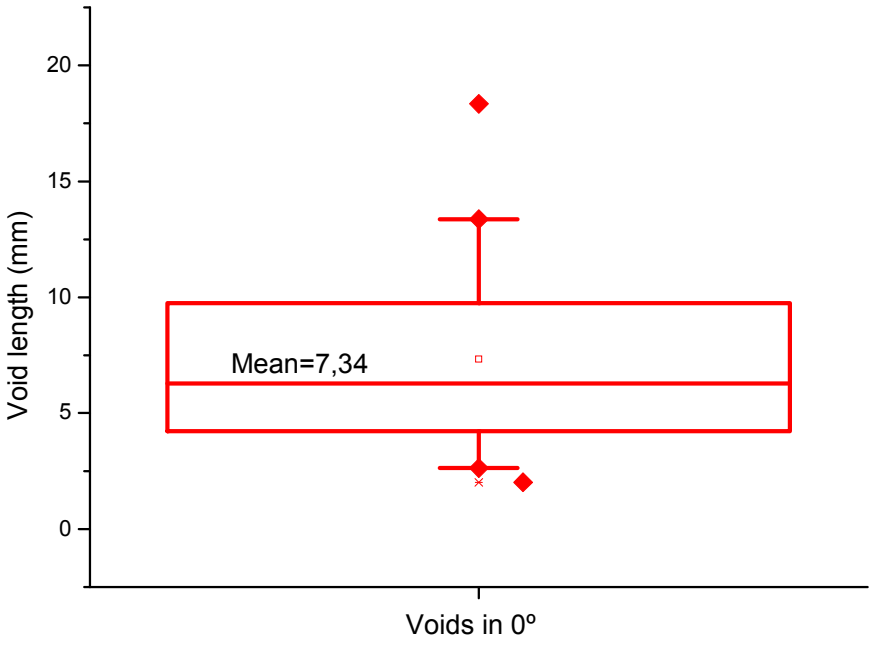

Figure 4.24. Box diagram for void length in 0º voided specimens

In order to interpret graphic 4.5 it has to be mentioned that the box represents the 50% of the values, the border lines include the 95% of the data and the single points represent outliers, considered non-regular data.

Voids were located within the specimens as stated in *Annex 1.*

For the non-voided and voided zones defined in the experimental part, both zones were analysed by studying the behaviour of equal void and non-voided areas in each specimen.

Thus, results obtained for the non-voided region are presented. The relation between crack density, measured in $\frac{1}{mm}$ for a certain length of the specimen, and the stress applied is shown in *Figure 4.25.*

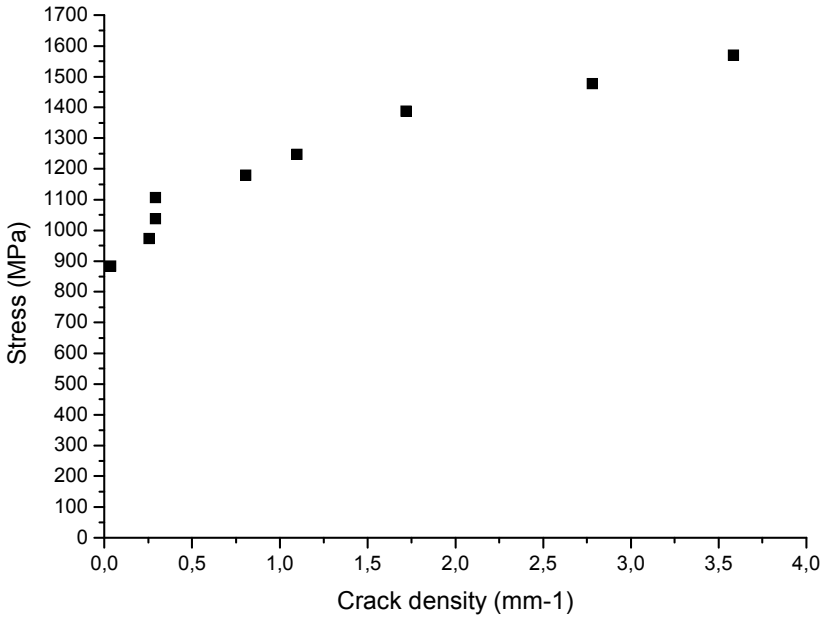

a)

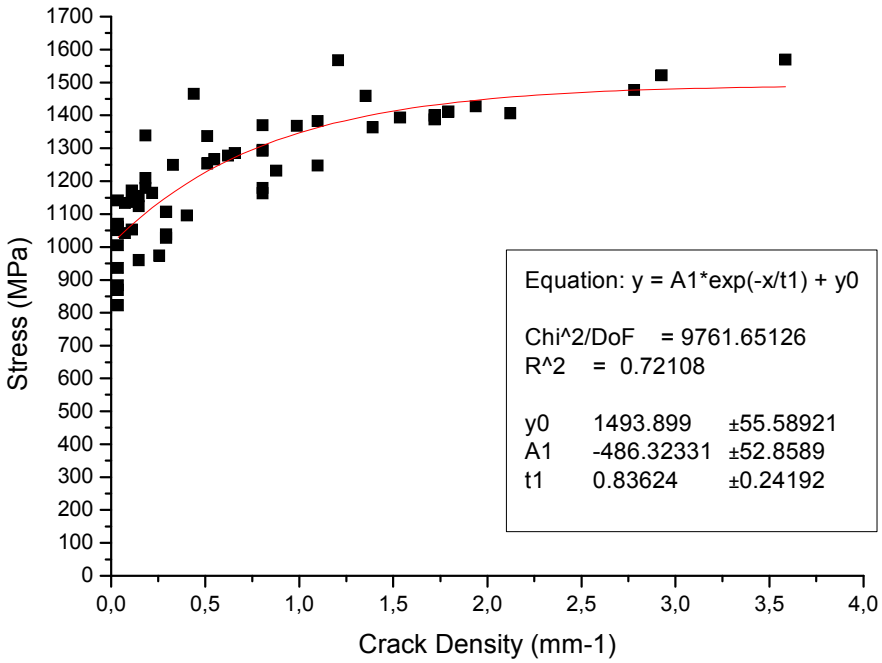

Figure 4.25 Crack density per stress in the non-voided zone of a 0º voided specimen. a) for a certain specimen b) for all the measured specimens.

In order to compare and discuss these results, a first order exponential equation was fitted to the data points.

$$y = -486{,}32e^{\left(\frac{-x}{0{,}83624}\right)} + 1493{,}90 \qquad (4.1)$$

It has to be noted that a good correlation was achieved as stated with the correlation coefficient R=0,84916. This can be explained by the rather big variation of void size, distribution and number of voids in the tested area.

Next, results obtained in the voided region of the specimens are presented.
As before, the relation between the stress applied in a specimen and the crack density produced is characterized in *Figure 4.26*

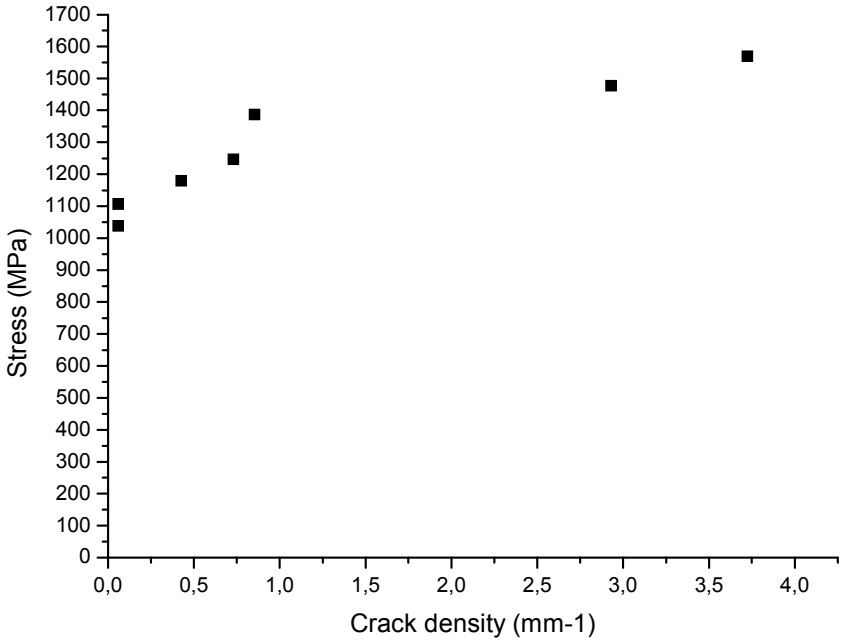

a)

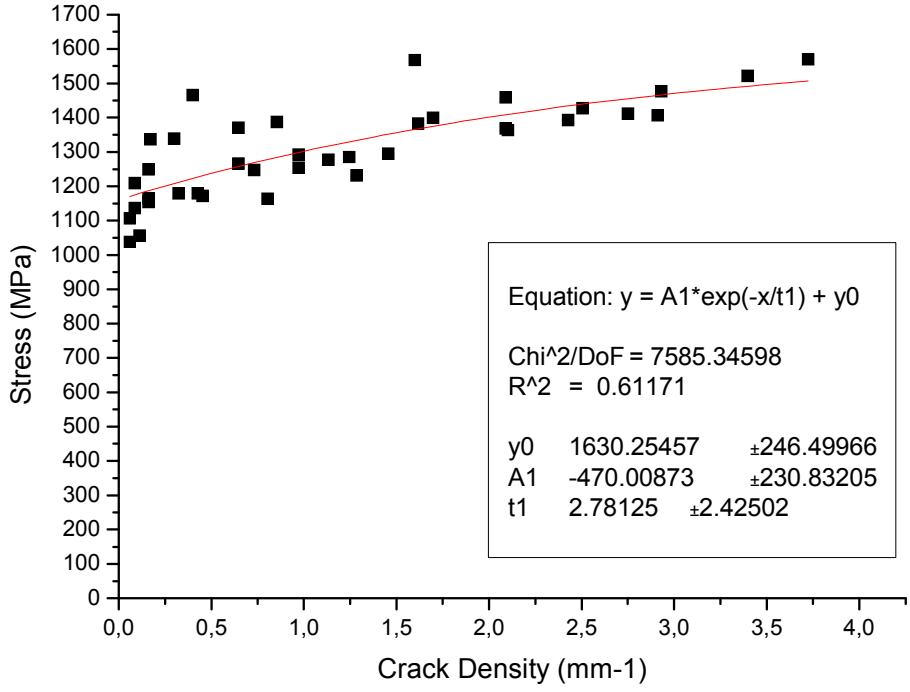

b)

Figure 4.26 Crack density per stress in the voided zone of a 0° voided specimen. a) for a certain specimen b) for all the measured specimens.

In this case, a first order exponential equation was fitted to the data points as well.

$$y = -470{,}01e^{\left(\frac{-x}{2{,}78125}\right)} + 1630{,}25 \qquad (4.2)$$

It has to be noted that a good correlation was achieved as stated with the correlation coefficient R=0,78212.

As a complement, the behaviour of both regions is presented in the following *Figure 4.27*

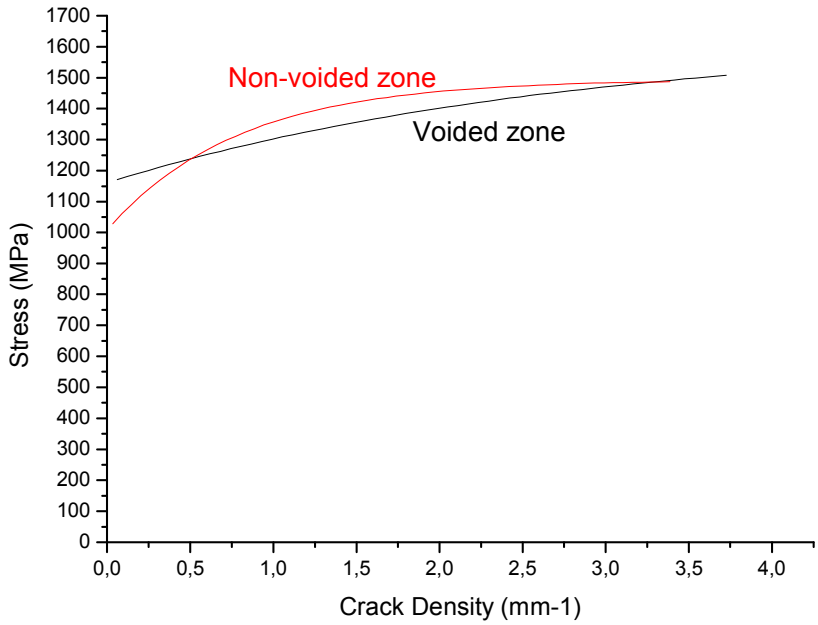

Figure 4.27 Comparison between crack density and stress in voided and non-voided regions for a 0º voided laminate.

This graphic shows that the crack density is higher in the non-void zone than in the void zone.

The relation between first crack and void area is shown in *figure 4.28*. This is the influence in the stress, at which the first crack appears, of the total void area within the specimens measured in the XY plane.

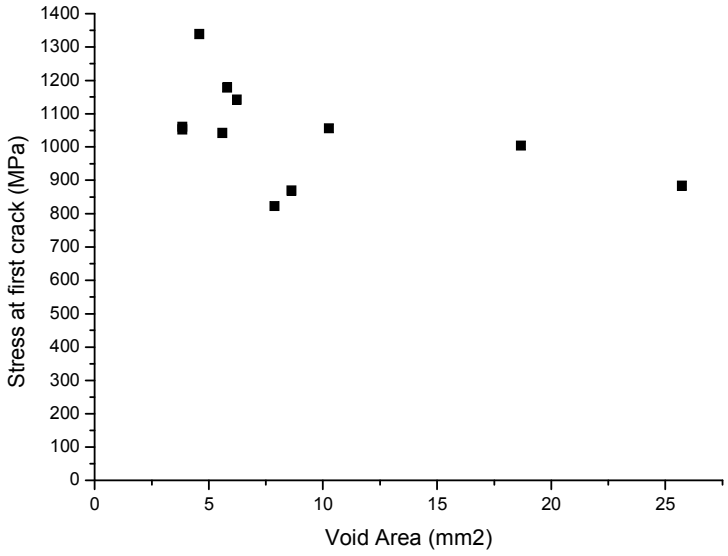

Figure 4.28 Stress at first crack in specimen per total void area for 0º voided specimens.

It can be noticed that the stress at which the first crack appears is related to the void area, although a real dependency can not be seen because of the scatter. As the voided area grows, the first crack appears at a lower applied stress. Nevertheless, it seems that very small areas do not influence that much the first crack.

The length of the void in the specimen was studied too.

Most of the voids overlapped in the transversal direction. Because of this reason, instead of considering the length of each single void, the length of the longest void was taken into consideration in order to study when the first crack in the specimen appeared. *Figure 4.29*

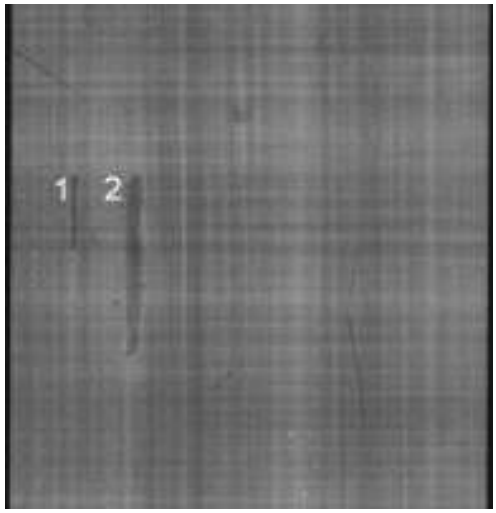

Figure 4.29Two overlapped voids in transverse direction. Length of void 2 was considered for Stress/Void length graphic.

Thus, the relation between the maximum void length in a specimen and the stress at which the first crack appeared is presented in *Figure 4.30.*

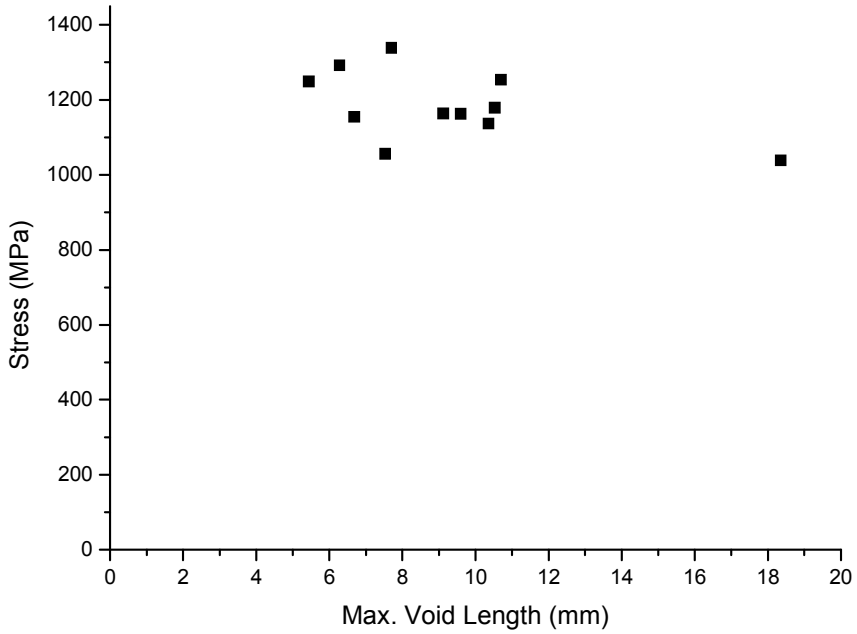

Figure 4.30 Maximum void length per stress at first crack in 0º voided specimens.

It is noted that this relation presents a decreasing tendency. As the maximum void length measured increases, the stress at which the first crack appears decreases.

4.2.4 Results obtained from the tensile test for specimens with voids oriented in 90º direction

In order to study the influence of the direction in which the void is applied, a further study was made concerning 90º voided specimens. This time, a total of 17 CFRP specimens were tested.

All data required for characterizing the specimens can be consulted in *Annex 2.* The process of creating voids result highly variable concerning void number and void length. Thus, a mean of 2 voids per specimen was achieved and distributed as shown in *Figure 4.31*.

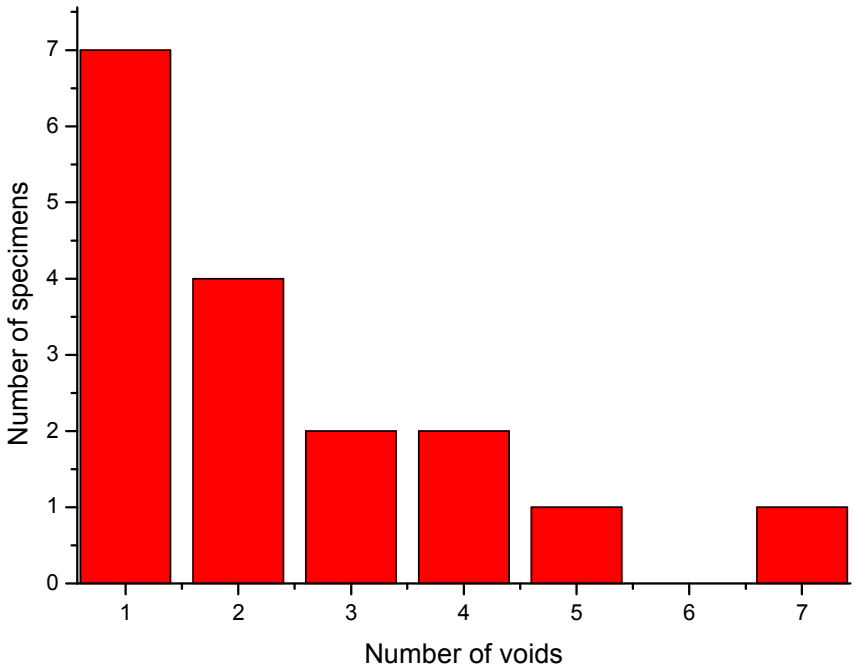

Figure 4.31. Number of voids per number of 90º voided specimens manufactured

These voids were located within the specimens as shown in *Annex 1*
Through the image treatment of the x-rays, voids were measured so that it could be stated that a mean length of 6,10968mm was achieved as shown in *Figure 4.32.* The interpretation of this graphic is as explained for the 0º Void.

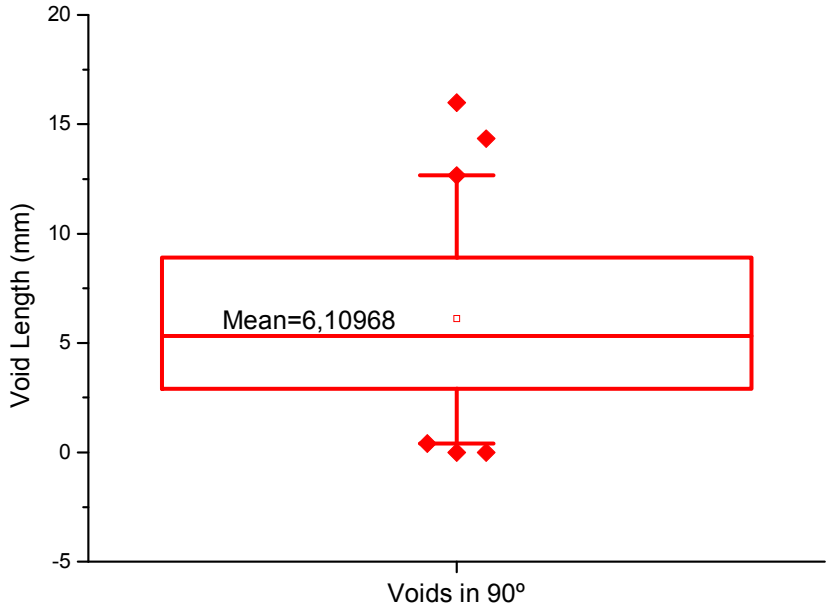

Figure 4.32. Box diagram for void length in 90º voided specimens

For 90º voided specimens, all lengths of the voids were taken into consideration.

Regarding the behaviour of the specimen under stress, the relation between crack density in the specimen and the stress applied is shown in *Figure 4.33*.

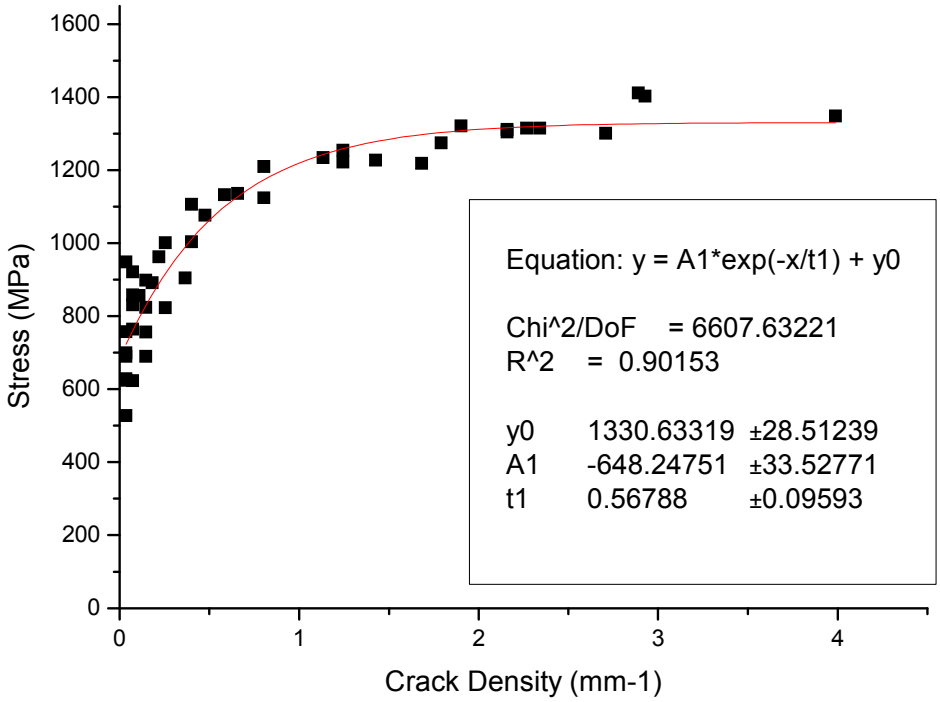

Figure 4.33. Crack density per stress in a 90º voided specimen.

For *figure 4.33*, it was found that a first order exponential equation fitted best the data point and presented a good correlation coefficient of R=0,949489

$$y = -648{,}25e^{\left(\frac{-x}{0{,}56788}\right)} + 1330{,}63 \qquad (4.3)$$

Next, the relation between the void areas, calculated through the projection of the void in the plane xy, and the applied stress at which the first longitudinal crack appears. *Figure 4.34.*

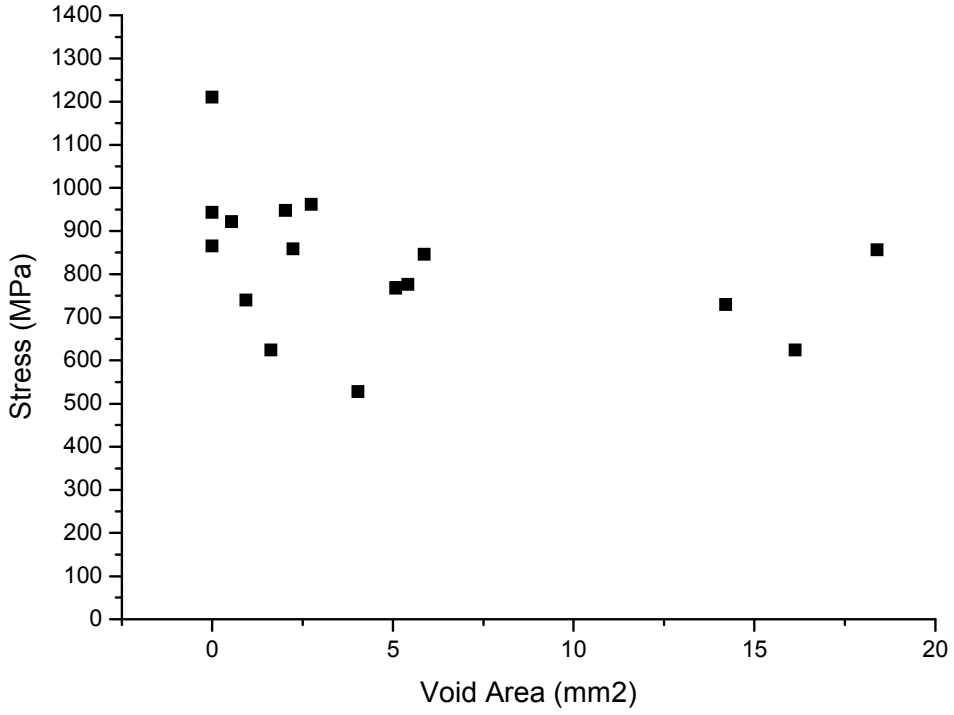

Figure 4.34. Relation between total void area in specimen and stress at the first crack in specimen for 90º voided specimens

As it can be noticed, this relation is not representative as data present not a good correlation. The reason for this fact may be that other parameters such as void dispersion, radius or its thickness influence in the appearance of the first crack.

The relation between length of the different voids against the stress at which a crack appeared in each void is presented in Figure *4.35.*

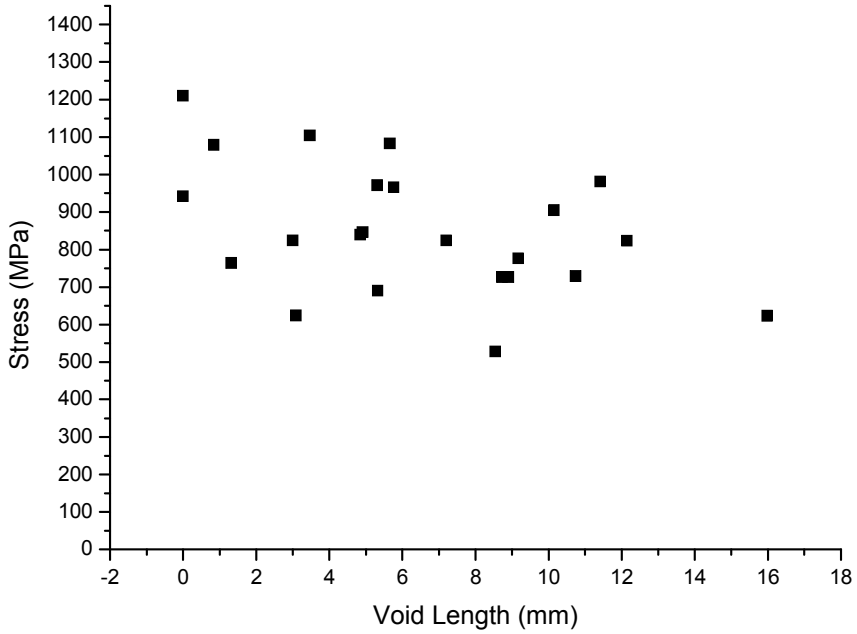

Figure 4.35. Relation between void length and stress at first crack in 90º voided specimens.

It can be seen that the stress at which the crack appears in a voided section, tends to decrease as the length of the void increases. The void length shows a better correlation. Due to the large scatter it can be noted that not just the length of the void is one parameter for the first crack than as well other geometrical parameters, such as the resin or fibre distribution.

4.2.5 Comparison between 0º voided and 90º voided laminates results

Results obtained for both kinds of voided laminates are compared in this section.

Because of testing requirements, these two morphologies present a different lay-up, $[0,0,90,0,90]_s$ for the 90º void and $[0,90,0,90,0]_s$ for the 0º void. This fact may influence the results obtained.

It can be seen in next graphic that the development of crack density under tensile load in both studied models at the voided area present a different behaviour. *Figure 4.36*

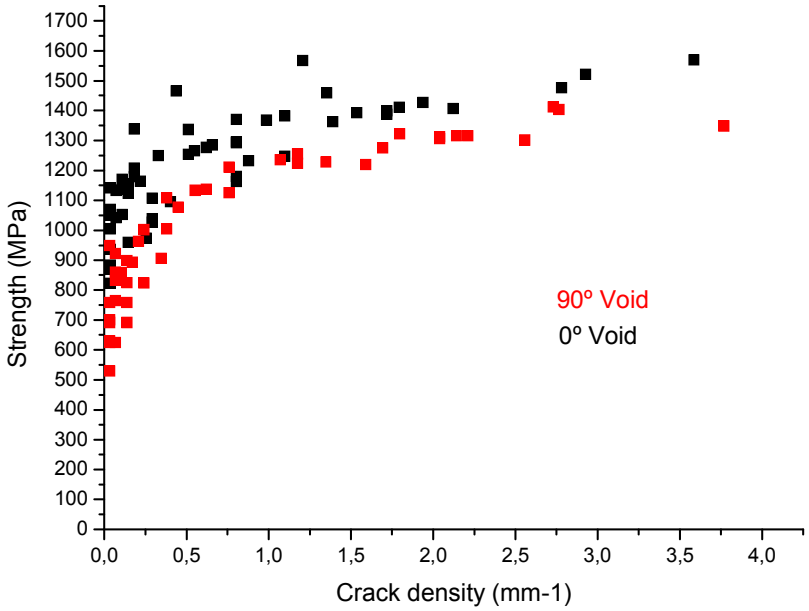

Figure 4.36 Comparison between crack growing in voided zone for 0º voided and 90º voided cross-ply laminates

A clearer view can be obtained by comparing the equations fitted to the respective data. *Figure 4.37*

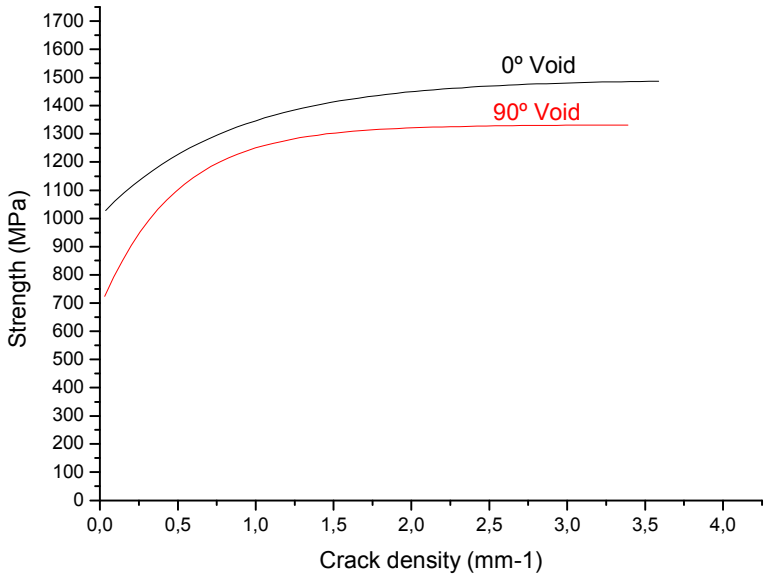

Figure 4.37 Comparison between crack growing tendency equations for 0º voided and 90º voided cross-ply laminates

The effect of the void area within the laminate and how it affects the first crack appearing in the voided area is compared for both 0º and 90º laminates. *Figure 4.38.*

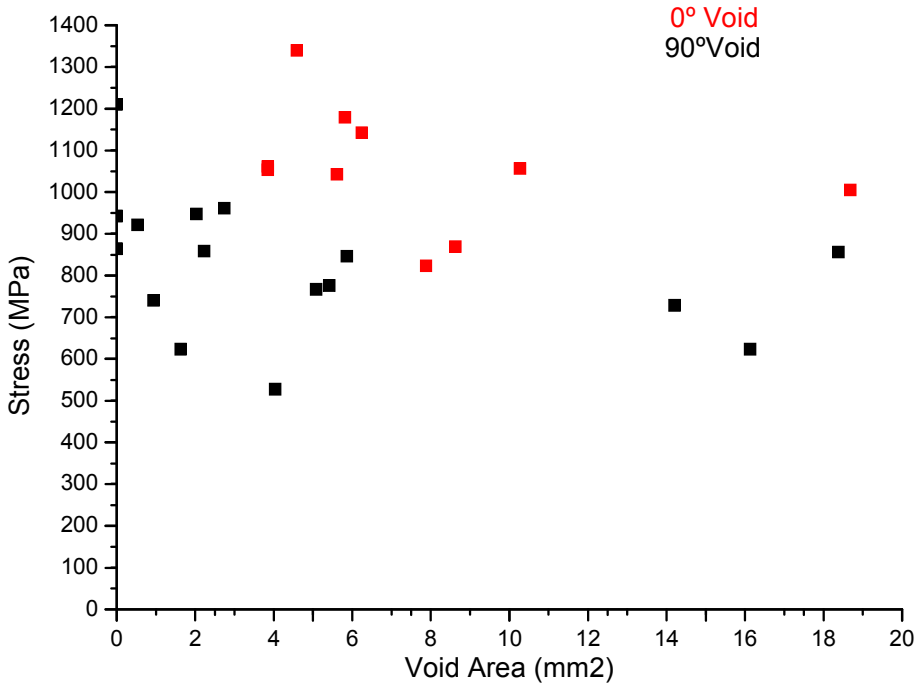

Figure 4.38. Comparison between global void area in the coupon and stress at which the first crack appears crack growing tendency equations for 0º voided and 90º voided cross-ply laminates

Effect of the void length in the stress at which a crack appears in a void is compared in *Figure 4.39.*

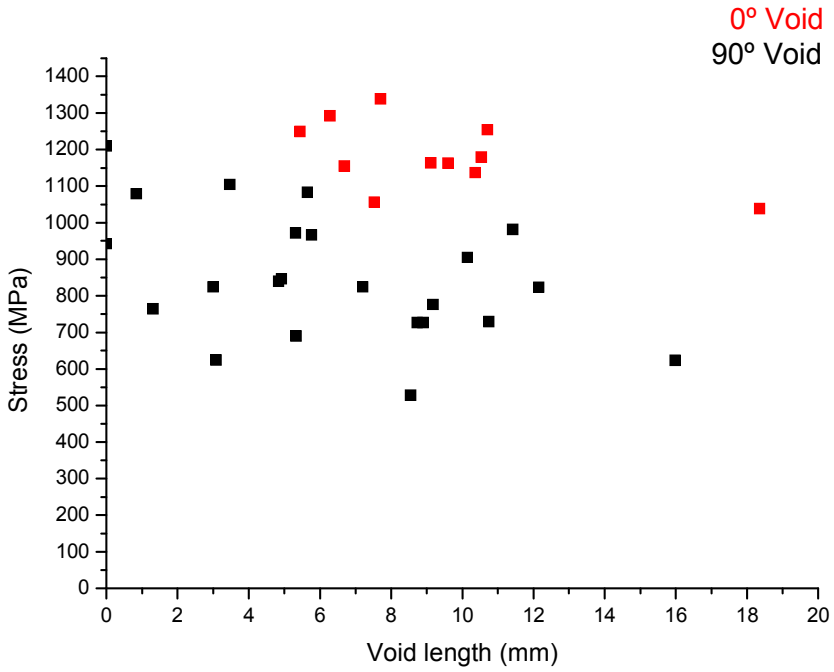

Figure 4.39. Comparison between void length and stress at which a crack appears at the void for 0º voided and 90º voided cross-ply laminates

5. DISCUSSION

The failure mechanism of a voided CFRP 0-90° cross-ply laminate under tensile loads applied in one direction was studied in this Final Degree Project.

For this purpose, voided coupons were manufactured and a FEA was done. Although in FEM the model was created with one void, it resulted difficult to produce just one void in the manufactured specimens.

Induced voids were thought to be of about 6mm length referring to the FEA model and to literature. Thus, a mean of 6,11±4,13961mm and a mean of 7,34±3,97 were obtained for 90º and 0º voided laminates respectively. As it can be noticed by the standard deviation, the range of void length was wide and dispersed.

Most of the voids presented a voided form like the one theoretically expected, as shown in *Fig. 4.18.*

Non-voided specimens were tested in order to act as a reference, obtaining a mean strength of 1572±124MPa and a mean strain of 1,5001±0,1422

If comparing the strength and strain of the voided specimens with non-voided specimens, it was noted that strength decreased in 3,56% for 90º voids and 3,43% for 0º voids, which is in good agreement to the results from the literature [12]. Strain increased in a 7,34% in 90º voided specimens and 2,02% for 0º voided specimens. Such an increase could be explained by some inaccuration while being tested. Another explanation can be that for 0º void, the fibre waviness along the 0º voided layer straightened inducing an increase in strain. In the case of 90º void, it could be explained due to the fact that as the elastic modulus decreased, stiffness decreased as well, which produced an increase in strain.

Regarding the failure mechanism under tensile stress of the cross-ply laminates, cracks in 90º voided laminates started to develop at the earliest at 35% of the ultimate strength for the stacking sequence $[0,0,90,0,90]_s$ and they

start to develop at around 50% of the ultimate strength for 0º voided laminates with the stacking sequence $[0,90,0,90,0]_s$. Such a difference in late appearing of the cracks can be because of the bigger thickness of the 90º inner layer in the laminate stacking sequence for 90º void. This fact agrees to the results seen in literature [8]

In both cases, cracks presented the same growing morphology. They started at the edges of the specimens because of the weakness in this region as seen in *Fig.4.19*. While increasing the load, they started to grow forming the first transversal crack. Nevertheless, it has to be mentioned that because of the used detection method (penetrant was applied at the edges), detecting inner failures such as delamination, longitudinal cracks or fibre fracture was not possible for low stresses. [27]

Considering the FEA for 0º voided coupons, this first crack should have occurred at the void. *Fig.4.5*, *Fig 4.13*. When the void is located along the 0° direction, the specimen presents maximum peak concentration stresses in the transversal plane located in the middle of the void, where its section is more width. So it was calculated that failure would occur at the void.

On the other side, when the void is aligned along the 90° direction, the specimen presents lower stresses but concentrated in the interface between the voided ply and the correlative to this one. As this zone is very vulnerable, a pick stress in there may produce delamination between plies. No relevant peak stresses were applied at the void section itself.

Both models predict a failure in the void section or in its vicinity. Nevertheless, the laboratory results showed a different behaviour where the final failure did not occur at the void.

For 0º void, calculated tensile stresses in FEM could lead to fibre failure, which occurs at about 3000MPa. Due to this calculation first fibre failure would be expected at strains of 1.2% instead of 1.5% due to the high stresses next to the void. But as it has been seen in tensile test results, final failure is not that much dependent on the 0º void. This can be produced because the model assumption, without undulated fibre, resin rich area and matrix-fibre debonding,

did not represent accurately enough the real behaviour, which produced overestimated high stresses to be calculated.
For 90º void, the simulation was more accurated to real behaviour, because lower stresses were applied at the 90º layer, this stresses when reaching a value of 200MPa would induce matrix crack at the void section as the stresses there where sensibly higher. This fact was confirmed by studying the first crack formation through the X-Ray pictures. It could be noted that in 90º voided specimens, the first crack appeared usually at the voided section,
Contrarily, for 0º specimens, the first crack was formed randomly through the length of the specimens.

If considering the first crack in the void, not the specimen, it has been noted that it generally appears before in 90º voids instead of 0º voids. *Graphic 4.38* Once again it has to be mentioned that the 90º layer was thicker at the 90º void lay up.

Considering the length of the void, it can be seen that in both cases there is a certain relation, the stress at which the crack appears decreases as the length of the void increases *Graphic 4.39.* Concerning 0º voids, this tendency may be due to statistic because the probability of having a crack in a void increases for longer voids. Anyhow, although a clear decreasing tendency can be noted, the results presented a lot of dispersion, may point that the length of a void is one parameter, but not defined enough. Some other parameters such as its radius or its thickness, the resin or fibre distribution or the void dispersion may influence in the appearance of the first crack.

The relation between the total void area in a specimen and the stress at the first crack was contemplated in *Graphic 4.38* too. There, it can be seen that in both cases the stress at which the first crack in the laminate appears decreases as the total voided area increases. As it happened with the length relation, the data points for the area presented a lot of scatter, mainly because of the fact that some other parameters as void dispersion do influence on the appearance of the first crack.

After the first transversal crack appeared, more cracks continued appearing until they reached a saturation point.
It was found that transversal crack density develops later in $[0,90,0,90,0]_s$ specimens than in $[0,0,90,0,90]_s$ specimens, most probably due to the thickness of the 90º layer and the later appearance of the first crack when the void is oriented in 0º direction. *Figure 4.37.*

Longitudinal cracks were formed and one time detected short before the final failure at about 95% of the ultimate strength. *Fig. 4.21*
The deformation of the laminate increased while the stress was increasing. This fact produced high stresses due to the mismatch of Poisson's ratio between adjacent cross-plied layers. The energy liberated by the transverse cracks influenced the formation of longitudinal cracks too.

Finally, fibre failure and delamination were observed once the specimen failed.
As seen in *Fig. 4.22* the failure of a voided specimen was progressive and related with the void, when it occurred at the void section, In one occasion, the fibres located next to a 0º void failed and trespassed the stress to the surrounding fibres, this process continued until the stress was too high to be stand for the section as it can be seen in figure 4.22. At this time, a brittle fracture propagated through the section provoking the final failure.
Apart from this punctual noted failure, other specimens did fail randomly along the length of the specimen, so it could be interpreted that void do not influence in the location of the final failure.

6. CONCLUSIONS

- Big discrete voids do not affect the location of final failure in cross-ply laminates.
- As expected from the literature strength decreases about a 3% in voided cross-ply laminates.
- Transversal cracks in 90º voided laminates start to develop at the earliest at 35% of the ultimate strength for the stacking sequence $[0,0,90,0,90]_s$ and they start to develop at around 50% of the ultimate strength for 0º voided laminates with the stacking sequence $[0,90,0,90,0]_s$
- Under unidirectional stress, first transversal crack usually occurs at the void when this is oriented in 90º. In contrast, 0º voids have no influence on the appearance of the first crack.
- The stress, at which the first crack occurs in a voided section, decreases for a higher length of a certain void. However, because of high scatter maybe its radius, thickness or the resin and fibre distribution could be better parameters.
- The stress, at which the first crack appears in a specimen, decreases for bigger voided areas. But as before, because of high scatter maybe void radius, thickness or the resin and fibre distribution could be better parameters.
- Transversal crack density develops later in $[0,0,90,0,90]_s$ specimens than in $[0,90,0,90,0]_s$ voided specimens, probably due to the different thickness of the 90º layer.
- 90º void FEA did show good agreement with the practical test.
- 0º void FEA did not result enough precise in order to get an accurate vision of the real laminate behaviour. Due to simplifications in the model, it overestimated the strength at the void. An improved model with fibre waviness, resin reach area and matrix-fibre debonding could achieve a more realistic view.

7. BIBLIOGRAPHY

[1] DANIEL, M. I. ; ISHAI, O. : *Engineering Mechanics of Composite Materials*, Oxford University Press, 1994.

[2] HOBBIEBRUNKEN, T. : *Modellierung und Implementierung der thermomechanischen Eigenschaften und induzierten Mikroschädigungen in Faserverbundwerkstoffen,* Technische Universität Hamburg-Harburg, AB. Kunst- und Verbundwerkstoffe, Diplomarbeit, 2002.

[3] HULL, D. : *An introduction to composite materials*, Cambridge university press, 1981.

[4] CALLISTER W.D. : *Materials science and engineering An introduction*, fifth edition, John Wiley & Sons, 2000.

[5] 977-2 HD Datasheet

[6] SCHULTE, K. ; FIEDLER, B : *Structure and properties of composite materials,* 2nd Edition, Pg.117.

[7] CLEMENTS, L.L. ; LEE, P.R. : ASTM-STP 768 (1982), 161,171.

[8] LAFAIRE-FRENOT, M.C. ; HÉNAFF-GARDIN, C. : Formation and growth of 90º Ply Fatigue Cracks in Carbon / Epoxy Laminates, Composites Science and Technology, Elsevier, 1990.

[9] ZHAN-SHENG GUO ; LING LIU ; BO-MING ZHANG ; SHANYI DU ; *Critical Void Content for Thermoset Composite Laminates*, Journal of Composite Materials, Vol. 00, 2006.

[10] OLIVIER, P. ; COTTU, J.P. ; FERRET, B. : Effects of cure cycle pressure and voids on some mechanical properties of carbon/epoxy laminates. Composites 1995;26:509-15.

[11] HUANG, H. : TALREJA, R. : *Effects of void geometry on elastic properties of unidirectional fibre reinforced composites*. P.2-5.

[12] BOWLES, K.J. ; FRIMPONG, S. : *Void effects on the interlaminar shear strength of unidirectional graphite-fiber-reinforced composites*. J Compos Mater 1992;26(10):1487-509

[13] JUDD, N. C. W. ; WRIGHT, W. W. : *Voids and their effects on the mechanical properties of composites – an appraisal*". SAMPE Journal, January/February 1978, 14 (1), 10-14.

[14] BIRT, E.A. ; SMITH, R.A. : *A review of NDE methods for porosity measurement in fibre-reinforced polymer composites*, The journal of the British Institute of NDT, Vol 46, No 11, pp 681-686, 2004.

[15] RUBBIN, A.M. ; JERINA, K.L. : *The effect of Porosity on Elastic Constants of Representative Aircraft Laminates,* J Adv Mater 1994: 21-30.

[16] J.SUMMERSCALES, S.A. FRY „ *Poisson's ratio in fibre-reinforced polymer composites with a high void content*". Journal of materials science letters 13. 1994. 912-914.

[17] www.wikipedia.org

[18] ZIENKIEWICZ, O.C. ; TAYLOR R.L. : The Finite Element Method, Elsevier, 2000

[19] Cycom 977-2 Matrix Datasheet. Cytec Engineered Materials.

[20] Fibre IMS Toho Tenax. Toho Tenax Europe GmbH www.tohotenax-eu.com

[21] Ansys Manual Elements Reference. Ansys Release 10.0, 2005

[22] Private information

[23] DAVE, R. ; KARDOS, J.L. ; DUDUKOVIC M.P. : *Process Modeling of Thermosetting Matriz Composites: A Guide for Autoclave Cure Cycle Selection*, Washington University. In: Proceedings of the American society for composites, *Technomic Publishing, 1986.*

[24] *ASTM : D3039/D 3039M, Standard Test Method for Tensile Properties of Polymer Matrix Composite Materials,* Annual book of ASTM standars 2004, volume 15.03.

[25] CLEMENTS, L.L. ; LEE, P.R. : ASTM-STP 768 (1982), 161,171.

[26] STONE, D.E.W. ; CLARKE, B. : *Ultrasonic attenuation as a measure of void content in carbon-fibre reinforced plastics*". Non-Destructive Testing. June 1975. pp 137-145.

[27] PRAKASH, R. „*Non-destructive testing of composites*" Composites 11 (1980) pp 217-224.

[28] SCOTT, I.G. ; SCALA, C.M. : *A review of non-destructive testing of composite materials*". NDT International. 1982, pp75-76.

[29] PENDLETON, R.L. ; MARK, E. T. : *Manual on Experimental Methods for Mechanical Testing of Composites*. Elsevier Applied Science Publishers. 1989 p.116.

[30] RASBAND, W.S. : *ImageJ*, U. S. National Institutes of Health, Bethesda, Maryland, USA, http://rsb.info.nih.gov/ij/, 1997-2006.

[31] ABRAMOFF, M.D. ; MAGELHAES, P.J. ; RAM, S.J. : *Image Processing with ImageJ*. Biophotonics International, volume 11, issue 7, pp. 36-42, 2004.

[32] CARLSSON, L.A. ; BYRON PIPES, R. : Experimental characterization of advanced composite materials, Prentice-Hall, 1987

8. APPENDIX

8.1 X-radiographies from the specimens before testing.

KvCLP_04: Non-Voided Reference

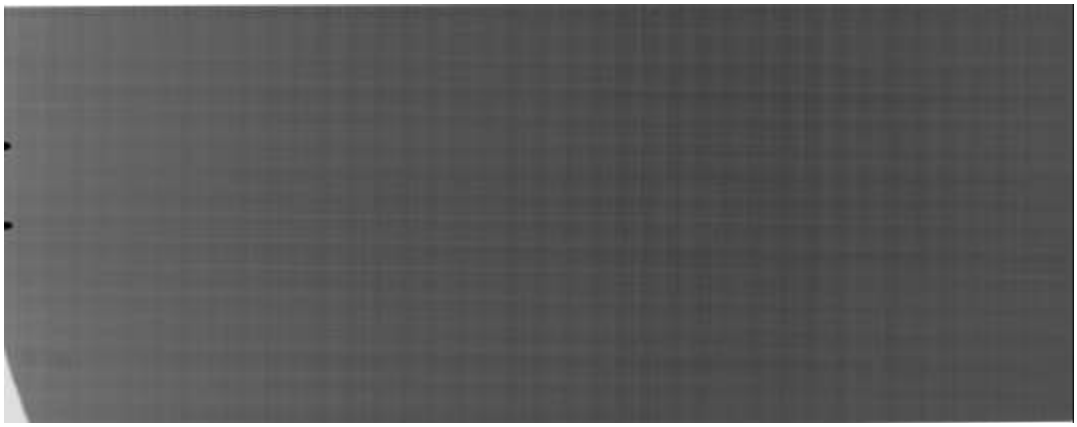

kvCLP_05: 90º Void

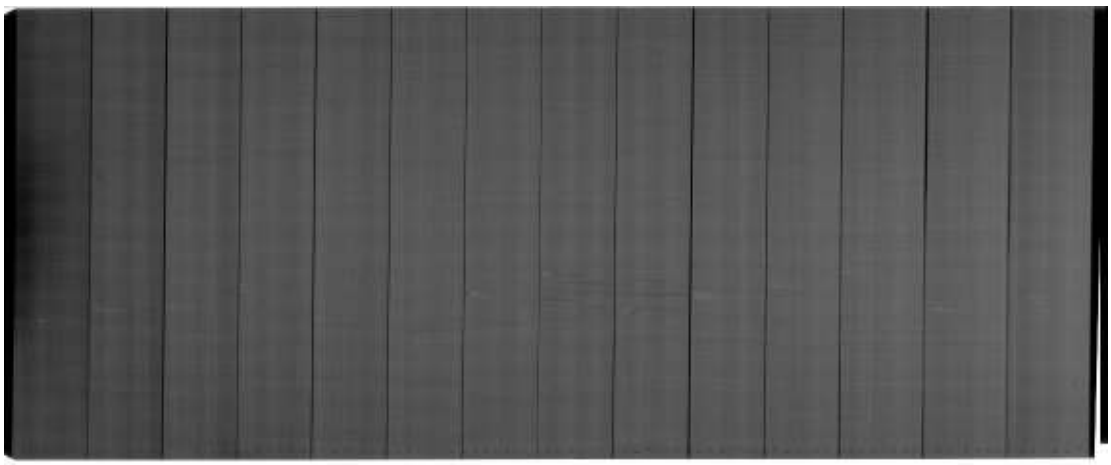

kvCLP_07: 90º Void

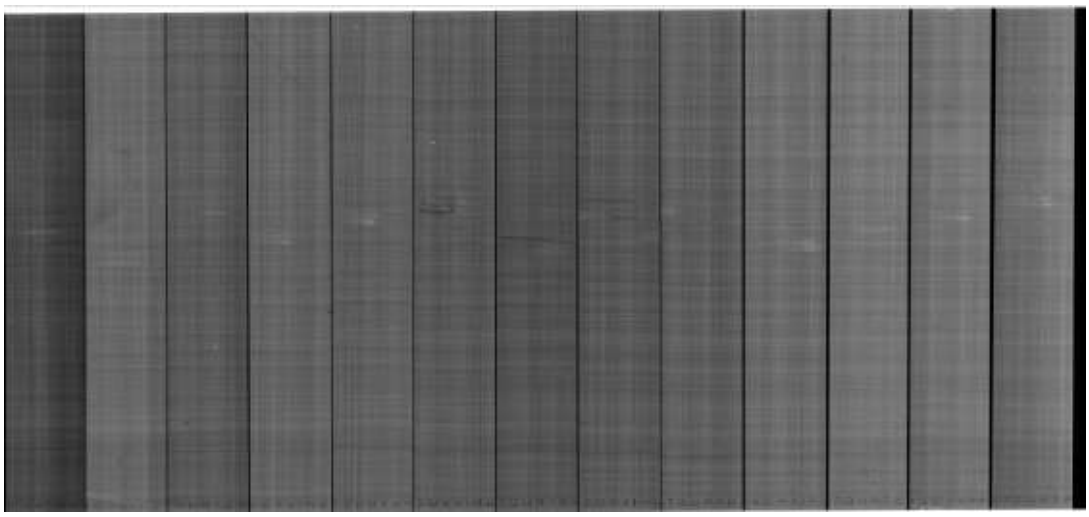

kvCLP_09: 0º Void

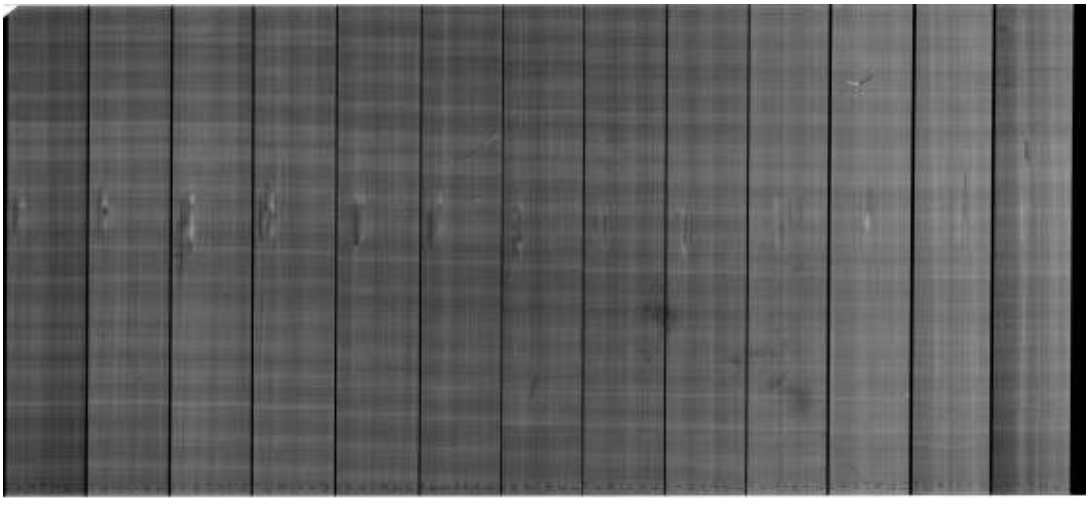

8.2 Specimen characterization

KvCLP_04: Non-Voided Reference

	Width	Thickness
KVCLP 4 1 R	**15,55**	**2,595**
KVCLP 4 2 R	**15,82**	**2,674**
KVCLP 4 3 R	**15,80**	**2,709**
KVCLP 4 4 R	**15,71**	**2,716**
KVCLP 4 5 R	**15,82**	**2,687**
KVCLP 4 6 R	**15,73**	**2,660**
KVCLP 4 7 R	**15,54**	**2,649**
KVCLP 4 8 R	**15,69**	**2,639**
KVCLP 4 9 R	**15,58**	**2,674**
KVCLP 4 10 R	**15,93**	**2,700**
KVCLP 4 11 R	**15,82**	**2,718**
KVCLP 4 12 R	**15,70**	**2,704**
KVCLP 4 13 R	**15,77**	**2,648**

kvCLP_05: 90º Void

	Width	Thickness
KVCLP 5 1 HV	**16,18**	**2,477**
KVCLP 5 2 HV	**15,81**	**2,576**
KVCLP 5 3 HV	**15,87**	**2,639**
KVCLP 5 4 HV	**15,87**	**2,744**
KVCLP 5 5 HV	**16,01**	**2,762**
KVCLP 5 6 HV	**15,97**	**2,800**
KVCLP 5 7 HV	**15,90**	**2,826**
KVCLP 5 8 HV	**15,96**	**2,823**
KVCLP 5 9 HV	**15,96**	**2,821**
KVCLP 5 10 HV	**15,77**	**2,832**
KVCLP 5 11 HV	**17,48**	**2,822**
KVCLP 5 12 HV	**17,73**	**2,710**
KVCLP 5 13 HV	**17,76**	**2,638**

kvCLP_07: 90º Void

	Width	Thickness
KVCLP 7 1 HV	**15,50**	**2,519**
KVCLP 7 2 HV	**15,65**	**2,642**
KVCLP 7 3 HV	**15,86**	**2,686**
KVCLP 7 4 HV	**16,15**	**2,706**
KVCLP 7 5 HV	**15,71**	**2,678**
KVCLP 7 6 HV	**15,86**	**2,634**
KVCLP 7 7 HV	**15,66**	**2,610**
KVCLP 7 8 HV	**15,98**	**2,607**
KVCLP 7 9 HV	**15,92**	**2,635**
KVCLP 7 10 HV	**16,13**	**2,694**
KVCLP 7 11 HV	**15,41**	**2,696**
KVCLP 7 12 HV	**15,65**	**2,669**
KVCLP 7 13 HV	**15,72**	**2,573**

kvCLP_09: 0º Void

	Width	Thickness
KVCLP 9 1 VV	**16,00**	**2,477**
KVCLP 9 2 VV	**16,29**	**2,695**
KVCLP 9 3 VV	**15,93**	**2,725**
KVCLP 9 4 VV	**16,31**	**2,756**
KVCLP 9 5 VV	**16,45**	**2,780**
KVCLP 9 6 VV	**15,91**	**2,743**
KVCLP 9 7 VV	**15,94**	**2,704**
KVCLP 9 8 VV	**16,03**	**2,710**
KVCLP 9 9 VV	**16,00**	**2,744**
KVCLP 9 11 VV	**15,84**	**2,797**
KVCLP 9 12 VV	**16,07**	**2,789**
KVCLP 9 13 VV	**15,78**	**2,747**
KVCLP 9 14 VV	**15,69**	**2,612**

8.3 X-radiographies from the tested specimens

8.3.1 90º voided laminates

Plate KvCLP_05

Specimen KvCLP_05_04, at 38,5, 45, 51, 55, 59 and 62kN unidirectional stress from left to right.

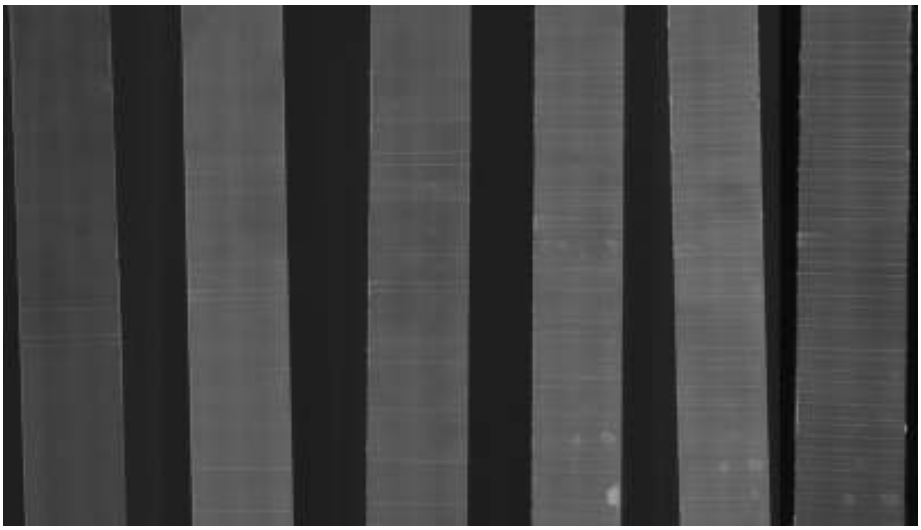

From now on all specimens are represented from left to right in the mentioned order.

Specimens KvCLP_05_01, KvCLP_05_02, KvCLP_05_03, KvCLP_05_06, KvCLP_05_07, KvCLP_05_08 at 38,5kN unidirectional stress.

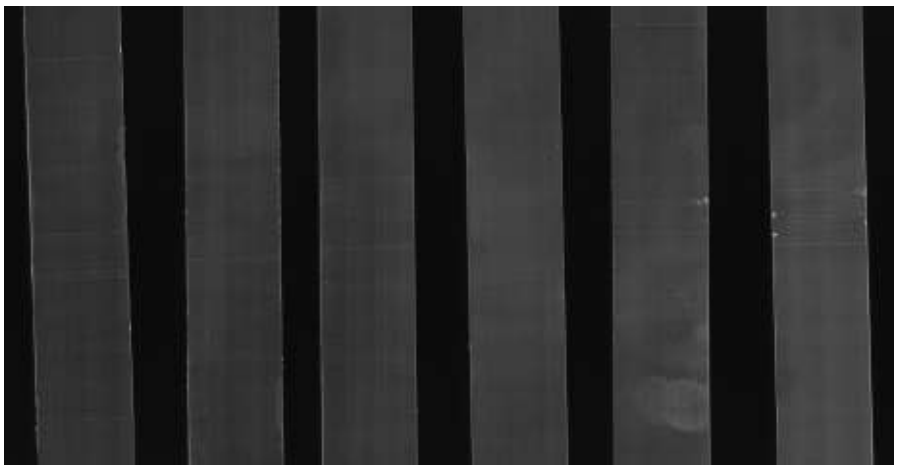

Specimens KvCLP_05_01, KvCLP_05_02, KvCLP_05_03, KvCLP_05_06, KvCLP_05_07, KvCLP_05_08 at 45kN unidirectional stress.

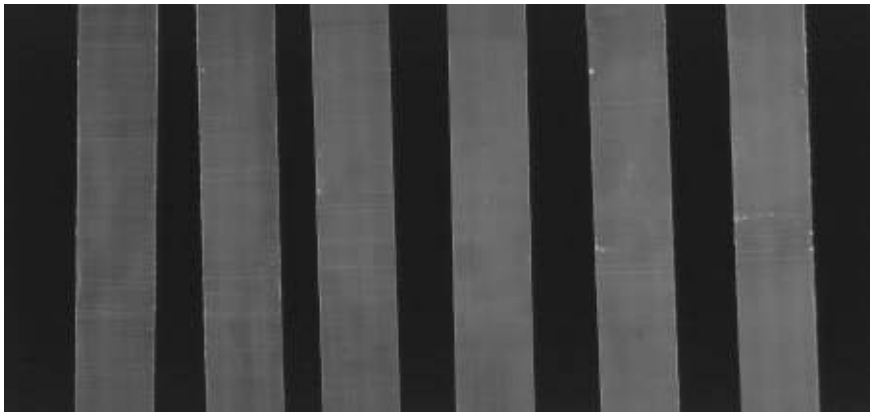

Specimens KvCLP_05_01, KvCLP_05_02, KvCLP_05_03, KvCLP_05_06, KvCLP_05_07, KvCLP_05_08 at 51kN unidirectional stress.

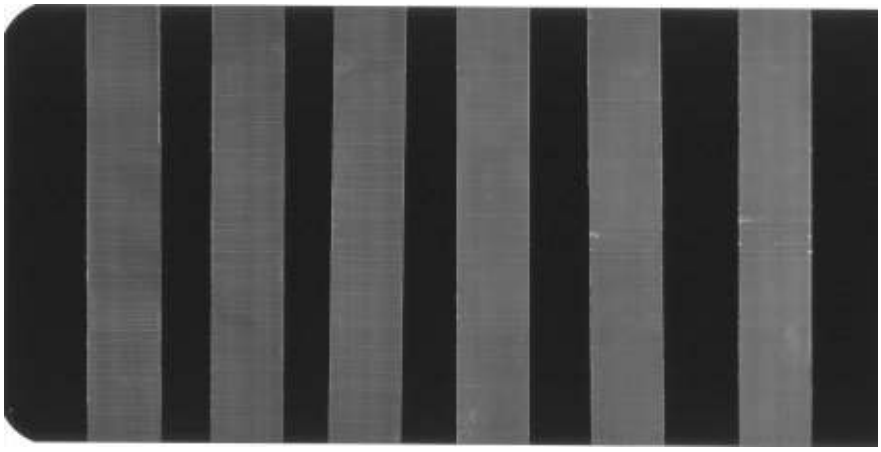

Specimens KvCLP_05_01, KvCLP_05_02 at 53kN and KvCLP_05_03, KvCLP_05_06, KvCLP_05_07, KvCLP_05_08 at 55kN.

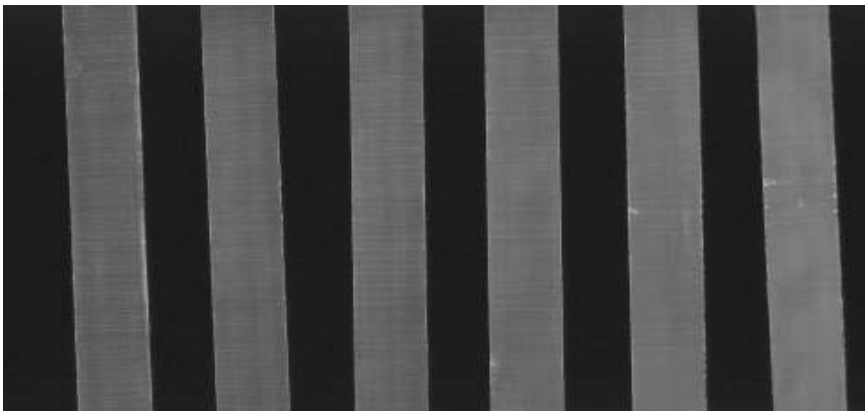

Specimens KvCLP_05_01, at 55kN KvCLP_05_02, at 57kN and KvCLP_05_03, KvCLP_05_06, KvCLP_05_07, KvCLP_05_08 at 59kN unidirectional stress.

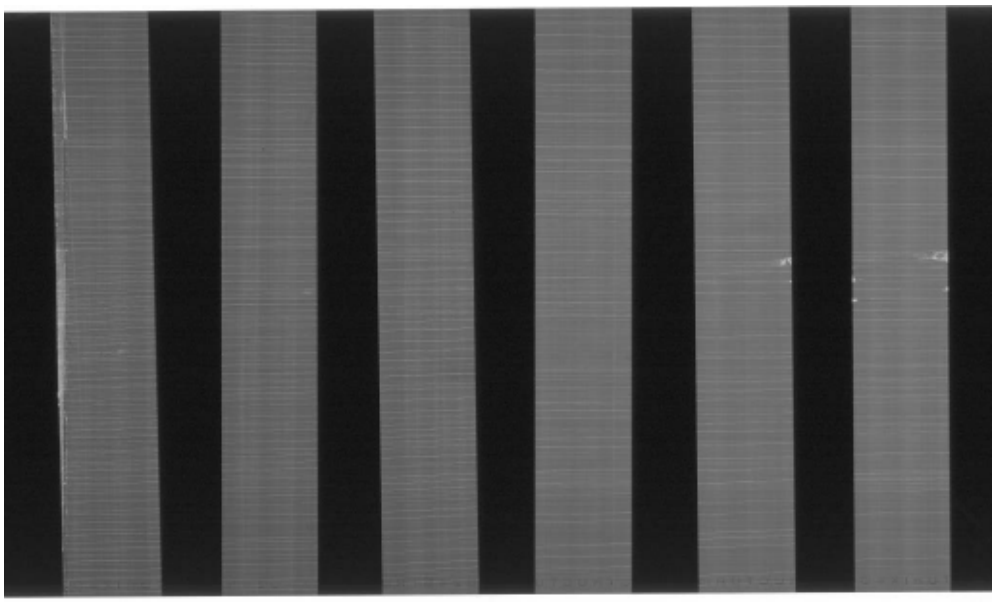

Specimens KvCLP_05_09, KvCLP_05_10, KvCLP_05_11 at 15kN unidirectional stress.

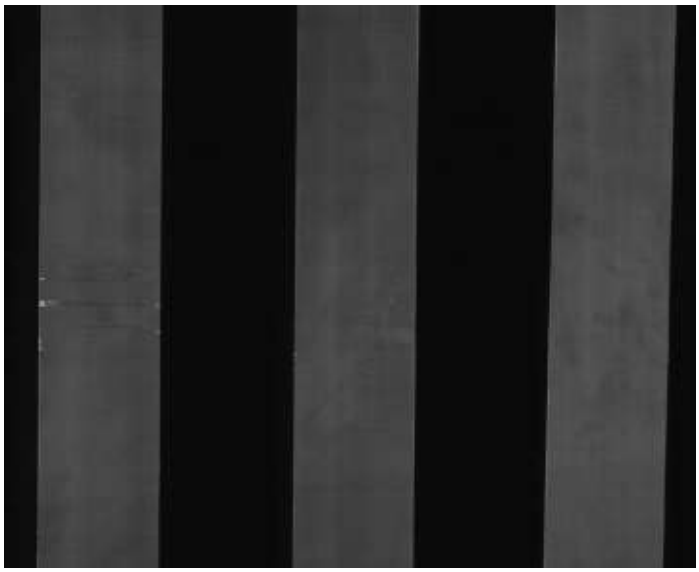

Specimens KvCLP_05_09, KvCLP_05_10, KvCLP_05_11 at 20kN unidirectional stress.

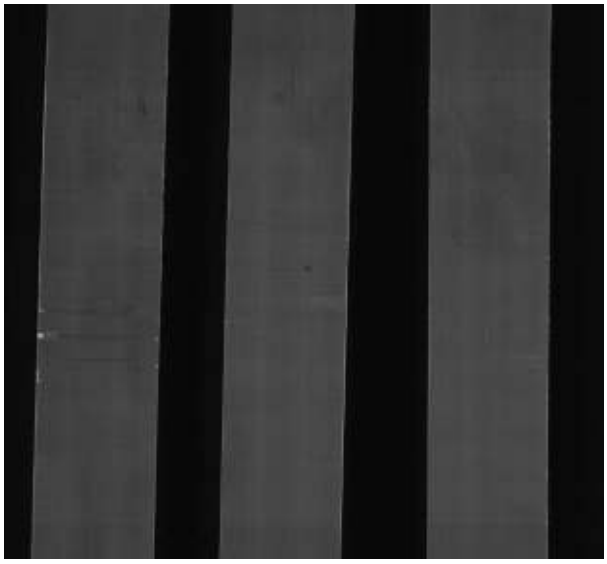

Specimens KvCLP_05_09, KvCLP_05_10, KvCLP_05_11 at 25kN unidirectional stress.

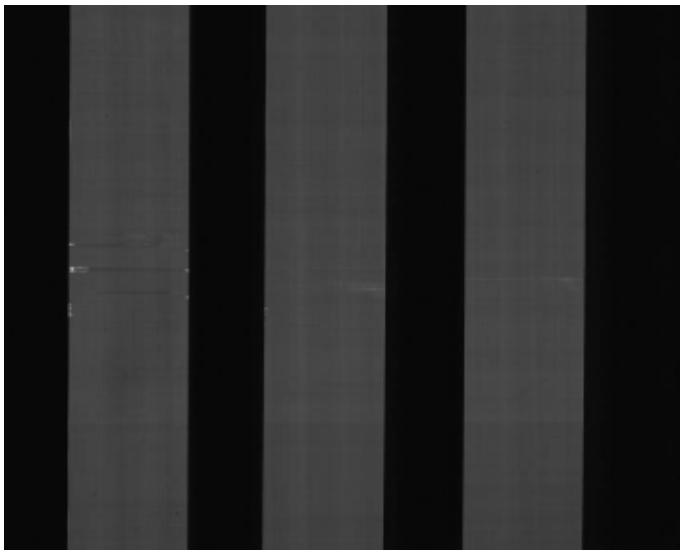

Specimens KvCLP_05_09, KvCLP_05_10, KvCLP_05_11 at 28kN unidirectional stress.

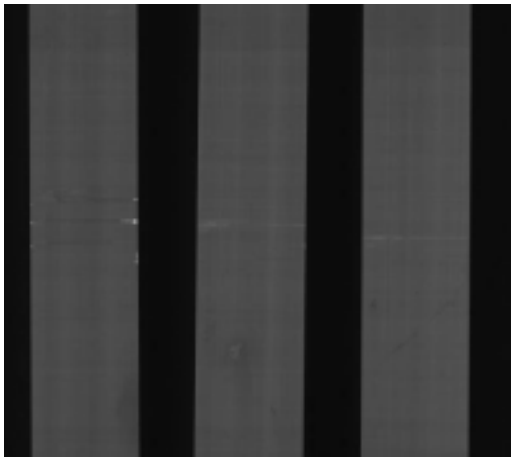

Specimens KvCLP_05_09, KvCLP_05_10, KvCLP_05_11 at 31kN unidirectional stress.

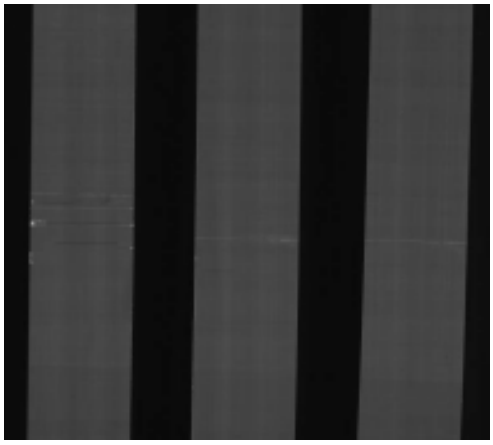

Specimens KvCLP_05_09, KvCLP_05_10, KvCLP_05_11 at 34kN unidirectional stress.

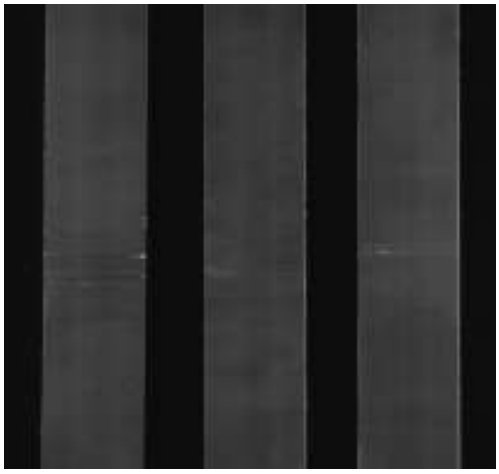

Specimens KvCLP_05_09, KvCLP_05_10, KvCLP_05_11 at 37kN unidirectional stress.

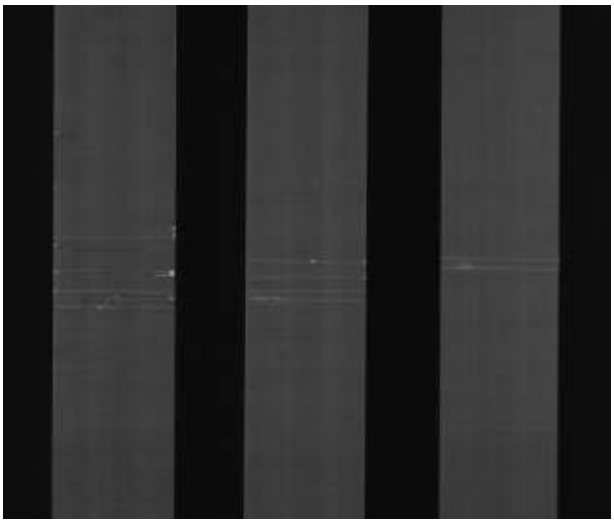

Specimens KvCLP_05_09, KvCLP_05_10, KvCLP_05_11 at 40kN unidirectional stress.

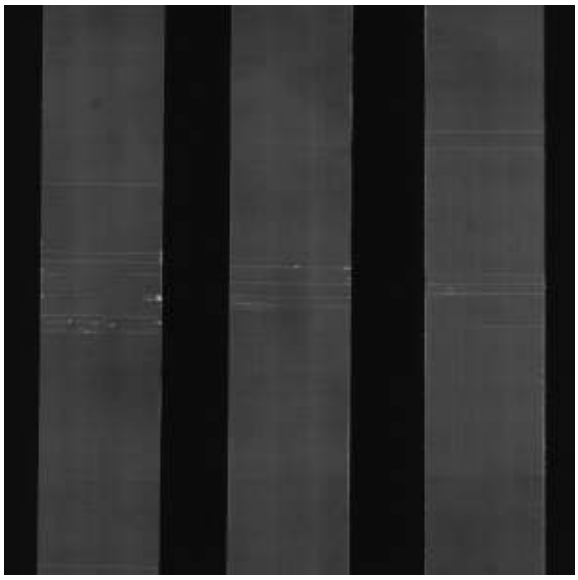

Plate KvCLP_07

Specimens KvCLP_07_01, KvCLP_07_02, KvCLP_07_03, KvCLP_07_06, KvCLP_07_07, KvCLP_07_08, KvCLP_07_09 at 25kN unidirectional stress.

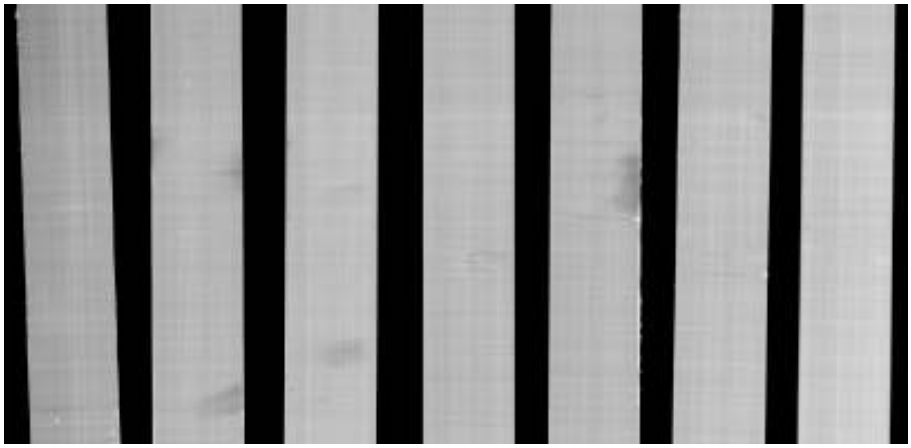

Specimens KvCLP_07_01, KvCLP_07_02, KvCLP_07_03, KvCLP_07_06, KvCLP_07_07, KvCLP_07_08, KvCLP_07_09 at 30kN unidirectional stress.

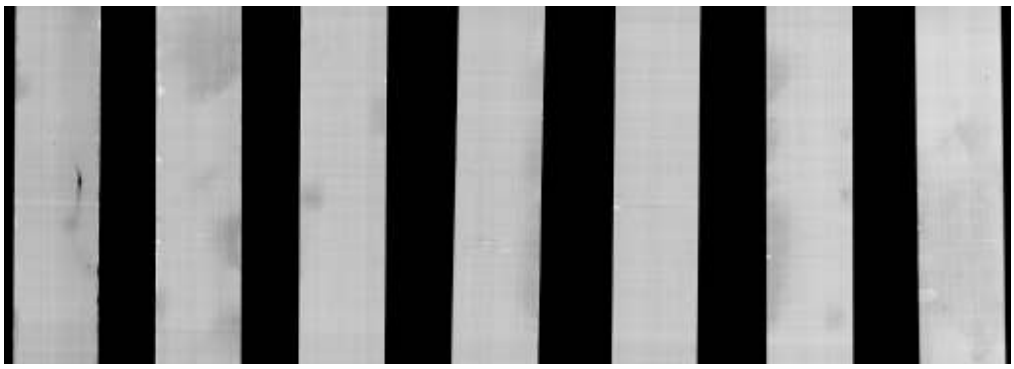

Specimens KvCLP_07_01, KvCLP_07_02, KvCLP_07_03, KvCLP_07_06, KvCLP_07_07, KvCLP_07_08, KvCLP_07_09 at 35kN unidirectional stress.

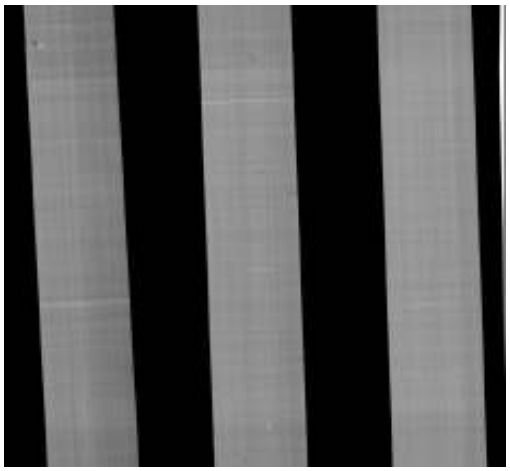

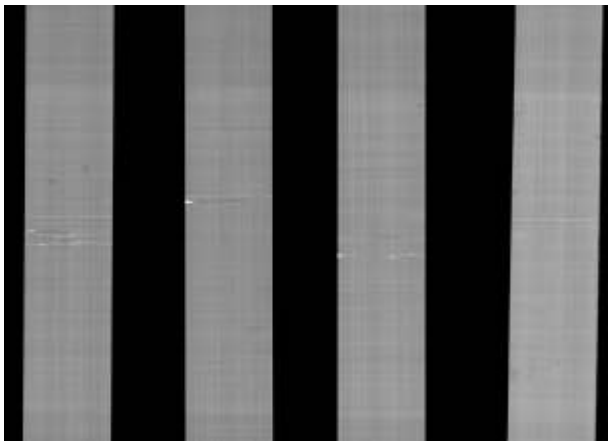

Specimens KvCLP_07_01, KvCLP_07_02, KvCLP_07_03, KvCLP_07_06, KvCLP_07_07, KvCLP_07_08, KvCLP_07_09 at 40kN unidirectional stress.

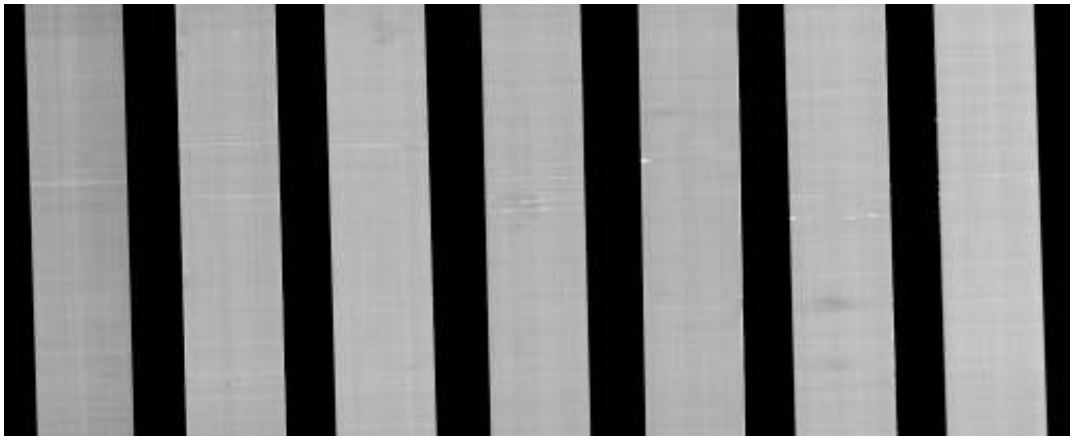

Specimens KvCLP_07_01, KvCLP_07_02, KvCLP_07_03, KvCLP_07_06, KvCLP_07_07, KvCLP_07_08, KvCLP_07_09 at 45kN unidirectional stress.

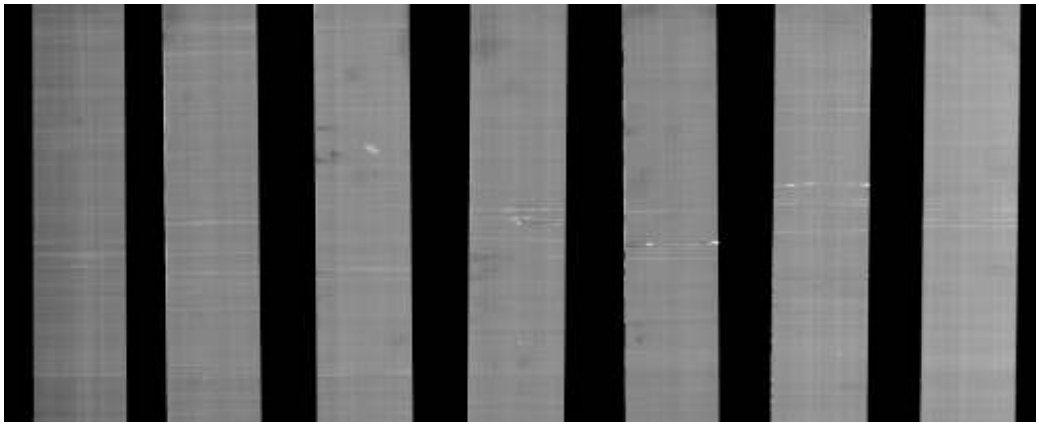

Specimens KvCLP_07_01, KvCLP_07_02, KvCLP_07_03, KvCLP_07_06, KvCLP_07_07, KvCLP_07_08, KvCLP_07_09 at 50kN unidirectional stress.

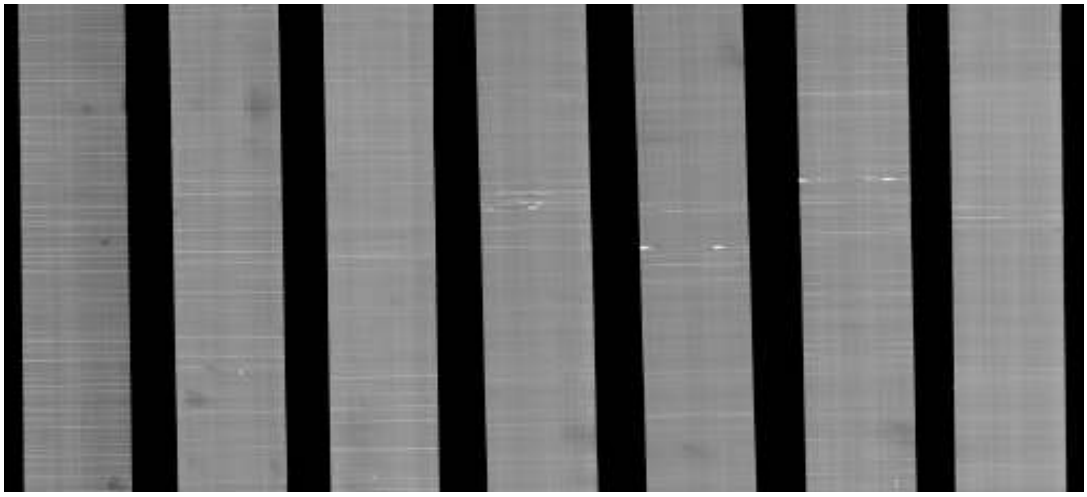

8.3.2 0º voided laminates

Plate KvCLP_09

Specimens KvCLP_09_01, KvCLP_09_02, KvCLP_09_03, KvCLP_09_04 at 15kN unidirectional stress.

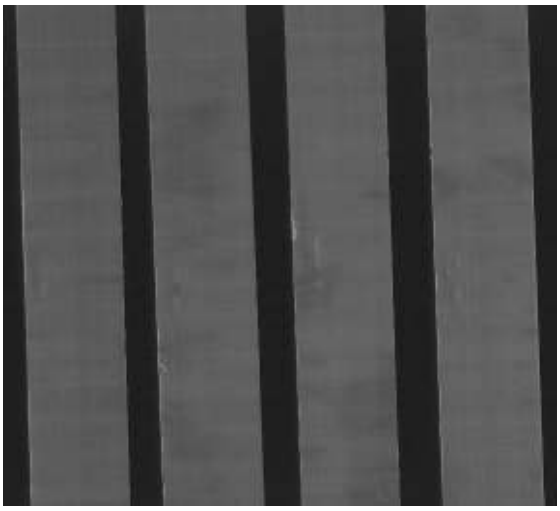

Specimens KvCLP_09_01, KvCLP_09_02, KvCLP_09_03, KvCLP_09_04 at 18kN unidirectional stress.

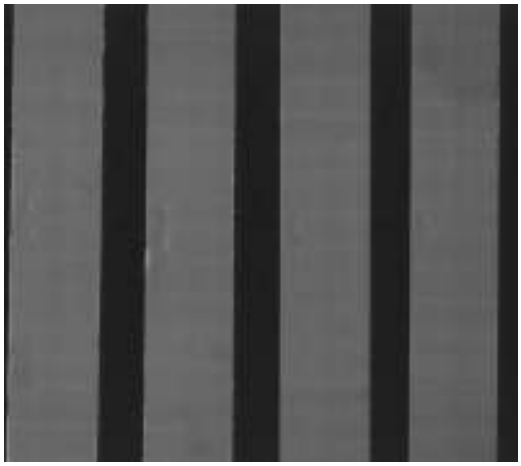

Specimens KvCLP_09_01, KvCLP_09_02, KvCLP_09_03, KvCLP_09_04 at 20kN unidirectional stress.

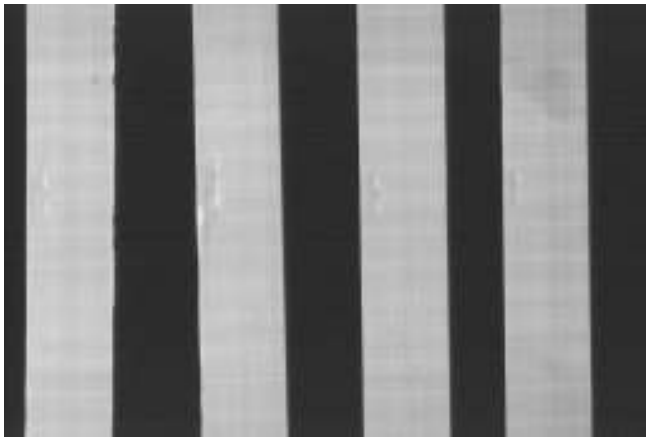

Specimens KvCLP_09_01, KvCLP_09_02, KvCLP_09_03, KvCLP_09_04 at 25kN unidirectional stress.

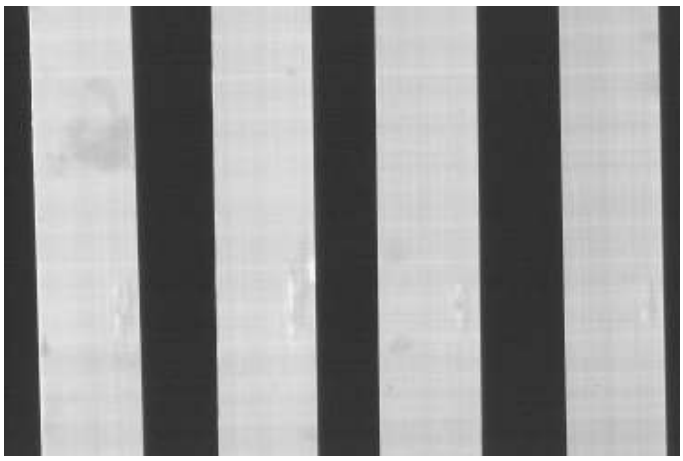

Specimens KvCLP_09_01, KvCLP_09_02, KvCLP_09_03, KvCLP_09_04 at 29kN unidirectional stress.

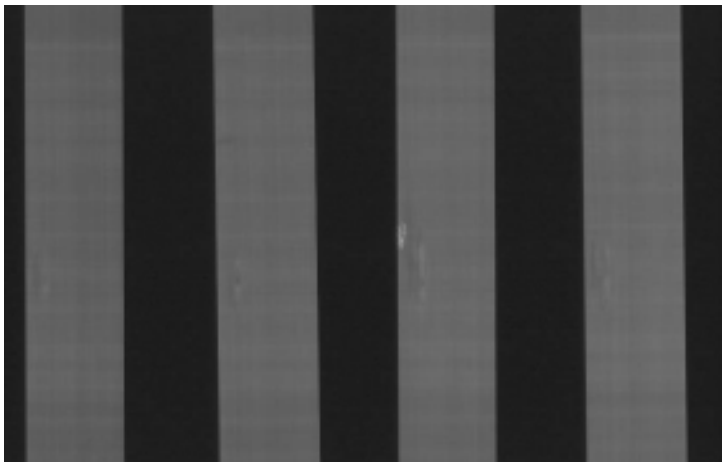

Specimens KvCLP_09_01, KvCLP_09_02, KvCLP_09_03, KvCLP_09_04 at 31kN unidirectional stress.

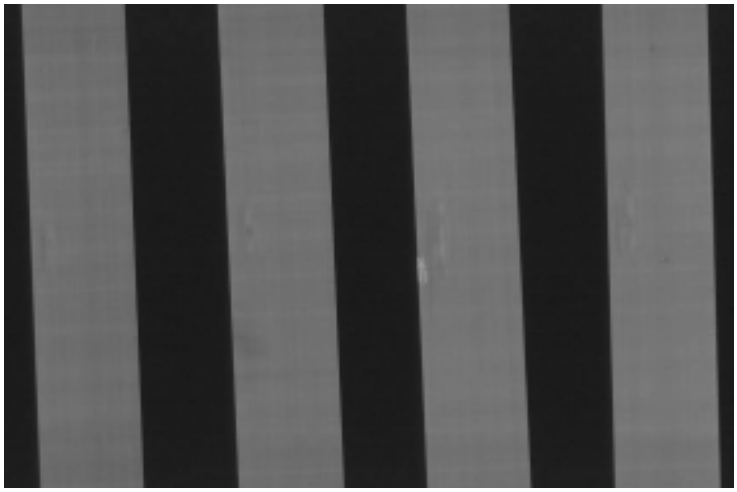

Specimens KvCLP_09_01, KvCLP_09_02, KvCLP_09_03, KvCLP_09_04 at 35kN unidirectional stress.

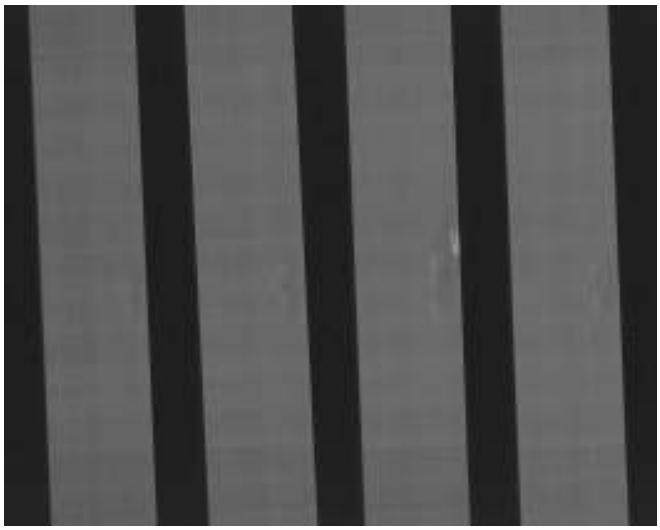

Specimens KvCLP_09_01, KvCLP_09_02, KvCLP_09_03, KvCLP_09_04 at 38kN unidirectional stress.

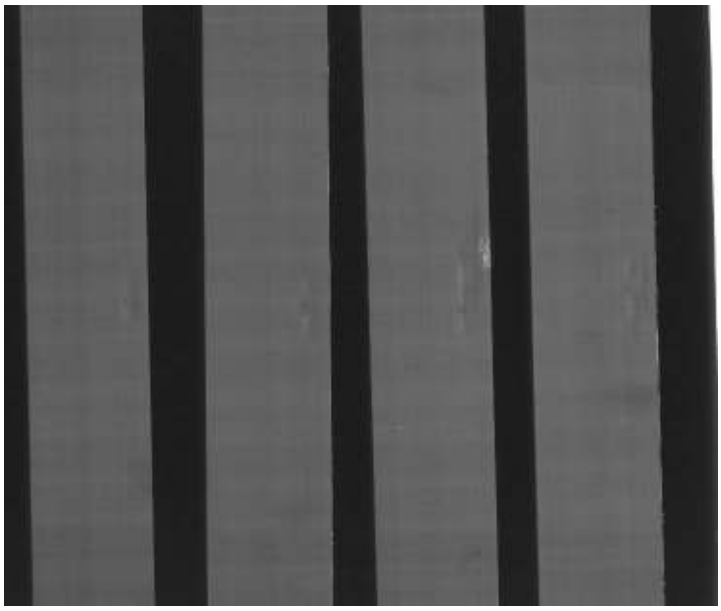

Specimens KvCLP_09_01, KvCLP_09_02, KvCLP_09_03, KvCLP_09_04 at 42kN unidirectional stress.

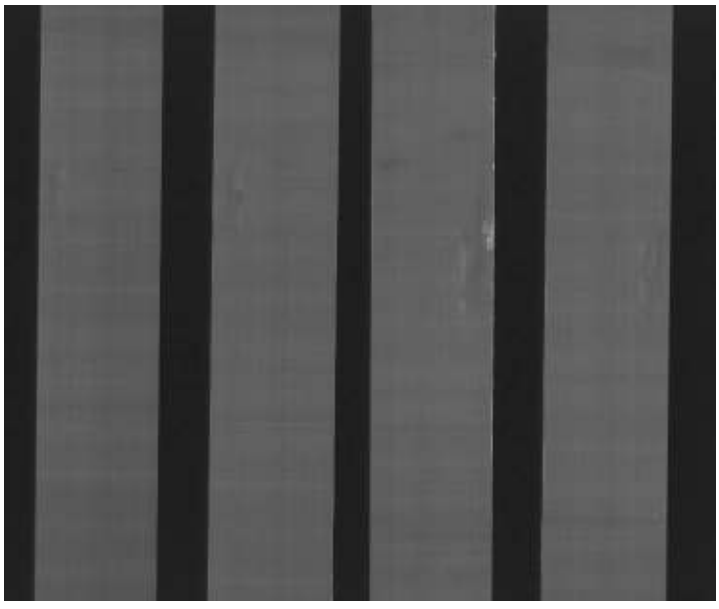

Specimens KvCLP_09_01 at 53kN and KvCLP_09_02, KvCLP_09_03, KvCLP_09_04 at 45kN unidirectional stress.

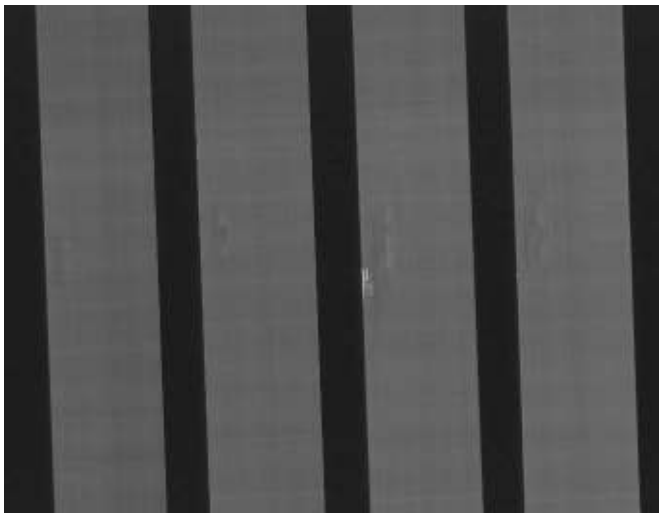

Specimens KvCLP_09_01, KvCLP_09_02 and KvCLP_09_03 at 48kN unidirectional stress.

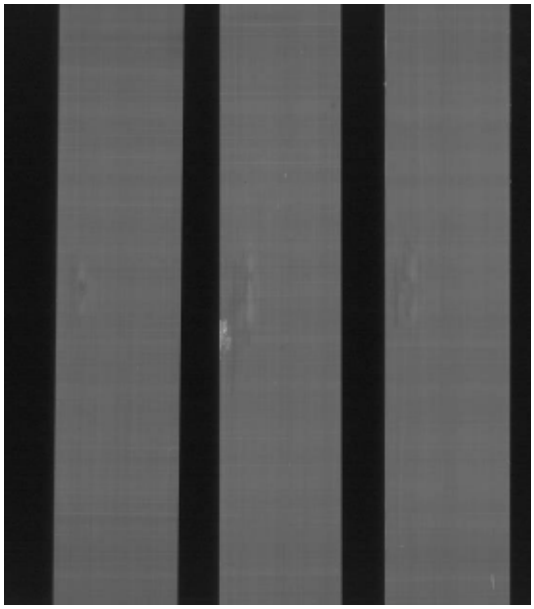

Specimens KvCLP_09_01, KvCLP_09_02, KvCLP_09_03 at 51kN unidirectional stress.

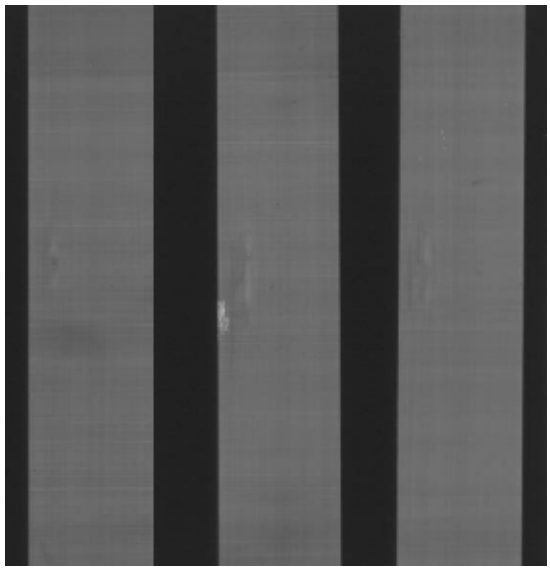

Specimens KvCLP_09_01 at 58kN and KvCLP_09_02, KvCLP_09_03, KvCLP_09_04 at 54kN unidirectional stress.

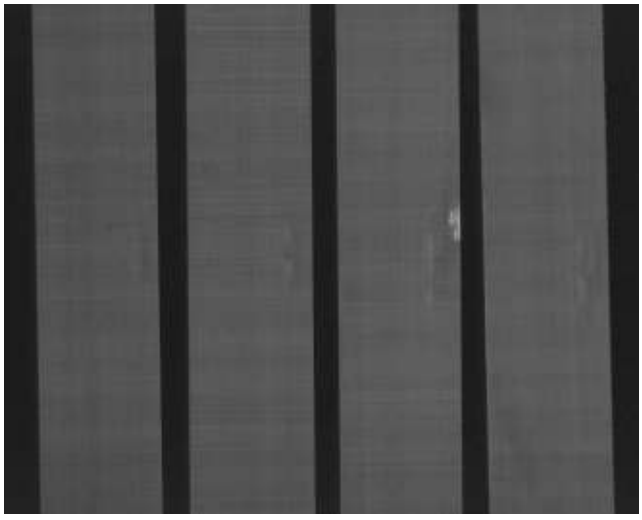

Specimens KvCLP_09_01 at 62kN and KvCLP_09_02, KvCLP_09_03, KvCLP_09_04 at 60kN unidirectional stress.

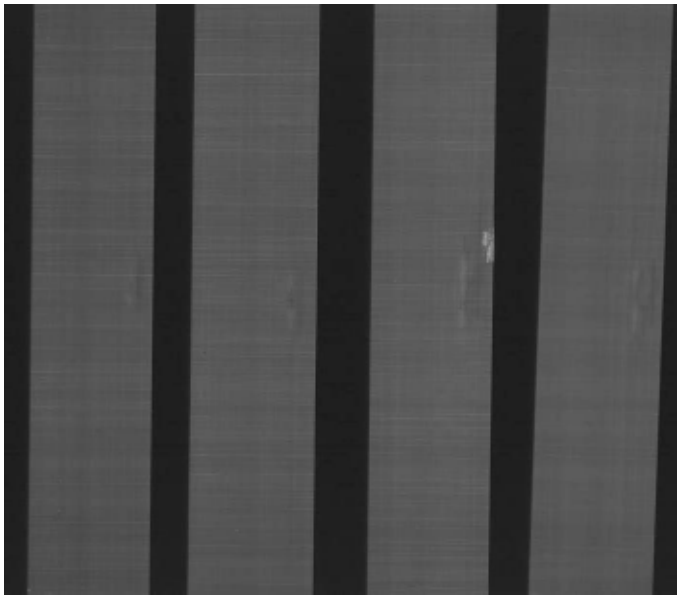

Specimens KvCLP_09_02, KvCLP_09_03, KvCLP_09_04 at 64kN unidirectional stress.

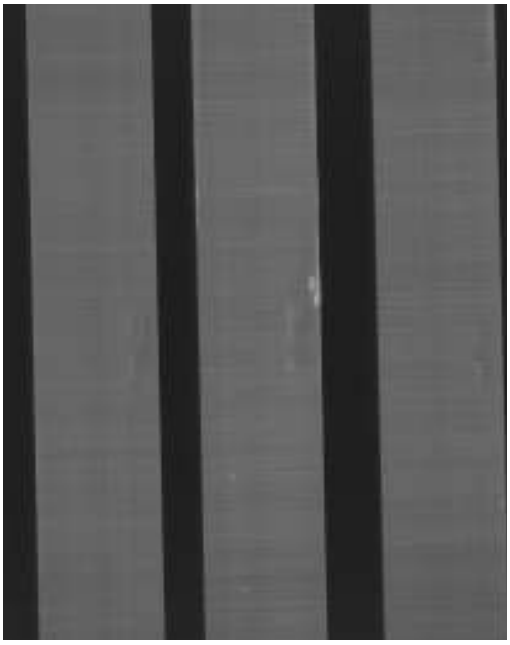

Specimen KvCLP_09_04 at 68kN unidirectional stress.